Aus der Medizinischen Klinik und Poliklinik III

Experimentelle Leukämie- und Lymphomforschung (ELLF)

Deutsches Konsortium für Translationale Krebsforschung (DKTK)

Dissertation

zum Erwerb des Doctor of Philosophy (Ph.D.)

an der Medizinischen Fakultät der

Ludwig-Maximilians-Universität zu München

Characterization of CSF3R mutations in Core Binding Factor Leukemia

vorgelegt von:

Anja Susanna Swoboda, geb. Wilding

aus:

Ingolstadt

Jahr:

2024

Mit Genehmigung der Medizinischen Fakultät der

Ludwig-Maximilians-Universität zu München

First evaluator (1. TAC member):	Prof. Dr. Philipp A. Greif
Second evaluator (2. TAC member):	Prof. Dr. Oliver Weigert
Third evaluator:	Prof. Dr. Irmela Jeremias
Fourth evaluator:	Priv. Doz. Dr. Johanna Tischer

Dean: **Prof. Dr. med. Thomas Gudermann**

date of the defense:

09.07.2024

_____

Table of content

Dedication

I dedicate this thesis to my children,

Nikolas and Christian

my wonderful boys,

my greatest source of joy.

Abstract

Predicting treatment success of acute myeloid leukemia (AML) is highly dependent on different factors. It is an extremely heterogeneous disease which is in progression and outcome vastly depending on genetic subtypes and interplay of aberrations, which are often poorly understood. In AML patients, somatic mutations of the colony-stimulating factor-3 receptor (*CSF3R*) gene show eminent correlation with the presence of altered hematopoietic transcription factors. In particular, *CSF3R* proximal membrane domain mutations were found in either *CEBPA* double mutated AML or t(8;21) core binding-factor (CBF) leukemia, leading to proliferative advantage and disrupted differentiation as direct consequence of ligand independent receptor activation.

In this thesis, the oncogenic collaboration between the CSF3R mutant T618I and RUNX1-RUNX1T1 fusion was studied. Generally, the fusion gene *RUNX1-RUNX1T1*, associated to translocation t(8;21) positive AML indicates a favorable prognosis, however, full understanding of the influence of *CSF3R* mutations during AML development and treatment outcome is missing. RUNX1-RUNX1T1 induces partial block of myeloid differentiation, but does not cause leukemia on its own, advocating for the requirement of additional genetic lesions. It was discovered that both may activate specific pathways synergistically – beyond disturbing differentiation and driving proliferation. In immature donor HSPCs, expression of both oncogenes induced a prominent clonal advantage, increased self-renewal potential, as well as a distinct immunophenotype and blast-like, immature morphology. Hedgehog signaling could be uncovered as a putative mechanism, with upregulated *GLI2* as a putative pharmacological target. Both experimental systems, primary cells and cell line model, were sensitive to treatment with the GLI-inhibitor GANT61 upon CSF3R T618I expression. Those results suggest that RUNX1-RUNXT1 and mutated CSF3R act synergistically during leukemogenesis via induction of hedgehog signaling which can be targeted therapeutically.

List of figures

List of tables

List of Abbreviations

Abbreviation	
%	Percentage
°C	Degree Celsius
µ	Micro
aCML	atypical Chronic Myeloid Leukemia
ALL	Acute Lymphocytic Leukemia
AML	Acute Myeloid Leukemia
AMML	Acute Myelomonocytic Leukemia
Ara-C	Cytarabine
bp	Basepairs
BSA	Bovine serum albumin
CBF	Core-binding factor
CD	Cluster of Differentiation
cDNA	complementary DNA
CIN	Chronic Idiopathic Neutropenia
CML	Chronic Myeloid Leukemia
CMML	Chronic Myelomonocytic Leukemia
CMP	Common myeloid progenitor
cMPO	cytoplasmic Myeloperoxidase
CNL	Chronic Neutrophilic Leukemia
CR	complete remission
CRH	Cytokine receptor homology
CSF1R	Colony-stimulating factor 1 receptor
CSF3R	Colony-stimulating factor 3 receptor
DC	Dendritic cell
Dest	Distilled
Dhh	Desert Hedgehog
DMEM	Dulbecco´s modified eagle medium
DMSO	Dimethyl Sulfoxide
DNMT	DNA methyltransferase
DNR	Daunorubicin
EDTA	Ethylene diamine tetraacetic acid
ELN	European LeukemiaNet
EMA	European Medicines Agency
EV	Empty vector
FAB	French-American-British
FBS	Fetal bovine serum
FDA	Food and Drug administration
FISH	Fluorescence in-situ hybridization
FN	Fibronectin
G-CSF	Granulocytic colony-stimulating factor
GFP	Green fluorescent protein
GLI	Glioma-Associated Oncogene Family Zinc Finger

GM-CSF	granulocyte-macrophage colony-stimulating factor
GO	Gemtuzumab Ozogamizin
HDAC	Histone deacetylase
Hh	Hedgehog
HSC	Hematopoietic stem cells
HSPC	Hematopoietic stem and progenitor cells
IFN	Interferon
Ig	Immunoglobin
Ihh	Indian Hedgehog
IL	Interleukin
JAK	Janus kinase
JNK	Jun N-terminal kinase
LSC	Leukemic stem cell
M	Molar (mol/l)
m	Milli
MAPK	Mitogen activated protein kinase
M-CSF	macrophage colony-stimulating factor
MDS	Myelodysplastic syndrome
min	Minute(s)
MPO	Myeloperoxidase
MPP	Multipotent progenitor
MRD	Minimal/measurable residual disease
mRNA	Messenger RNA
NGS	Next-Generation Sequencing
OS	Overall survival
PB	Peripheral Blood
PBPC	Peripheral blood progenitor cells
PBS	Phosphate buffered saline
PCR	Polymerase chain reaction
PI3K	Phosphatidylinositol 3-kinase
qPCR	quantitative PCR
RFS	Relapse free survival
RNA	Ribinucleic acid
ROS	Reactive oxygen species
rpm	Rounds per minute
RT	Room temperature
RTK	Receptor tyrosine kinase
RT-PCR	reverse transcriptase PCR
SCN	Severe Congenital Neutropenia
SMO	Smoothened
SOCS	Suppressor of cytokine signaling
STAT	Signal transducer and activator of transcription
SYK	Spleen associated tyrosine kinase
TYK	Tyrosine kinase
WHO	World Health Organization
WT	Wildtype

1 Introduction

1.1 Preface

A great variety of gene mutations and chromosomal aberrations are the underlying cause of malignant cell transformation and cancer progression. Mutations in the colony-stimulating factor 3 receptor (*CSF3R*) gene are frequently observed in some forms of leukemia but are extremely rare in de novo acute myeloid leukemia (AML).[1] Where they are found, they are mostly accompanied by core-binding factor (CBF) leukemia or *CEBPA* mutations[1–3], deteriorating therapy outcome[4]. Different types of *CSF3R* mutations are thereby distinctively correlated to either one CBF rearrangement[2]. The central hypothesis of this work was that the unique combination of chromosomal translocation t(8;21) and the transmembrane mutation T618I of *CSF3R* provide an decisive advantage for hematopoietic cells. Therefore the main objective was an experimental setup in different cellular systems, allowing for the exploration of biological consequences following CSF3R T618I expression in a t(8;21) background. Given the high proportion of *CSF3R* mutated CBF leukemia patients eventually relapsing, the experimental work for this thesis is ultimately intended to investigate druggable targets in support of patients that might not benefit from standard therapy alone.

1.2 Acute myeloid leukemia

Leukemias are malignancies of the hematopoietic system causing an accumulation of dysfunctional leukocytes. While lymphoblastic leukemias originate from lymphatic progenitors, myeloid leukemia cells stem from myeloid progenitors which fail to give rise to mature granulocytes and monocytes.[5–7] Clinically, both lymphoblastic and myeloid leukemias can be divided into rapidly progressing, aggressive acute leukemias and slowly progressing chronic leukemias. Among acute leukemias, acute myeloid leukemia (AML) is the most frequent subtype with 80% of cases.[8] AML is characterized as a cancer of hematopoietic stem and progenitor cells, often poorly or aberrantly differentiated. Malignant cells infiltrate blood, bone marrow and other tissues by dysregulated clonal expansion and proliferation. Therefore, healthy cells are suppressed by malignant cells, impairing normal hematopoiesis, and eventually leading to bone marrow failure.[9]

1.2.1 Incidence and pathogenesis

In 2020, more than 19 million people worldwide were diagnosed with some form of cancer. In the same year, the World Health Organization (WHO) documented nearly 10 million cancer-related deaths, making it one of the leading causes of death worldwide. Hematologic malignancies, including myeloma, lymphoma and leukemia accounted for approximately 8% of all cancer-related deaths.[10]

Every year statistically between 2.5 and 3 people per 100 000 individuals are diagnosed with a form of acute myeloid leukemia. AML is considered a disease of age, with an emerging average age of 68.[11] In contrast, in children under 15, only 10-15% of acute leukemias are classified as AML.[12] While it was still considered incurable 50 years ago, better understanding of the disease, modern diagnostics, especially Next Generation Sequencing, and specific targeting of selected genomic lesions helped to raise the survival rate to 29% in total, with 35-40% survival rates in patients under the age of 60 and 5-15% in patients older than 60.[9,13] AML is generally considered a rapidly progressing disease with poor prognosis, yet, response to treatment as well as prognostic risks are highly heterogeneous. If patients respond well to initial treatment and show complete remission, 40-50% of young adults and the vast majority of elderly patients eventually relapse, highly limiting treatment options. Relapsing patients commonly show clonal evolution of the disease.[14]

Four to six weeks before initial diagnosis, patients often present early symptoms of AML including general weakness, fever, paleness, infections, or bleeding. Less commonly, impaired normal hematopoiesis and infiltration of leukemic cells can lead to localized symptoms as myeloid sarcomas, or disorders of the central nervous system.[15]

1.2.2 Diagnostic methods

Precise differential diagnosis, discerning AML from other leukemia, as chronic myelogenous leukemia (CML) or acute lymphocytic leukemia (ALL) has vital implications and is crucial for therapeutic decisions. As initial diagnosis, blood count from bone marrow or peripheral blood is sufficient, as 20% or more immature blast count is a clear sign for AML.[16,17] Moreover, cytogenetic differences are key to differential risk assessment between patients. Bone marrow aspirate provides material for morphology, cytogenetic and molecular analysis as well as surface marker staining. Irrespective of blast count, presence of balanced rearrangements as translocations t(16;16), t(15;17), t(8;21), or inversion of chromosome 16 (inv(16)) are sufficient to diagnose AML.[13,16,17] In leukemogenesis of 30-50% of young adults and children, the initiating event is the generation of fusion genes due to translocation or inversion events in hematopoietic progenitor cells. In contrast, balanced chromosomal rearrangements are only present in a minority of elderly patients.[18]

For solid diagnosis after WHO standards, intersecting results of the following four methods must be taken into consideration:

1.2.2.1 Morphology

Morphologic examination using May-Grünwald-Giemsa or Wright-Giemsa staining is considered the gold-standard in routine diagnostic. Cytomorphology is used for AML classification according to recommendations of both the French-American-British (FAB) system and the World Health Organization (WHO). [12,16,17,19]

1.2.2.2 Immunophenotyping

Complementary to cytomorphology, immunophenotyping by multiparameter flow cytometry is used to characterize the lineage of diagnosed acute leukemia. [13,16,20,21]

Expression of markers for diagnosis	
Diagnosis of acute myeloid leukemia (AML)	
Precursor stage	CD34, CD38, CD117, CD133, HLA-DR
Granulocytic markers	CD13, CD15, CD16, CD33, CD65, cytoplasmic myeloperoxidase (cMPO)
Monocytic markers	Nonspecific esterase (NSE), CD11c, CD14, CD64, lysozyme, CD4, CD11b, CD36, NG2 homologue
Megakaryocytic markers	CD41 (glycoprotein IIb/IIIa), CD61 (glycoprotein IIIa), CD42 (glycoprotein 1b)
Erythroid markers	CD235a (glycophorin A)
Diagnosis of mixed phenotype acute leukemia (MPAL)	
Myeloid lineage	MPO or evidence of monocytic differentiation (at least 2 of the following: NSE, CD11c, CD14, CD64, lysozyme)
B-lineage	CD19 (strong) with at least one of the following: CD79a, cCD22, CD10, or CD19 (weak) with at least 2 of the following: CD79a, cCD22, CD10
T-lineage	cCD3, or surface CD3

Table 1: Expression of cell-surface and cytoplasmic markers for the diagnosis of acute myeloid leukemia and mixed phenotype acute leukemia.
Adapted from Döhner et al (2010).[13]

While immunophenotyping of leukemic cells is crucial to delineate AML from ALL and other leukemias, surface expression patterns alone are not sufficiently specific to distinctly determine FAB or WHO classification and cytogenetic subtype.[22]

1.2.2.3 Cytogenetics

Upon conjectured AML diagnosis, cytogenetic analysis becomes an inevitable component for diagnostic evaluation. Cytogenetic abnormalities are key for WHO classification and have high prognostic impact.

1.2.2.4 Molecular genetics

Especially for core binding factor abnormalities, screening via reverse transcriptase-polymerase chain reaction (RT-PCR) is a valuable detection technique in case cytogenetic methods fail or are not applicable. It should, however, only be used complementary to cytogenetic analysis.[23,24] While PCR based techniques like endpoint PCR or quantitative PCR (qPCR) remain a vital instrument of AML diagnosis,[25] modern Next-Generation sequencing (NGS) allows for rapid screening with high sensitivity,[26] providing the basis not only for disease classification,[19] but also risk stratification.[25]

1.2.3 Diagnostic classification and prognostic risks

AML subtypes are discerned after either of the two main classification systems: the French-American-British (FAB) or the more recent World Health Organization (WHO) classification.

1.2.3.1 FAB classification

The older of the two classification systems has been suggested as early as 1976, when a group of experts started discriminating AML subtypes based on morphology and immune phenotype. The subgroups were categorized according to a number system from M0-M7.[27]

M0	Acute myeloid leukemia with minimal differentiation
M1	Acute myeloblastic leukemia with no maturation
M2	Acute myeloblastic leukemia with maturation
M3	Hypergranular promyelocytic leukemia
M4	Myelomonocytic leukemia
M5	Monocytic leukemia
M6	Erythroleukemia
M7	Megakaryoblastic leukemia

Table 2: French-American-British (FAB) classification of AML.
Modified from Bennett et al. (1976).[27]

1.2.3.2 WHO classifications

Emerging new technologies and unparalleled gain of knowledge called for revision of AML classification according to the FAB system. Ever since the WHO re-classified AML with different entities in 2001, the classification had been revised in 2008, 2016 and 2022.[16,17,19,28,29] In contrast to FAB classification, precise AML classification can only follow analysis of combined diagnostics taking into consideration all available methods.

WHO classification of acute myeloid leukemia (AML) and related neoplasms
AML with defining genetic abnormalities
AML defined by differentiation

Table 3: WHO classification of acute myeloid leukemia (AML) and related neoplasms.
Modified from Khoury et al. (2016)[17].

Furthermore, WHO classification provides the basis for prognostic risk assessment as recommended by the European LeukemiaNet (ELN). Whereas earlier risk stratification proposed to classify patients risk as favorable, intermediate I, intermediate II and adverse,[13] the updated recommendation advises classification within only three groups:

Risk stratification European LeukemiaNet
Favorable
Intermediate
Adverse

Table 4: ELN risk stratification.
Modified from Döhner at al.[25]

In addition, detection of MRD by digital PCR and NGS has vital implications on both risk stratification and therapy options and is therefore monitored carefully.[25]

1.2.4 Therapy

Albeit being a highly heterogeneous disease, treatment of AML stays mainly universal. Throughout recent years, approaches towards individualized precision medicine have been undertaken, yet the classical 3+7 treatment remains state of the art.

Patients eligible for intense induction therapy are treated with a continuous infusion of 100-200mg/m^2 cytarabine (AraC) for 7 days in combination with 3 days of treatment with an anthracycline. Historically, 45-60mg/m^2 daunorubicin (DNR) are the drug of choice, the 2017 ELN recommendation calls for at least 60mg/m^2.[25,30] Escalating dosages to 90mg/m^2 may only be beneficial for a small subset of patients while leading to higher mortality rates due to increased toxicity. Idarubicin presents an alternative to high dose daunorubicin, showing comparable complete remission (CR) rates, overall survival (OS) and mortality at a dose of 12mg/m^2. Intense induction therapy represents the standard therapy for favorable and intermediate risk patients, leading to CR rates of 60-80% for adults younger than 60 years and only 40-60% for older patients.[9,13,30,31]

In addition, patients with specific biomarkers benefit from treatment options accompanying the “3+7” treatment. CD33+ AML, for example, may be treated with gemtuzumab ozogamizin (GO), a drug conjugated monoclonal antibody. Two independent studies suggest prolonged relapse free survival (RFS) in favorable risk CBF leukemia,[30,32,33] with a higher benefit in older patients.[34–37] FLT3 mutations are druggable by administration of midostaurin.[38–40] Recently, both FDA and EMA approved the smoothened (SMO) inhibitor Glasdegib as the first Hedgehog pathway inhibitor for treatment of adult AML patients who are not eligible for standard induction therapy, in combination with low dose Ara-C.[41,42]

1.3 CBF leukemia

1.3.1 Normal hematopoiesis and leukemic transformation

Hematopoiesis is the maturation process during which the cellular components of peripheral blood are produced. Those, mainly short-lived, cells are required for hemostasis, oxygen delivery, and protection against infections. Self-renewing hematopoietic stem cells (HSC) within the bone marrow give rise to immature progenitor cells which are differentiating into a series of increasingly lineage committed effector cells, influenced by the exposure to cytokines. The process needs to be tightly regulated to keep the large number of cells required in peripheral blood in balance.[43]

AML results from deranged hematopoietic development (**Figure 1**), starting as early as in HSCs, multipotent progenitors (MPP) or common myeloid progenitors (CMP).[44] In a multistep process, epigenetic and genetic alterations accumulate and transform a healthy cell into a leukemic cell with survival advantages, enhanced proliferation, and impaired differentiation. Dormant leukemic stem cells (LSC) may sustain self-renewing capacity or give rise to immature leukemic progenitor cells due to clonal hematopoiesis.[43,45,46] Those leukemic blasts proliferate in an uncontrolled manner, infiltrating peripheral blood and subsequently organs while ousting mature blood cells.[9]

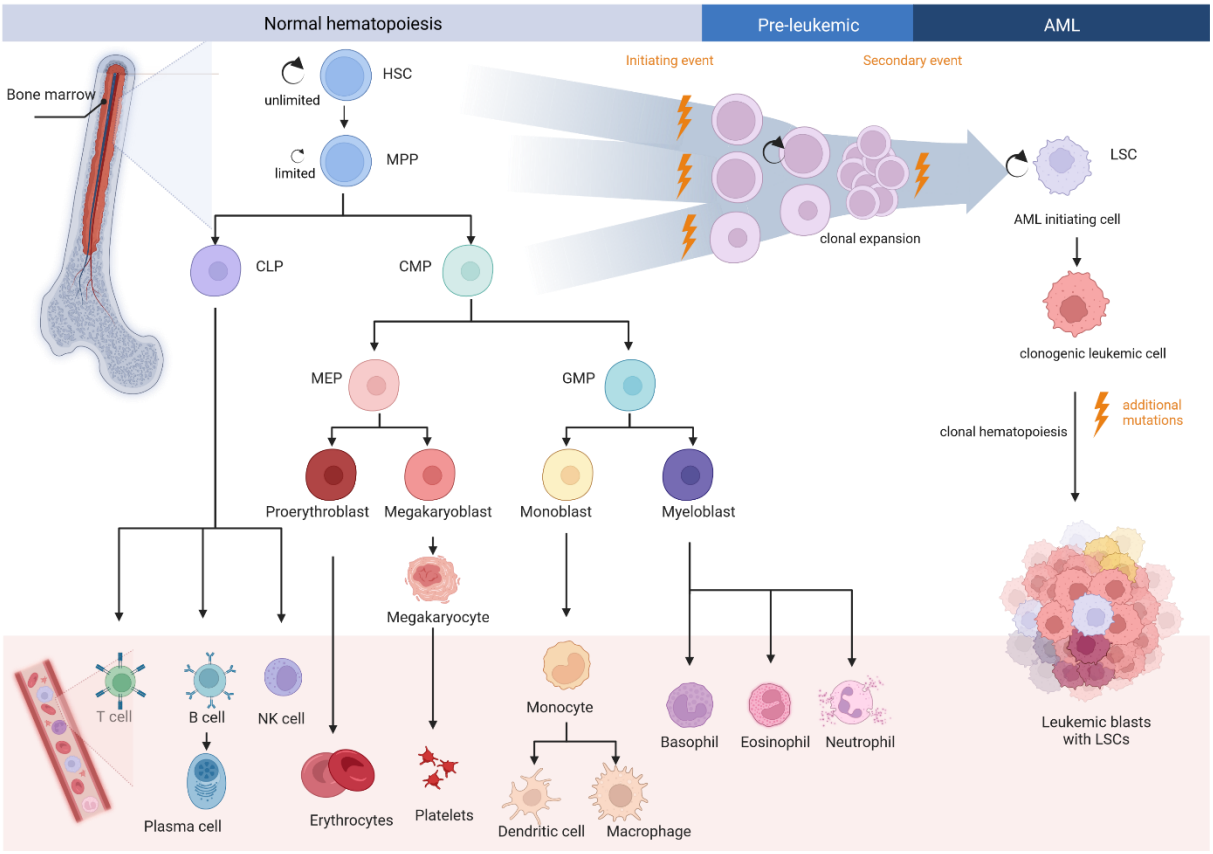

Figure 1: Schematic depiction of normal hematopoiesis versus leukemic transformation. During normal hematopoiesis, HSCs possess unlimited self-renewal potential. Differentiation occurs through a defined series of progenitor populations with restricted lineage potentials. Modified from Speck et al. (2002), Cozzio et al. (2003), Tan et al. (2006) and Chopra et al. (2019).[43–46]

1.3.2 Core-binding factor complex

In the 1970s Janet Rowley and colleagues discovered recurring cytogenetic aberrations in leukemic cells of patients. Using new chromosome banding techniques, they were able to identify the translocation of chromosomes 8 and 21 (t(8;21)) in acute myeloid leukemia[47] and t(15;17) in acute promyelocytic leukemia.[48] This pioneering work further led to the identification of genes disrupted by chromosomal breakpoints and therefore todays understanding of AML as a genetic disease.[18] The translocation that Rowley found in AML patients, t(8;21), targets runt-related transcription factor 1 (*RUNX1*), a distinct subunit of the core-binding factor (CBF) complex. The complex is formed by one DNA binding transcription factor subunit CBFα (RUNX1, RUNX2 or RUNX3) heterodimerized to the CBFβ subunit (CBFB) (**Figure 2 A**).[43,49] Depending on the biological context, selection of the CBFα subunit varies: While RUNX1

subdomain is inevitable for definitive hematopoiesis[50,51], RUNX2 is revealed to play an important role in osteoclast development[52,53]. RUNX3 has been found to be crucial in various ways, as it regulates blood cell development and function,[54–57] neurogenesis[58–60] and TGF-β signaling in gastric epithelium.[61–64]

Dimerization of RUNX1 and CBFβ leads to enhanced DNA binding capacity of RUNX1,[65,66] protection from proteolysis[67] and recruitment of several co-factors, finally resulting in target gene transcription (**Figure 2 b**).[43,68] Both RUNX1 and CBFB are key to HSC emergence and are essential in regulation of hematopoietic development.[50,51,69] Disruption of the complex leads to impaired differentiation and is, not surprisingly, a frequent target of genetic alterations. *RUNX1* is involved in t(8;21)(q22;q22), resulting in expression of the fusion protein RUNX1-RUNX1T1. Likewise, inv(16)(p13;q22) leads to *CBFB-MYH11* resulting in expression of the fusion transcript CBFβ-SMMHC. While both genetic rearrangements are linked to impaired hematologic differentiation, mode of action and associated phenotype are distinct.

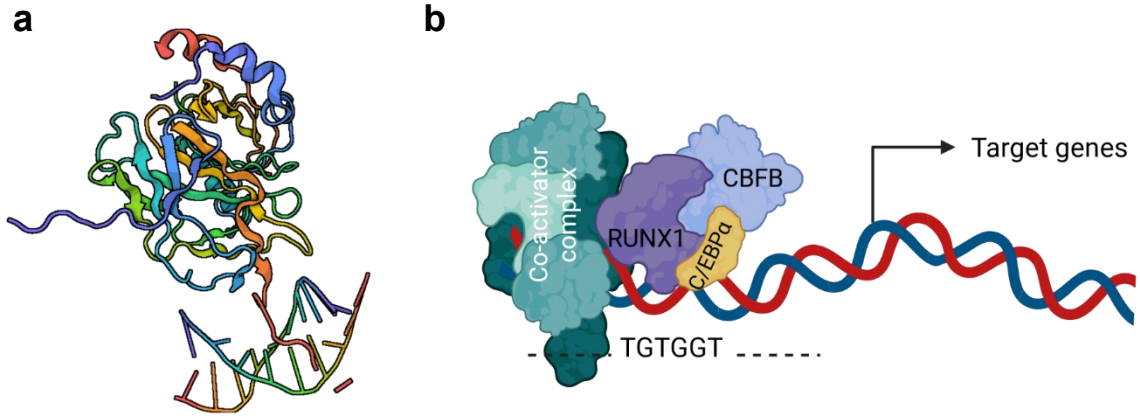

Figure 2: Core binding factor complex in normal hematopoiesis.
a) Protein structure of the core-binding factor (CBF) complex RUNX1-CBFβ bound to DNA. (PDB-ID: 1H9D) **b**) Schematic representation of CBF transcriptional activation complex. RUNX1 mediates DNA binding at the consensus sequence and heterodimerization with core-binding factor β (CBFβ) via its Runt domain, leading to recruitment of co-factors like C/EBPα and transcriptional activators, and consequential activation of target gene transcription. Modified from Beghini et al. (2019).[49]

1.3.3 Inversion of Chromosome 16

CBFB-SMMHC presents an additional RUNX1 binding site, increasing its binding affinity. Thus, CBFB-SMMHC sequesters RUNX1 away from sites of transcription onto actin filaments within the cytoplasm, thereby inhibiting RUNX1-mediated transcription activation in a dominant-negative manner (**Figure 3**)[70,71]. While this is true for expression of GATA2, KLF1 and others, resulting in blocked megakaryo- and erythropoiesis,[72] inv(16) is not only involved in impaired hematopoietic differentiation. The transcriptional activation of several distinct target genes is only triggered by formation of a new complex between CBFB-SMMHC and RUNX1 in concert with specific recruitment of histone deacetylases (HDAC) as well as several transcription co-activators.[49,73–75] Emerging evidence suggests that not only transcriptional repression,[76] but also altered expression activation is key for inv(16)-induced leukemogenesis.[43,49]

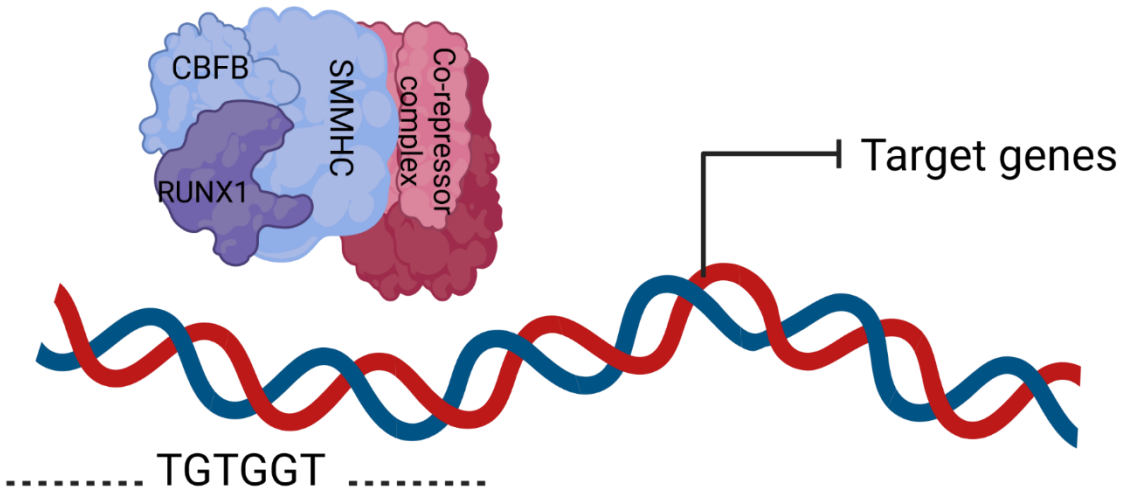

Figure 3: Core-binding factor complex with inv(16).
Schematic representation of core-binding factor complex with inv(16). Fusion of CBFB to SMMHC leads to abrogation of DNA binding at the consensus sequence via RUNX1. Consequently, target gene expression is inhibited. Modified from Lukasik et al. (2002), Huang et al. (2004), Yi et al. (2019) and Beghini et al. (2019).[49,70–72]

1.3.4 Translocation of Chromosomes 8 and 21

In contrast, leukemogenic effects of t(8;21) lie in the lack of transcription activation in combination with active repression of tumor-suppressor genes. Fusion of RUNX1T1 to RUNX1 physically disrupts the transactivation domain of RUNX1 while DNA binding remains intact (**Figure 4**). RUNX1-RUNX1T1 is still recruited to binding sites, exerting a dominant inhibitory effect on RUNX1, actively repressing RUNX1-dependent transcription[49,77]. PU.1 and CEBPα, important transcription activators interacting with RUNX1, are inactivated by RUNX1-RUNX1T1, blocking granulocytic maturation.[78,79] Nevertheless, interaction with wildtype RUNX1 seems to be inevitable for functionality of the fusion protein. In addition, RUNX1-RUNX1T1 holds capacity to actively recruit DNA methyltransferases (DNMTs) and transcriptional repressors to distinct promotor regions of tumor-suppressor genes, impairing gene expression and resulting in a unique DNA hypermethylation signature (**Figure 4**).[49,80–86] However, despite impairing granulopoiesis, RUNX1-RUNX1T1 has been reported to indirectly transactivate the promotor regions of both macrophage (CSF1R) and granulocytic (CSF3R) colony-stimulating factor receptors, further contributing to leukemogenesis.[43,87,88]

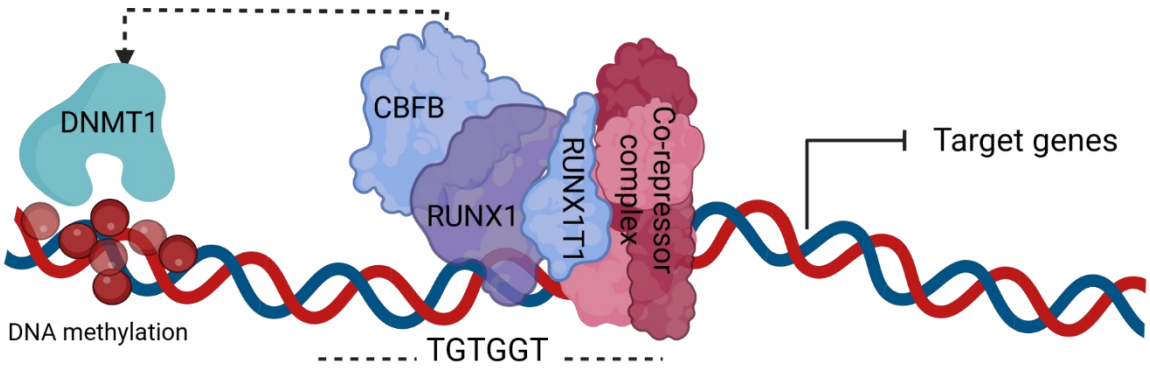

Figure 4: Core-binding factor complex with t(8;21).
Schematic representation of core-binding factor complex with t(8;21). Fusion of RUNX1 to RUNX1T1 inhibits target gene expression by recruitment repressor proteins. Furthermore, DNMT1 is recruited to distinct promotor regions of tumor-suppressor genes. Modified from Beghini et al. (2019).[49]

1.3.5 Secondary mutations

It is important to recognize that CBF mutations represent a necessary initiating event in the curse of leukemogenesis and have important clinical impact. Presence of inv(16) or t(8;21) represent distinct entities in AML with recurrent genetic alterations and lead to diagnosis of AML regardless of blast count.[13,16,19,28] Risk assessment by the ELN considers CBF leukemia as favourable in patients receiving high-dose AraC induction therapy.[25]

Nevertheless, CBF rearrangements are not sufficient for leukemic transformation, but rather provide fertile soil for secondary mutations.[89–93] Acquisition of differentiation modulators, like CBF rearrangements, are considered class II mutations and are necessary for priming cells to a pre-leukemic state with clonal expansion.[49,94,95] So-called class I mutations, perturbing cell cycle and proliferation, then cooperate with the initiating event and progress leukemogenesis.[43,92,96–102] The most frequent genetic alterations cooperating with CBF rearrangements are activating mutations in receptor tyrosine kinases (RTKs) or small GTPases.[90,103,104] Although t(8;21) and inv(16) lead to a similar phenotype involving the CBF-complex, they perturb distinct signaling pathways and therefor present different spectra of cooperative mutations (**Figure 5**).[95,105–107] Pre-leukemic clones positive for the t(8;21) associated RUNX1-RUNX1T1 were extremly cytokine dependent, suggesting that mutations leading to cytokine mediated survival and proliferation advantages might be crucial collaborators in leukemogenesis.[94,108–110] In line with that, Opatz et al. found that alterations in the gene encoding for the granulocytic cytokine receptor Colony Stimulating Factor 3 Receptor (*CSF3R*) as well as in cytokine transduction members as *JAK2*, *JAK3* and *TET2* were highly associated with RUNX1-RUNX1T1.[2]

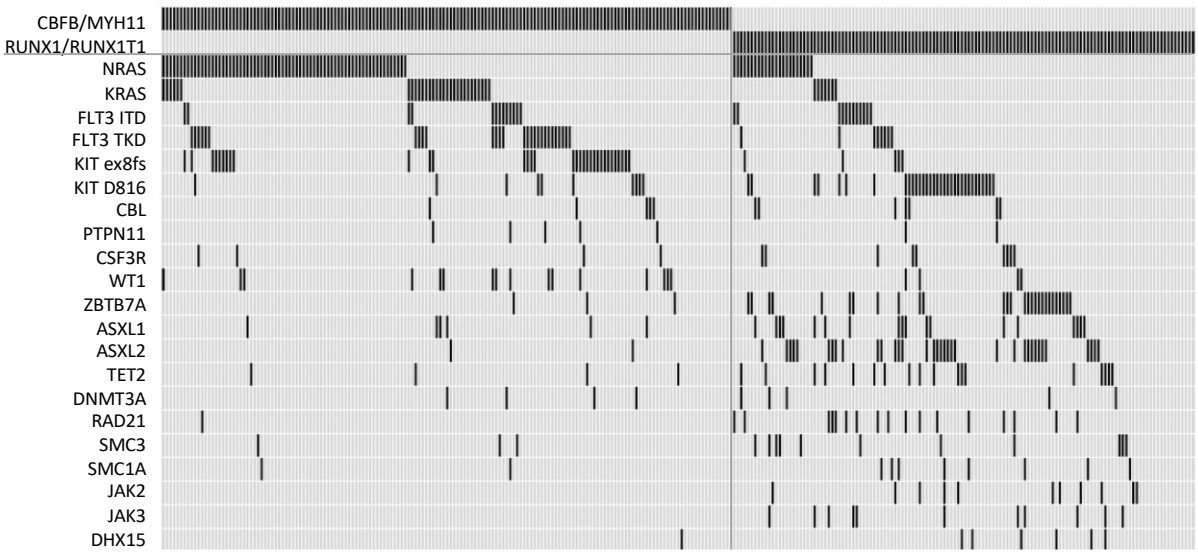

Figure 5: Secondary Mutations.
Amplicon sequencing of patients with either inv(16) or t(8;21). CBFB-SMMHC and RUNX1-RUNX1T1 fusion present distinct spectra of cooperating secondary mutations. (Black: positive; grey: negative.) Adapted from Opatz et al. (2020).[2]

1.4 Receptor of Granulocytic Colony stimulating factor 3 (CSF3R)

Cytokine receptors located on the cell surface are activated by binding to their cognate cytokine. Physical interaction between cytokine and receptor mediates transduction of a signaling cascade in response, allowing for targeted stimulation of the effector cell. During healthy human hematopoiesis, cytokines like macrophage colony-stimulating factor (M-GSF), macrophage-granulocyte colony-stimulating factor (GM-CSF) or granulocyte colony-stimulating factor (G-CSF) orchestrate differentiation throughout various stages of maturation. G-CSF receptor, also known as receptor of granulocytic colony-stimulating factor 3 (CSF3R), is mainly expressed on myeloid lineage cells, modulating proliferation, differentiation and survival.

1.4.1 Protein structure

Throughout this work, transcript RefSeq NM_000760.4 is used for nomenclature, including the 23 amino acid long N-terminal signal peptide.[111–113] CSF3R is a type I membrane protein and member of the cytokine receptor superfamily with a single-chained protein structure, expressed from a single gene encoded on chromosome 1p35-p34.3[114]. Molecular cloning revealed a protein structure consisting of 813 amino acids, including an extracellular domain from amino acids 24-627, a short transmembrane domain (amino acids 628-650) and an intracellular cytoplasmic domain ranging from amino acid 651-836.[115,116] The extracellular domain consists of one N-terminal immunoglobin-like (Ig-like) domain followed by five fibronectin type III (FN III) domains. Two FN III domains adjacent the Ig-like domain form the cytokine receptor homology (CRH) region, a domain characteristic for various hematopoietic growth factor receptors including receptors for GM-CSF, numerous interleukins and erythropoietin.[117–119] A conserved cluster of four cysteine residues as well as a W-S-X-W-S motif are shared structural features within the CRH domain, crucial for ligand binding and receptor activation (**Figure 6 a**).[115–117,120] Upon binding of G-CSF, the receptor homodimerizes through helix-helix interactions within the transmembrane domain [113,121] and allows downstream signaling, mediated by the cytoplasmic domain.[122]

Unlike M-CSFR, being a receptor tyrosine kinase, the cytoplasmic tail of CSF3R lacks intrinsic kinase activity. Signal transduction is mediated by three conserved Box motifs (boxes 1-3) (**Figure 6 a, b**) in concert with four tyrosine residues at amino acids 727, 752, 767 and 787 (**Figure 6 b**).[123–125] Boxes 1 and 2 are important regions for proliferation signaling, while Box 3 is essential for induction of myeloid differentiation[124,126] and cell survival.[127] The tyrosine residues, in turn, provide docking sites for important downstream effector proteins containing the Src homology 2 (SH2) domain, including suppressor of cytokine signaling (SOCS) 3, signal transducer and activator of transcription (STAT) 3, the adaptor proteins SH2-containing (Shc) and growth-factor receptor bound protein 2 (Grb2), as well as the SH2-containing protein tyrosine phosphatase 2 (Shp2) (**Figure 6 a**).[128] The major signaling pathways following CSF3R activation are JAK/STAT, PI3K/AKT and MAPK/ERK pathways.[115]

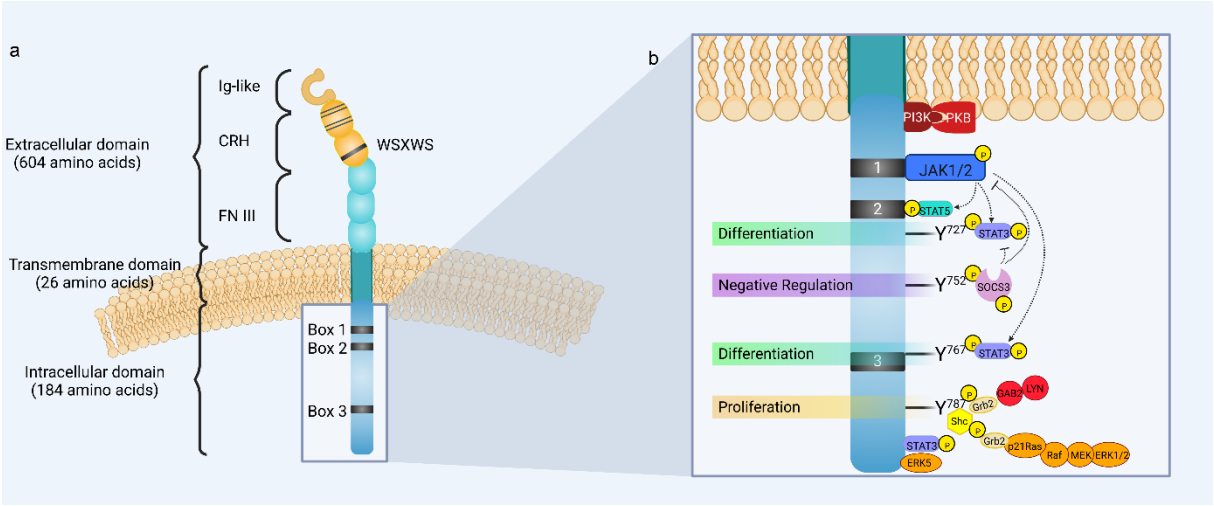

Figure 6: CSF3R protein structure and signaling.
a) Schematic representation of CSF3R monomer. The extracellular domain is comprised of one Ig-like domain, the CRH region containing four conserved cysteine residues (thin black lines) and the WSXWS-motif (thick black line), and three FN III repeats. A short transmembrane domain enables receptor dimerization. The intercellular domain consists of three important Box-motifs. **b**) Signaling mechanisms activated by dimerized wildtype CSF3R upon ligand binding. Four tyrosine residues provide docking sites for downstream signaling molecules (RefSeq NM_ 000760.4). Modified from Touw et al. (2007), Ward et al. (2007), Beekman et al. (2010), Touw et al. (2013), Palande et al. (2013) and Liongue et al. (2014).[113,120,121,128–130]

1.4.2 CSF3R-mediated signaling pathways.

1.4.2.1 JAK/STAT

Activation of CSF3R leads to conformational changes to recruit and stimulate multiple tyrosine kinases. One major signaling route follows activation of members of the Janus kinase (JAK) family, especially JAK1, JAK2 and Tyrosine kinase 2 (TYK2),[115,117,122,131,132] SRC family members like LYN[117,122,133–135] and HCK[136] as well as the spleen associated tyrosine kinase (SYK) and TNK.[112,134,135] While the mechanism of SRC activation is not fully understood yet,[115,134] JAK signaling has been studied in detail. Phosphorylation of JAK1 and JAK2 is facilitated by binding to CSF3R at the tryptophane residue 650 (**Figure 6 b**).[137] Activated JAK proteins then further bind the proximal cytoplasmic region. Tyrosine residues 727 and 767 provide docking sites for STAT3 in close proximity to activated JAK, which phosphorylates tyrosine residues of STAT3 and STAT5, as well as CSF3R itself. Of note, STAT5 phosphorylation is facilitated at a different binding site within the box 2 region of CSF3R and

does not necessarily require JAK activity[138]. Activated STAT proteins thus dimerize and translocated into the nucleus, where they transcriptionally activate their target genes.[122,130,131,134,135,138–140]

Activated STAT3 promotes differentiation in myeloid cells[120] and regulates CSF3R signaling in a negative feedback loop. Suppressor of cytokine signaling (SOCS) 3, recruited to Y752, binds, inhibits and marks both the activated G-CSF receptor[120,128] and JAK2 for degradation.[141,142] In contrast, STAT5 induces both proliferation and positively modulates cell survival.[115,138,139]

1.4.2.2 PI3K/AKT

Additional to JAK binding regions, CSF3R facilitates binding and stimulation of phosphatidylinositol 3-kinase (PI3K) at its proximal membrane region.[115,117] The mechanism of PI3K activation, however, remains unclear.[115] While there is evidence, that CSF3R mediated signaling through PI3K is at least partially independent of JAK signaling,[143] other studies suggest that the presence of LYN might be crucial for pathway activation.[120,133,144–147] Downstream signal transduction *via* the protein kinase B, also known as AKT serine/threonine kinase 1 (AKT) has a direct impact on proliferation and cellular quiescence,[113,115,122,128,135] as well as cell survival.[133]

1.4.2.3 MAPK/ERK

Phosphorylated tyrosine residue 764 serves as a docking site for the SH2 domains of the adaptor proteins Shc and Grb2. Binding of p21Ras activates the Ras/Raf/MAPK/ERK pathway in a cascade-like manner.[120,128] Activation of ERK1/2 MAP kinases in myeloid progenitor cells is mainly associated with proliferation, and the main downstream effector of p21Ras. Y787 of CSF3R also activates signaling through Jun N-terminal kinase (JKN) and p38MAP kinase downstream of p21Ras. The role of these kinases in response to G-CSF, however, is not fully understood yet.[120]

In contrast, activation of ERK5 following CSF3R activation seems to be independent of receptor tyrosine phosphorylation but is rather facilitated by binding to its C-terminus.

Activation of ERK5 is dependent on the cellular context, as it is strongly activated in neuronal cells stimulated by G-CSF, promoting neuronal survival.[120]

1.4.3 Biologic effects

Initially, granulocytic colony-stimulating factor (G-CSF) was described as a hematopoietic growth factor stimulating neutrophil precursors into proliferation and maturation. Soon it became evident, that G-CSF plays an important role during various stages of hematopoiesis, with the receptor of granulocytic colony stimulating factor 3 (CSF3R), being expressed on hematopoietic cells as immature as multipotent HSCs and as mature as megakaryocytes, neutrophils and monocytes, as well as B- and T-cells. CSF3R is also found on non-hematopoietic cells like neuronal progenitors, vascular endothelial cells, cardiomyocytes, as well as various fetal tissues. The effect on non-myeloid cells, however, is not yet fully clear. Leukemic cells of both lymphatic and myeloid lineage are also frequent expressors of CSF3R. Within the myeloid lineage, receptor surface expression increases with maturation. With 50-500 receptors per cell, mature neutrophils show the highest surface expression of CSF3R.[114] While maintenance of steady state neutrophil numbers due to induction of maturation, proliferation and survival is a crucial task of G-CSF induced CSF3R signaling, it also plays a pivotal role in emergency granulopoiesis.[120,148–153]

Physiologic exposure to G-CSF during bacterial infections, but not viral or fungal infections,[151,152,154,155] mobilizes immature cells from the bone marrow and exhausts them into peripheral blood (PB).[114,156] In parallel, also effector functions of neutrophils, such as phagocytosis and bactericidal degranulation are activated.[157] At the same time, serum levels of G-CSF are elevated 10-30 times from 25 pm/mL – 78 pg/mL[150,153,158] in healthy subjects, to more than 700 pg/mL during acute infections or chronic inflammatory diseases[150,151,153] and close to 3000 pg/mL in patients with septic shock.[159] Production of G-CSF by bone marrow stromal cells, macrophages, fibroblasts and endothelial cells is mainly induced by pro-inflammatory mediators and transcription factors.

In addition to inflammatory functions in neutrophils, CSF3R signaling has cell context dependent effects on other hematopoietic cells. In response to CSF3R activation, proliferation and mobilization of PB monocytes is induced.[114,160] Studies following exogeneous G-CSF administration, however, suggest an immune-suppressive role of CSF3R in monocytes.[160] Following G-CSF dependent expansion, monocytes showed suppressed proinflammatory cytokine production as well as increased production of the anti-inflammatory cytokine IL-10. In a feedback loop, IL-10 binds, among others, to immature monocytes, where signaling, in turn, requires activated STAT3.[161,162] In a similar manner, G-CSF induces the mobilization of tolerant dendritic cells (DCs), deriving from bone marrow. Those type 2 DCs induce the expression of anti-inflammatory cytokines IL-4 and IL-10, while reducing IFNγ production in lymphocytes, thus inhibiting T-cell activation.[156,160,163,164]

These effects can be used therapeutically as well, as G-CSF injection of patients undergoing chemotherapy or suffering from severe congenital neutropenia (SCN) can correct an underlying neutropenia and prevent infection-related mortality.[113,165] Furthermore, G-CSF administration to healthy subjects leads to mobilization of peripheral blood progenitor cells (PBPC). Donation of those cells allows for allogeneic PBPC transplantation.[114,166,167] A major concern, however, is the risk of progression from SCN to AML under G-CSF treatment. While the underlying role of G-CSF administration in disease progression remains unclear and could be due to increased survival rates,[114] development of AML in SCN patients is correlated with a gain of mutations in *CSF3R*.[113,115,121]

1.4.4 Mutations of CSF3R in disease

The first mutations found in *CSF3R* were discovered in SCN patients receiving G-CSF treatment.[113] Depending on the localization of *CSF3R* variants (**Figure 7**), they can cause varying biological and clinical consequences primarily affecting the myeloid lineage.[130]

1.4.4.1 Extracellular mutations

Variants within the extracellular domain are extremely rare as they are only described in distinct case reports of one patient suffering from chronic idiopathic neutropenia (CIN) and a small

number of SCN patients.[120,130,168] Those variants result in expression of a “crippled” receptor, that is not only defective, but also exerts a dominant negative effect on the co-expressed wildtype form of CSF3R.[130] The most prominent of these mutations, P229H, disrupts a proline rich hinge within the CRH domain, essential for ligand binding.[169] Other mutations within this class lead to frame shifts within the open reading frame, consequently resulting in premature stop codons within the WSXWS motif. Those truncated receptors were found to constitutively heterodimerize with wildtype receptor, negatively affecting its trafficking and signaling.[170,171] The CIN patient presented a variant truncating the receptor after the FN III-type domains, leading to abrogation of receptor signaling in response to G-CSF.[172]

1.4.4.2 Transmembrane mutations

The *CSF3R* mutation T618I was initially described in one SCN patient progressing to AML.[111] Subsequently, however, it has been identified as one of the most common *CSF3R* mutations in CNL[112,173], as well as, less commonly, atypical CML, *de novo* AML[112] and chronic myelomonocytic leukemia (CMML).[174] N579Y, identified in AML and CNL patients,[2,175] has only recently been shown to mimic the activating phenotype of T618I.[175] Another mutation localized at threonine 615 (T615A) was found in both CNL and aCML patients,[112] while the variants T640N and the alternative T640I have been identified as rare somatic mutations in AML patients.[176–178] Interestingly, germline T640N mutations have been found to be an underlying cause for hereditary neutrophilia, capable of progressing to a myelodysplastic syndrome (MDS).[179]

CSF3R mutations affecting the transmembrane domain and adjacent domains stabilize helix-helix interactions of neighboring receptor monomers even in absence of G-CSF, thereby creating a constitutively activated dimeric receptor configuration.[178] Experimental data retained from Ba/F3 cells, human CD34+ hematopoietic stem and progenitor cells (HSPCs) suggests ligand independent proliferation and constitutive signaling *via* the JAK/STAT and MAPK pathways.[112,175,178,179] Markedly, activating transmembrane domain mutations in core binding factor AML are associated with t(8;21), but not inv(16) (**Figure 7**).[2]

1.4.4.3 Intracellular truncation mutations

Missense and nonsense mutations within the intracellular domain, truncating approximately 100 amino acids from the cytoplasmic domain of the receptor are by far the most frequent and best studied *CSF3R* mutations in SCN patients[180,181] and are highly associated with progression to MDS and AML.[182] Similar mutations affecting the c-terminal domain have also been described in CNL and aCML[112] as well as in inv(16) positive AML (**Figure 7**).[2] Truncated receptors lack 2 to 3 tyrosine residues as well as important internalization motifs located between amino acids 772-778 and 779-792,[183–185] leading to impaired receptor endocytosis, surface overexpression and hyperproliferative response to G-CSF stimulation in myeloid progenitor cells.[130,135,186] Negative receptor regulation is severely blunted by the loss of critical recruitment sites for receptor associated tyrosine phosphatases, members of the SOCS family,[187,188] as well as STAT3, leading to diminished *SOCS3* transcription.[189] Shifted balance between STAT3 and STAT5 activation may increase proliferative advantages and clonal expansion in HSPCs.[113,130,135,190,191] In addition, activation of truncated CSF3R is associated with excessive production of reactive oxygen species (ROS), further increasing genotoxic stress and contributing to leukemogenesis.[133] Recently, it has been shown, that truncating mutations distal of amino acid 793 might also harbor oncogenic potential due to decreased receptor degradation.[183] Of note, truncating mutations of CSF3R are not leukemogenic itself, but rather co-operate with other mutations to further induce hematologic malignancies. In CNL, truncating mutations are often found alongside activating point mutations,[192] while in pediatric AML they were detected mutually exclusive.[193]

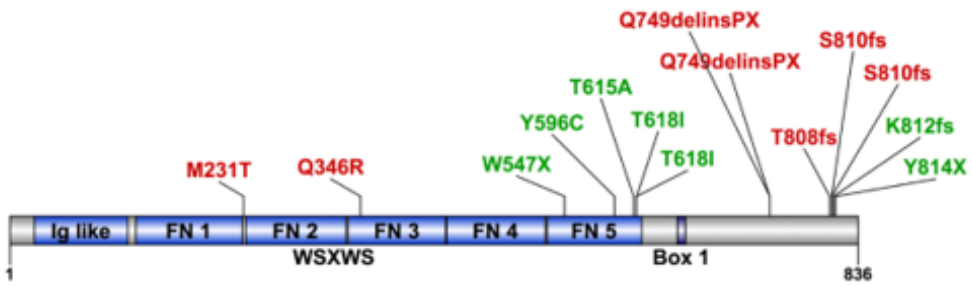

Figure 7: Graphic depiction of recurrent mutations in CSF3R.
Red: CBFB-SMMHC rearranged samples; Green: RUNX1-RUNX1T1 rearranged samples. Adapted from Opatz et al.[2]

1.5 Objective of the thesis

Translocation of chromosomes 8 and 21 is regarded as an initiating event of leukemogenesis, leading to clonal expansion and disturbed differentiation. Therefore, immature cells are primed in a pre-leukemic state that provide fertile soil for secondary mutations. Those so-called class II mutations recurrently cooperate with class I mutations, providing survival and proliferation advantages. Mutations in the *CSF3R* gene are extremely rare in de novo AML, where they are highly associated with CBF leukemia.[1,2] Among CBF-rearranged patients, the activating *CSF3R* mutation T618I is almost exclusively found in the t(8;21) background, suggesting a very specific cooperation. This study is based on the suspicion that *CSF3R* T618I represents a classical class I mutation, but further hypothesizes that the biological relevance in the context of t(8;21) CBF-leukemia might go beyond increased proliferation. To gain deeper insight, a model system mimicking the onset of leukemic transformation in primary cells from healthy donors (**Figure 8**) is used in this study. Wherever applicable, results are verified using a cell line model. The main objective of this thesis is the characterization of cells expressing CSF3R T618I in combination with RUNX1-RUNX1T1tr on a cellular and molecular level and consequentially compare to cells with forced expression of RUNX1-RUNX1T1tr alone. Understanding the molecular mechanisms facilitating malignant transformation caused by this unique cooperation is key to reveal therapeutically exploitable targets. Ultimately, the experimental work for this thesis is intended to investigate druggable targets in support of patients that might not benefit from standard therapy alone.

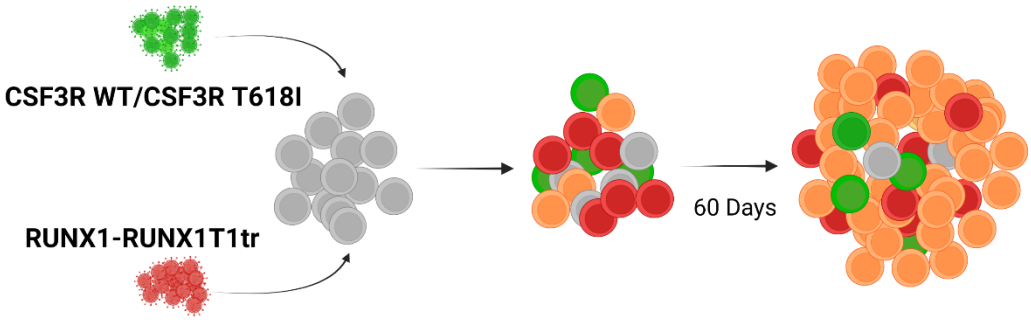

Figure 8: Schematic outline of the experimental setup.
HSPCs were virally transduced with CSF3R WT or T618I (GFP) and RUNX1-RUNX1T1tr (dtTomato). Competitive growth was assessed by flow cytometry every 2-3 days over a period of 60 days. Previously published (Swoboda et al.)[194,195].

2 Results

2.1 CSF3R T618I confers a clonal advantage to RUNX1-RUNX1T1 expressing progenitors.

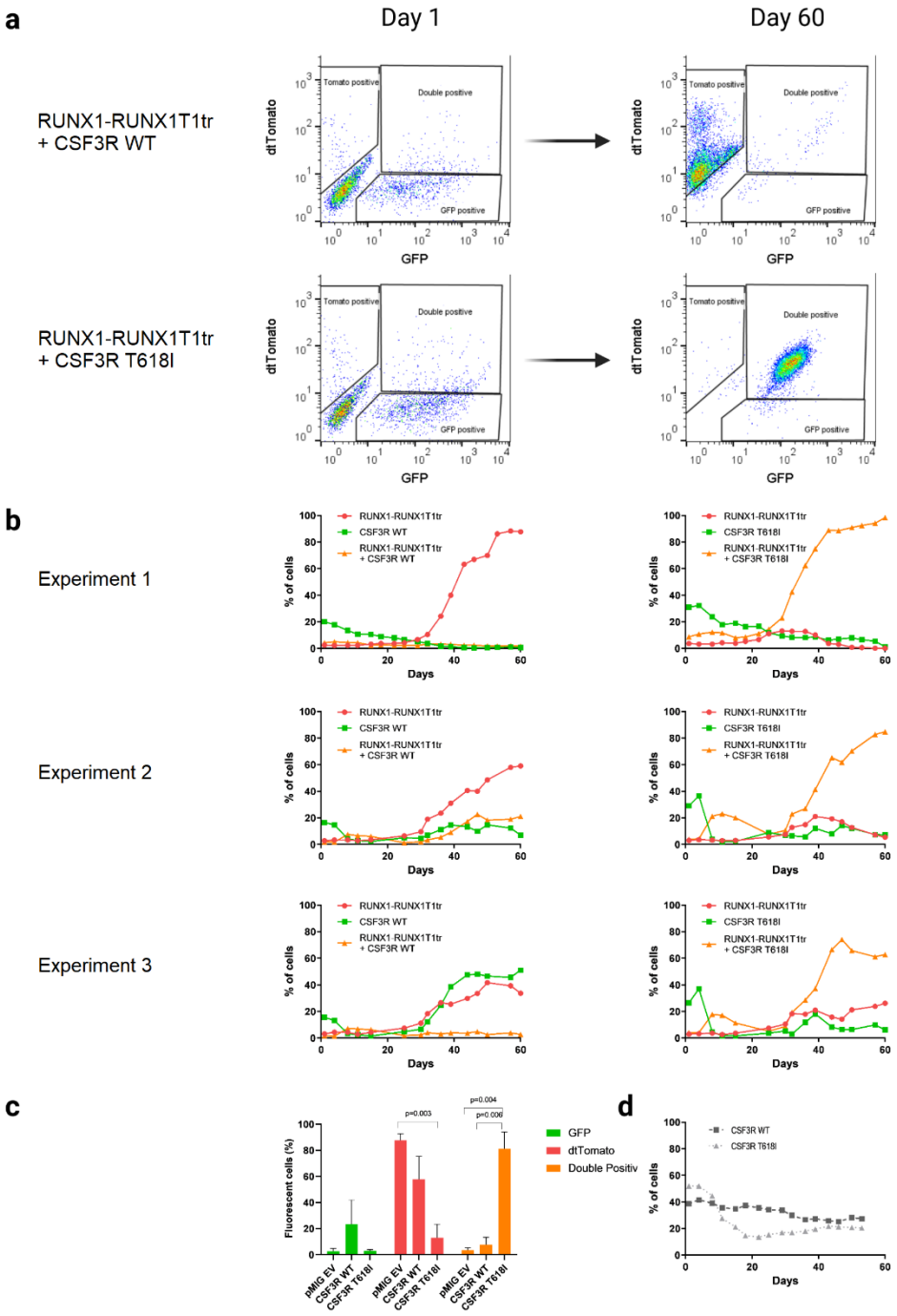

Figure 9: CSF3R T618I collaborates with RUNX1-RUNX1T1tr to expand HSPCs.
a) Flow cytometry gating strategy. Representative measurements on day 1 and day 60 of experiment 1 are displayed. **b**) Flow cytometry measurements of three independent experiments. The read out assessed was expansion of GFP-dtTomato double positive cells **c**) Summary of three independent experiments on the endpoint of expansion. Error bars represent ± standard error of the mean. **d**) Viral transduction of HSPCs with CSF3R WT or CSF3R T618I only, assessed by flow cytometry. Previously published.[194,195]

Expression of a truncated form of the t(8;21) related RUNX1-RUNX1T1 (RUNX1-RUNX1T1tr) fusion was confirmed sufficient to expand hematopoietic progenitor cells. In a mixed population, co-expression of the CSF3R mutant T618I (CSF3R T618I) but not CSF3R wildtype (WT) reproducibly led to competitive outgrowth of cells (**Figure 9 a, b, c**)[194,195]. In contrast, over-expression of either CSF3R WT or CSF3R T618I alone did not lead to considerable cell expansion (**Figure 9 d**).[194,195] HPSCs ectopically expressing CSF3R WT or mutant only started to differentiate concordant with unsuccessfully transduced cells and lost their proliferative potential therein. Due to decreasing cell numbers, withing 50 days neither culture was sufficient for flow cytometry (Data not shown).

2.2 CSF3R T618I induces an immunophenotype resembling acute myelomonocytic leukemia.

After *ex vivo* expansion and outgrowth, surface marker expression patterns were analyzed using flow cytometry. CD34, a marker of immature cells, was detected on a small fraction of RUNX1-RUNX1T1tr single positive cells, with the majority of cells expressing myeloid markers[195], consistent with previous reports.[94,109,196] CSF3R T618I co-expressing cells were entirely negative for CD34, but highly positive for the pan-myeloid marker CD13 and the monocytic marker CD14. In addition, double positive cells expressed HLA-DR, CD11b, CD11c, CD33, CD18 and partly CD49a (**Figure 10 a**)[195]. In patients suffering from acute myelomonocytic leukemia (AMML), monocytic cells, including monoblasts and promonocytes show a resembling surface marker pattern.[197–199]

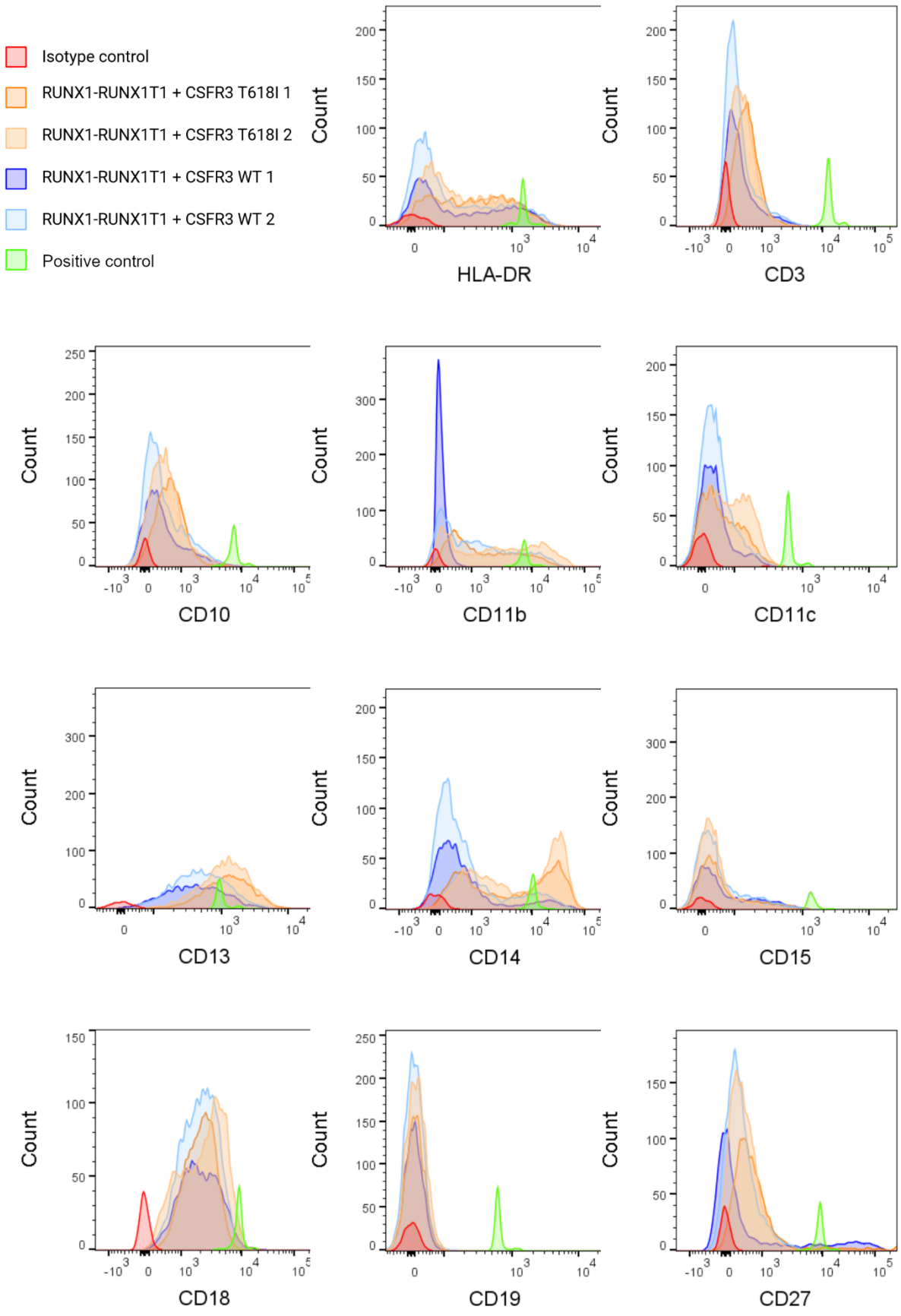
Isotype control
RUNX1-RUNX1T1 + CSFR3 T618I 1
RUNX1-RUNX1T1 + CSFR3 T618I 2
RUNX1-RUNX1T1 + CSFR3 WT 1
RUNX1-RUNX1T1 + CSFR3 WT 2
Positive control
Count
HLA-DR
CD3
CD10
CD11b
CD11c
CD13
CD14
CD15
CD18
CD19
CD27

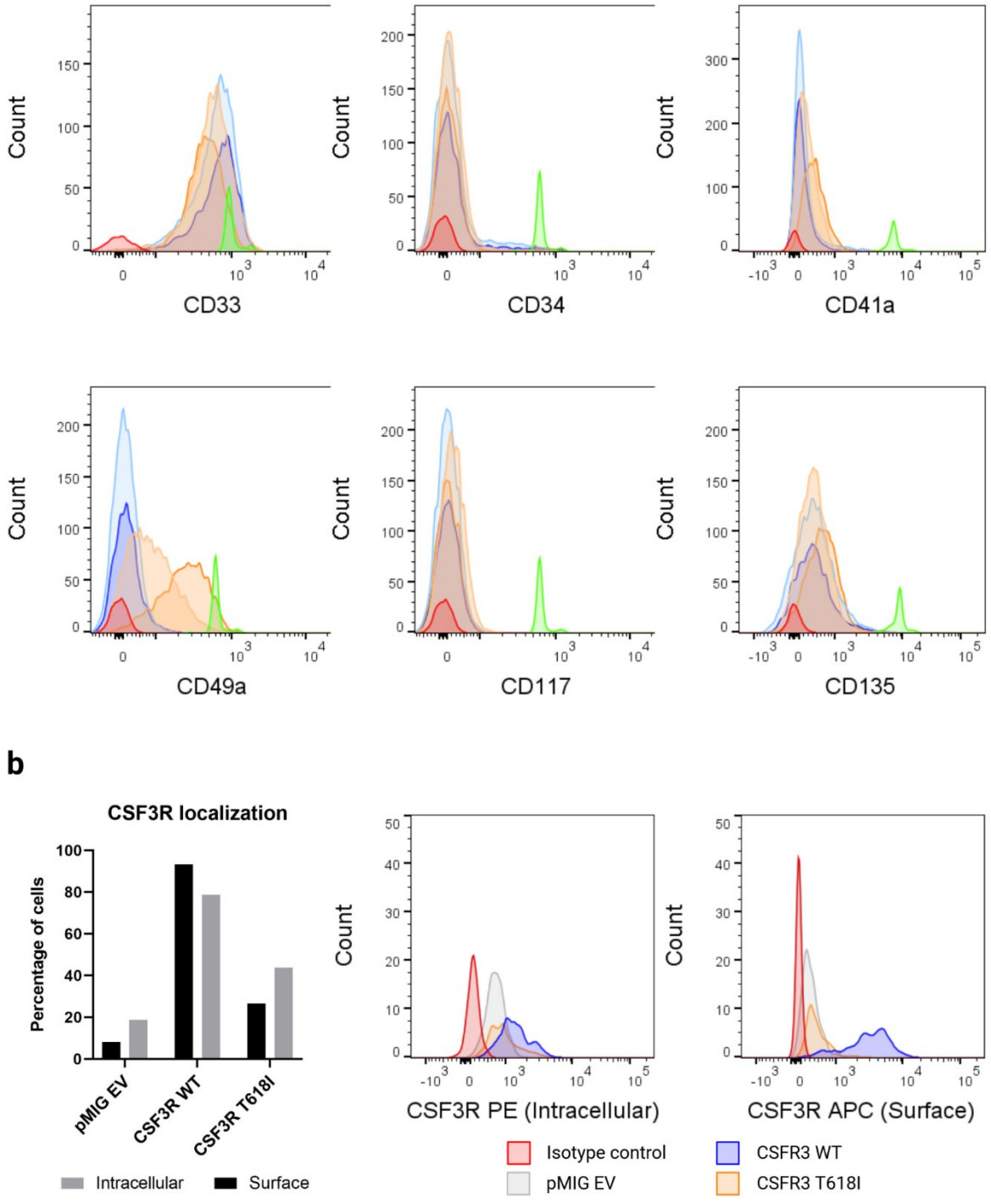

Figure 10: CSF3R T618I induces an immunophenotype resembling acute myelomonocytic leukemia.
a) Flow cytometry panel staining of two representative, independent experiments on day 60 of expansion (double transduced human HSPCs). **b**) CSF3R localization assessed by flow cytometry in SKNO-1 cells. The bar plot summarizes the CSF3R quantification on the right panels. Previously published.[195]

In healthy cells, activation of the receptor is induced by binding to its ligand, G-CSF. Subsequently, two receptor protein homo-dimerize and are internalized by the cell. Therefore, localization of CSF3R on the cell surface and intracellular were tested. To this end, the patient derived cell line SKNO-1, harboring the translocation t(8;21), was stably transduced with the empty control vector pMIG (EV), CSF3R WT or CSF3R T618I. Sorted cells overexpressing CSF3R WT showed a higher abundance of receptor on the surface than intracellularly, while mutated CSF3R localized predominantly intracellularly, hinting towards an activated state of the mutated receptor. Nonetheless, the ratio of surface to intracellular localization resembled endogenous CSF3R expression (**Figure 10 b**).[194]

2.3 CSF3R T618I leads to increased self-renewal and blast morphology.

Serial and limiting dilution assays allow for an estimation and direct comparison of cell frequency capable of proliferation and asymmetric division over time. Increased proliferation frequency and self-renewal potential are central in leukemogenesis. Seeding $1x10^3$ and $5x10^3$ of RUNX1-RUNX1T1tr single positive, fully expanded HSP cells did not result in measurable proliferation after 7 or 11 days, whereas seeding of $1x10^4$ cells resulted in an increase of cell number by 50% after 11 days. Analysis of double oncogene expressing cells 11 days post seeding revealed an average increase of cell number by 15-30-fold (**Figure 11 a**).[195] Serial dilution to $1x10^5$ cells showed highly increased proliferation potential in double oncogene expressing cells as compared to RUNX1-RUNX1T1tr single positive cells (**Figure 11 b**).[195] Furthermore, single positive cells could not successfully repopulate the culture after five rounds of dilution, while double positive cells showed high self-renewal potential over the course of 40 days.

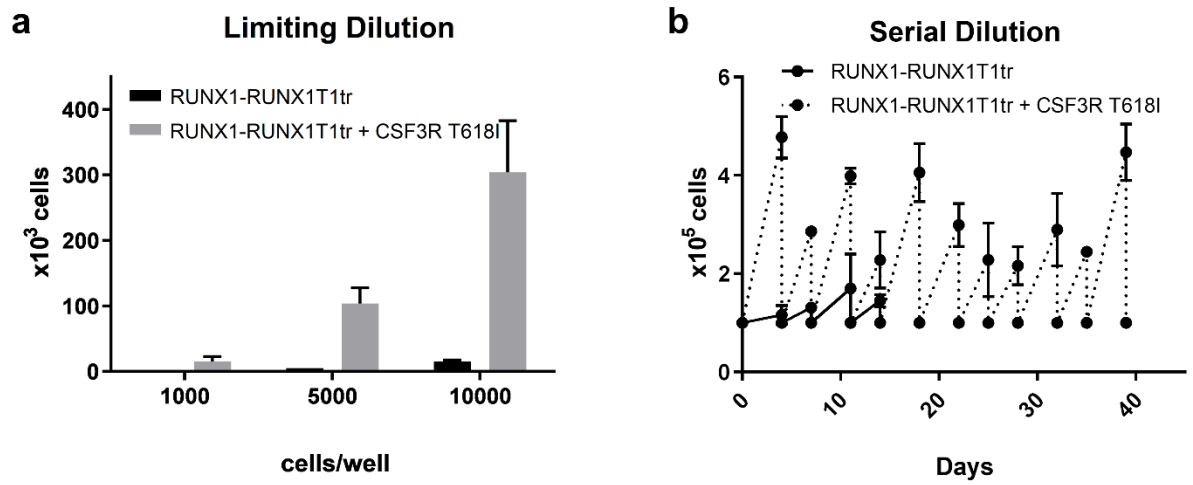

Figure 11: CSF3R T618I leads to increased self-renewal.
a) Limiting dilution assay: indicated cell numbers of transduced hCD34+ cells were seeded after expansion. Cell number was assessed 11 days post seeding. **b**) Serial dilution: 1x10^5 transduced hCD34+ cells were seeded after expansion. Cells were counted every 2-3 days and re-seeded at initial cell number (right). Error bars represent ± standard error of the mean. Previously published.[195]

Subsequently, primary HSPCs were transduced with RUNX1-RUNX1T1tr alone to simulate the sequential acquisition of genetic lesions leading to malignant transformation. Thereby, the cells clonally expanded, resulting in a culture composed of >95% fluorescence-marker positive cells. In a further step, a second hit was introduced by retroviral super-infection with CSF3R T618I (**Figure 12 a**).[195] This led to complete outgrowth of double positive cells over a period of another 60 days (**Figure 12 b**).[195] Cytomorphology of RUNX1-RUNX1T1tr single positive cells showed a heterogeneous mixture of mature and immature cells in RUNX1-RUNX1T1tr only expressing cells, whereas double positive cells remained mostly undifferentiated, featuring a homogeneous blast-like morphology (**Figure 12 c**).[195]

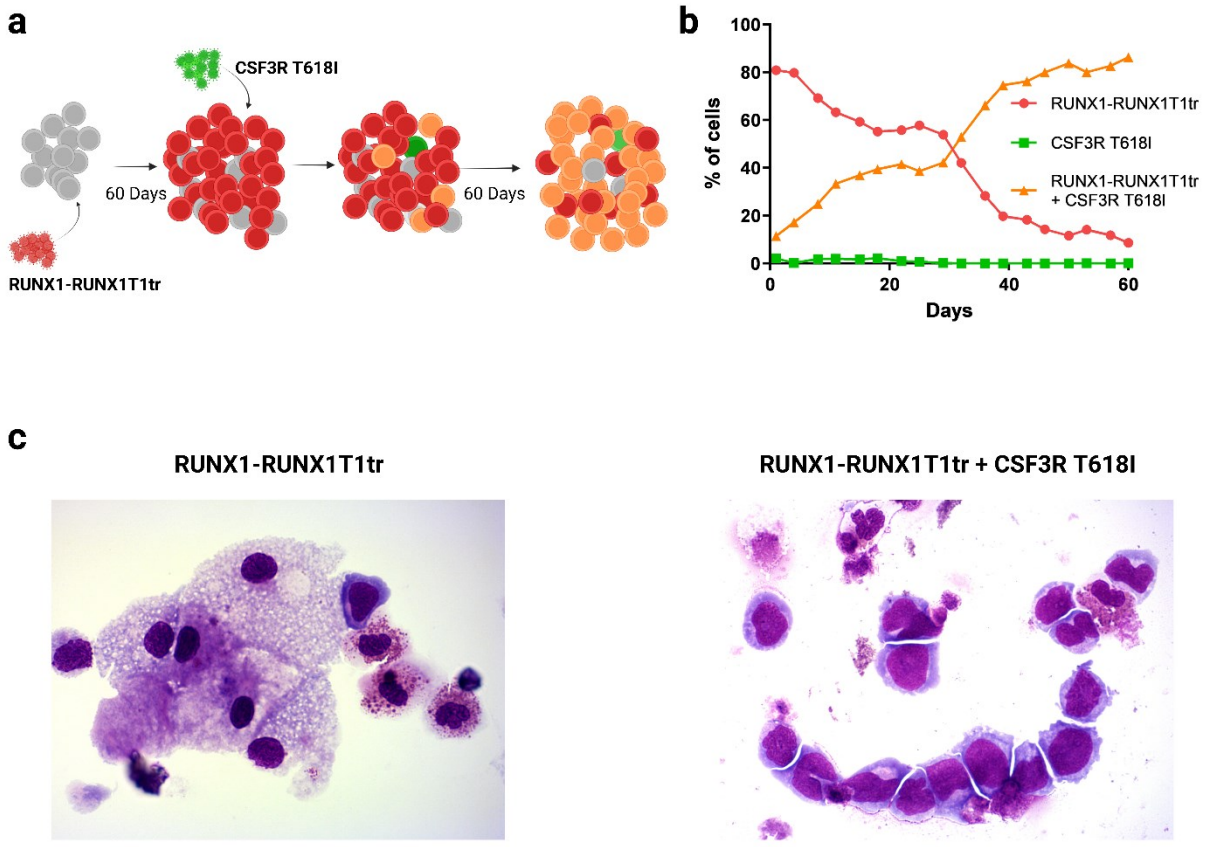

Figure 12: Forced expression of CSF3R T618I in a RUNX1-RUNX1T1tr background provides a competitive advantage and induces blast morphology.
a) Schematic outline of the experimental setup. hCD34+ cells were virally transduced with RUNX1-RUNX1T1tr and expanded over the period of 60 days. Expansion of dtTomato-positive cells was assessed every 2-3 days by flow cytometry. Post expansion, hCD34+ cells were superinfected with CSF3R WT or T618I. Competitive growth was assessed by flow cytometry every 2-3 days over a period of another 60 days. **b**) Flow cytometry measurement of one representative competitive growth assay after superinfection. **c**) Morphological analyses of cytospin/Giemsa preparations of hCD34+ cells 60 days post superinfection. Published previously.[195]

2.4 Double oncogene expressing progenitor cells do not engraft in non-irradiated NSG mice.

Additionally, the leukemic potential of CSF3R T618I in combination with RUNX1-RUNX1T1tr was tested in a murine NSG model. Per experimental arm, five mice (11 weeks old, female, not irradiated) were injected with HSPCs co-transduced with RUNX1-RUNX1T1tr and either wildtype or mutated CSF3R. The cells were expanded to <60% double or single positive cells prior to injection. The persistence of introduced cells was tracked in peripheral blood by measurement of CD34, CD45 and both fluorescence markers GFP and dtTomato. Although 6 months post injection, one mouse in the CSF3R WT group got sick and had to be sacrificed, no human cells were detectable in peripheral blood or bone marrow. The remaining mice were sacrificed 9 months post injection, since no human markers were evident in peripheral blood of both test groups (Data not shown). Subsequent bone marrow analysis revealed no engraftment of human cells in any mouse (**Figure 13**). Further tests with irradiated mice are inevitable to explore the leukemogenic behavior in *vivo*.

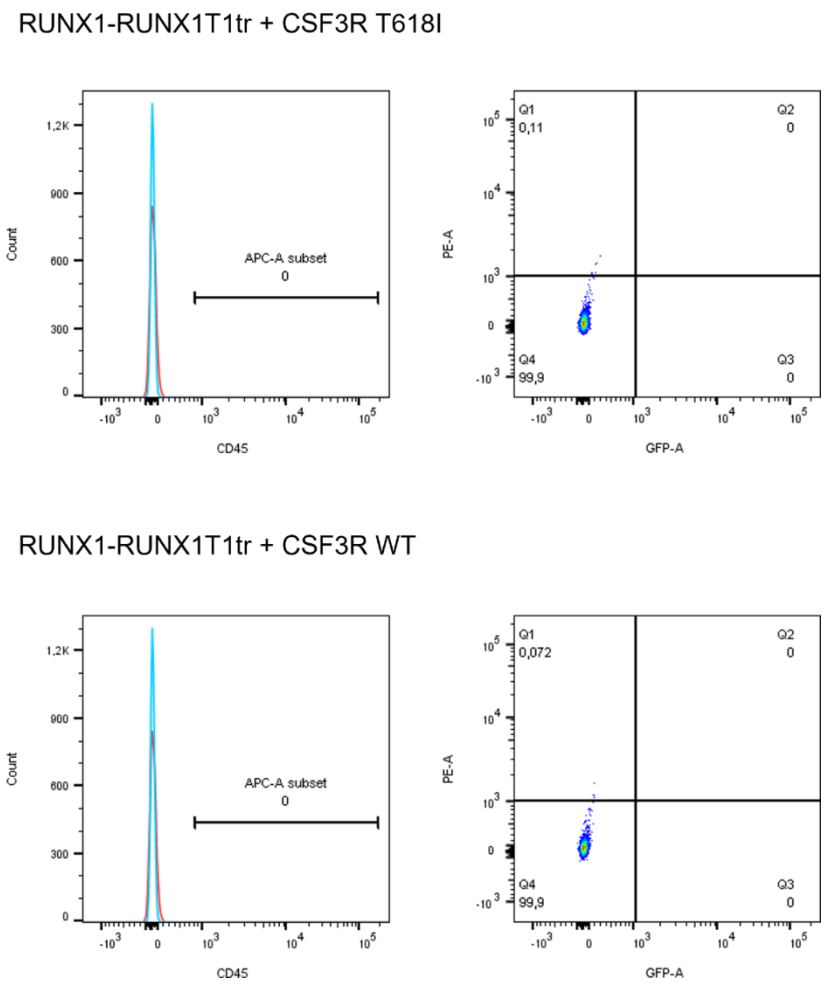

Figure 13: Bone marrow analysis.
Flow cytometry analysis of Mouse bone marrow. Bone marrow samples of one representative mouse per experimental arm are displayed. The samples were gated for CD45 staining (left) as well as GFP and dtTomato expression (PE-Channel) (right).

2.5 CSF3R T618I and RUNX1-RUNX1T1 synergistically alter specific pathways.

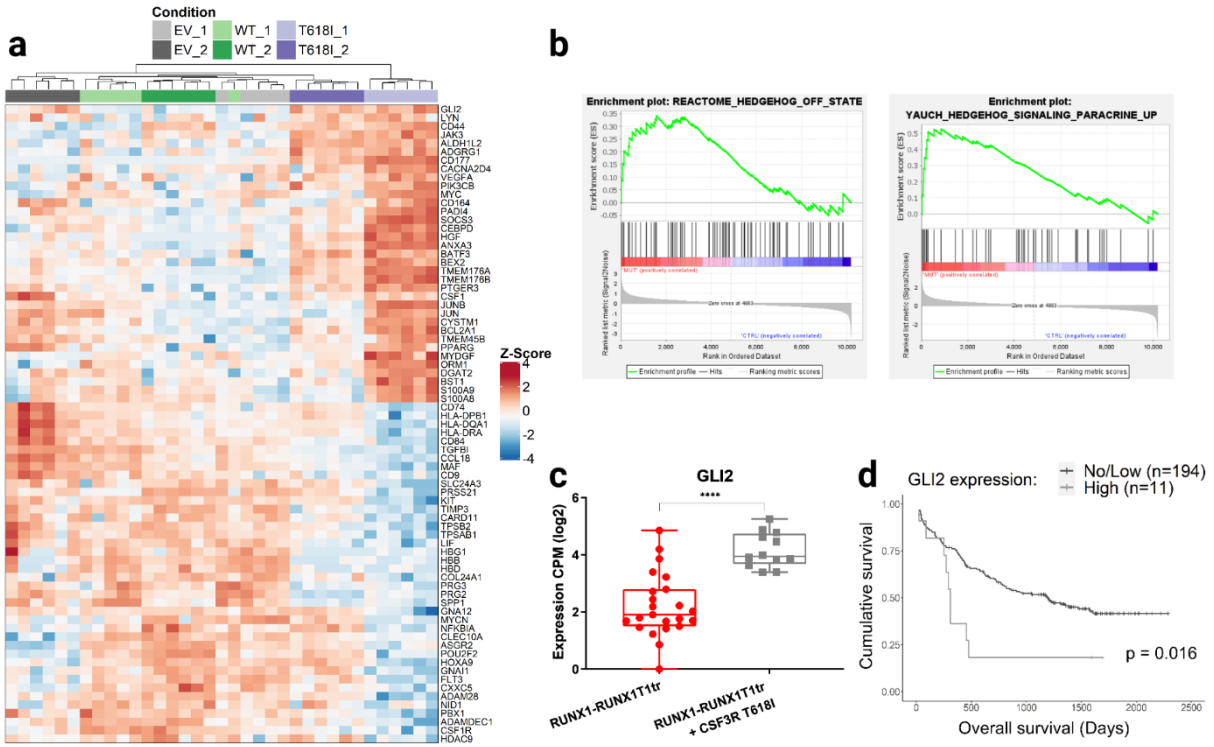

Figure 14: CSF3R T618I induces differential gene expression.
a) Heat map of significantly (p<0.05) deregulated genes in hCD34+ cells after 60 days of competitive outgrowth with RUNX1-RUNX1T1tr and CSF3R T618I compared to co-transduction of vector control (EV) or CSF3R WT. Data was obtained after performance of bulk RNAseq (SCRB-Seq) analysis. (n=2 independent transductions per construct; n=6 replicates per transduction). **b**) Gene set enrichment analysis (GSEA) of RNAseq data shows enrichment of hedgehog signaling genes in CSF3R T618I expressing cells. **c)** GLI2 expression as obtained from RNA-seq. Replicates of outgrown RUNX1-RUNX1T1tr populations (in red) resulting from double transduction with CSF3R WT (n= 12) and pMIG EV (n=11) were pooled together for this analysis, as they behave similarly in the growth competition assay. Differential expression analysis was performed with edgeR/limma package (**** p < 0.0001). **d)** Overall survival (OS) according to GLI2 expression of patients enrolled in the AMLCG-2008 study cohort (GSE106291). High expression was considered n(Transcripts)>=1; Low/No expression was considered n(Transcripts)<1. Published previously.[195]

In a next step, the molecular events leading to cooperative expansion of HSPCs were analyzed. Bulk RNA sequencing was performed on single and double oncogene expressing primary HSPCs (day 60; n=6). Expression of CSF3R T618I initiated the significant deregulation of 626 genes (**Figure 14**, **Supplementary Table 1**). Interestingly, CSF3R T618I expression resulted in significant enrichment of the Hedgehog signaling pathway (**Figure 14 b**), its downstream actor *Glioma-Associated Oncogene Family Zinc Finger 2* (*GLI2)* was one of the highest upregulated genes (**Figure 14 a, c**).[195] In Accordance with previous reports[200], patient samples of the AMLCG-2008 trial (GSE106291) presented shorter overall survival (**Figure 14 d**). Moreover, upregulation of *GLI2* in patients harboring *FLT3*-ITD was confirmed using gene expression data from the Beat AML cohort. AML patients with *CSF3R* mutations in the same cohort showed elevated levels of *GLI2* expression, comparable to *FLT3*-ITD positive samples (**Figure 15 a, Supplementary Table 2**). Deciphering the genomic localization of lesions in the *CSF3R* gene reveals a clear association of elevated *GLI2* expression with certain variants, but not others (**Figure 16**, **Figure 15 b, Supplementary Table 2**).[195] This further consolidates *GLI2* upregulation as a direct effect of activating CSF3R mutations in concert with translocation t(8;21).

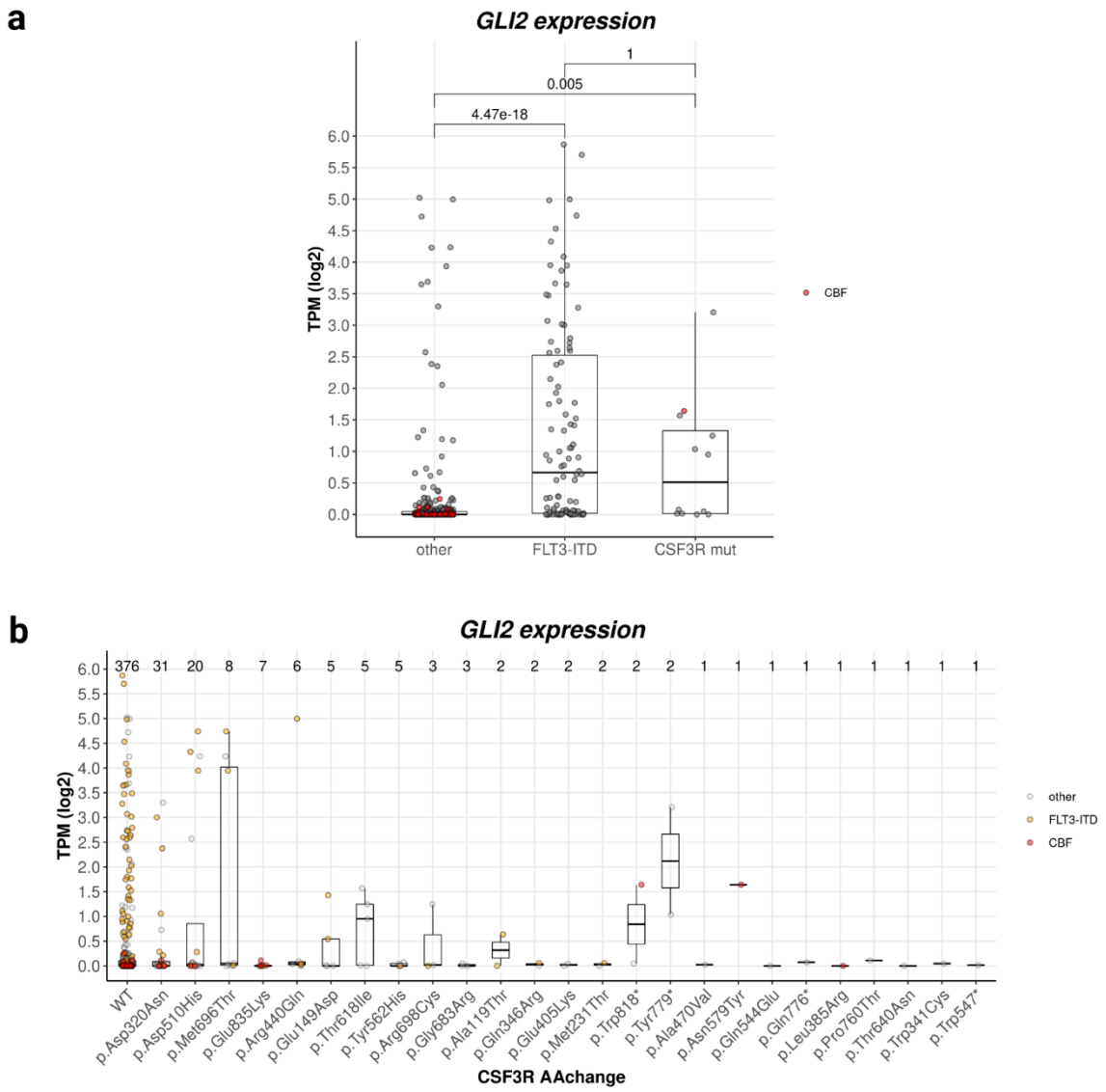

Figure 15: CSF3R T618I induces upregulated GLI2 expression in patients.
a) *GLI2* expression of patients within the Beat-AML cohort. Pathogenic and likely pathogenic *CSF3R* variants (ClinVar) were considered as mutations. Significance was determined using the Wilcoxon-Mann-Whitney U test. **b**) *GLI2* expression according to *CSF3R* variant status. Previously published.[195]

RT-qPCR in the cell line SKNO-1 confirmed differential expression of the majority of 20 selected genes tested, thus verifying the effect independent of the model system (**Figure 16 a**). Pathway analysis following RNA-seq revealed an enrichment of downstream actors within folate and pterine metabolism, a central mechanism of nucleotide synthesis and DNA methylation. Likewise, anti-inflammatory pathways such as IL-4, IL-10 and IL-13 signaling were altered (**Figure 16 b**).[195]

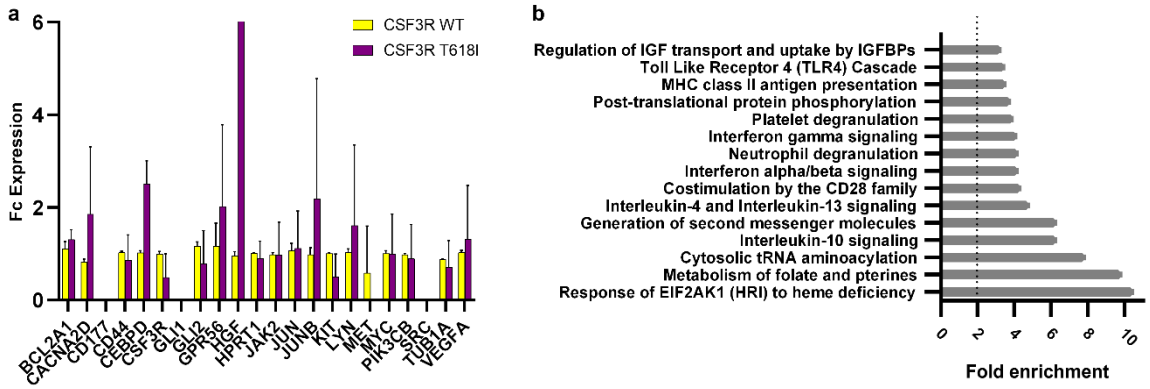

Figure 16: CSF3R T618I deregulates nucleotide biosynthesis and immune response.
a) RT-qPCR of SKNO-1 cells expressing CSF3R WT or T618I (n=3). Fold change expression of 20 selected genes is displayed. Error bars represent ± standard error of the mean. **b)** Gene set enrichment analysis (GSEA) of bulk RNAseq data that are enriched in CSF3R T618I expressing cells. Pathway analysis restricted to Reactome pathways.

2.6 CSF3R T618I and RUNX1-RUNX1T1 synergistically alter structure and dynamics of the cell population.

Performing bulk RNA-seq, changes in subpopulations are often underappreciated and cannot clearly be allocated. To visualize dynamic changes over time and directly only the desired cells within each population, single cell RNA-seq (scRNA-seq) was performed. Upon outgrowth (day 60) cells co-expressing RUNX1-RUNX1T1tr and CSF3R T618I showed a higher proportion of immature cells (HSC/MPP) (**Figure 17 a**) compared to RUNX1-RUNX1T1-driven expansion of single positive cells, originally co-transduced with CSF3R WT (see model **Figure 9**). This is congruent with the predominantly blast-like morphology in the double oncogene expressing culture (**Figure 12 c**). In turn, cycling cells and mast cells make up a great proportion of the single positive cells, while cycling cells are nearly absent and mast cells present only a small share of RUNX1-RUNX1T1tr and CSF3R T618I double positive culture (**Figure 17 a**, **Figure 18 b**).[195]

In accordance with bulk RNA-seq (**Figure 14**) and patient data (**Figure 15**), scRNA-seq showed enriched *GLI2* expression in double oncogene expressing cells. Using scRNA-seq, however, made it possible to match upregulated *GLI2* expression to distinct cell types. Within CSF3R T618I expressing cells, the two most abundant cell types, namely the “HSC/MPP compartment” and “macrophage-committed progenitors”, showed enriched *GLI2* expression. In both cultures, mast cells also presented slightly elevated abundance of *GLI2* transcripts (**Figure 17 b**, **c**).[195]

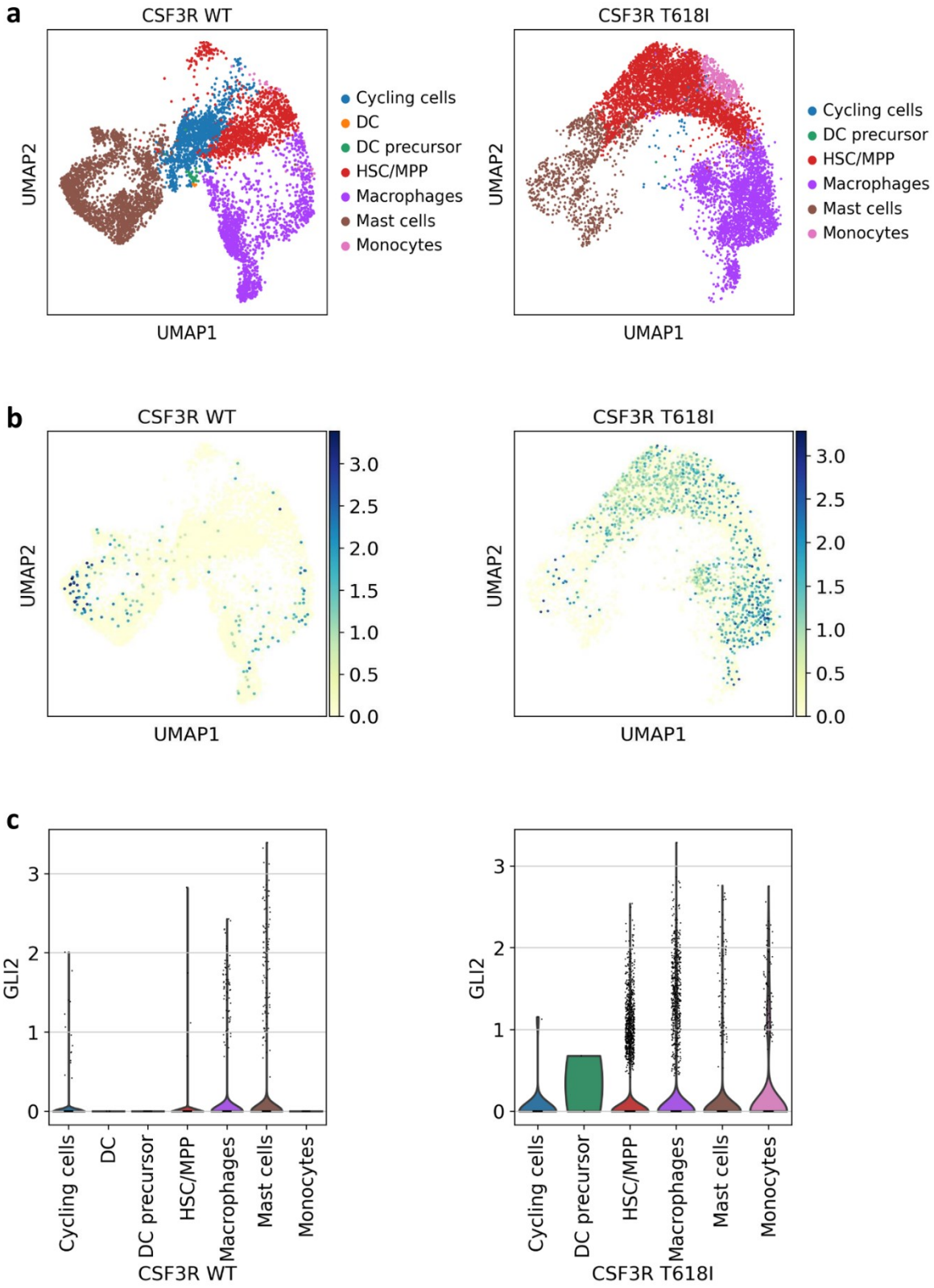

Figure 17: Single-cell RNA-seq shows enrichment of immature hematopoietic cells (HSC/MPP) and GLI2 upregulation in CSF3R T618I-mediated expansion.
a) UMAP showing different subpopulations annotated with CellTypist for CSF3R WT or T618I. **b**) UMAP showing GLI2 expression for CSF3R WT or T618I. **c**) Violin plots showing GLI2 expression across the subpopulations for CSF3R WT or T618I. CSF3R T618I sensitizes to GLI inhibition in a RUNX1-RUNX1T1tr background. Published previously.[195]

Comparing the composition of each group over time makes evident, that cooperation of RUNX1-RUNX1T1tr and CSF3R T618I not only blocks differentiation more efficiently than RUNX1-RUNX1T1tr alone. Closer examination further reveals expansion of HSC/MPP percentage over time upon double expression, while diminishing upon single expression (**Figure 18 a, b**).

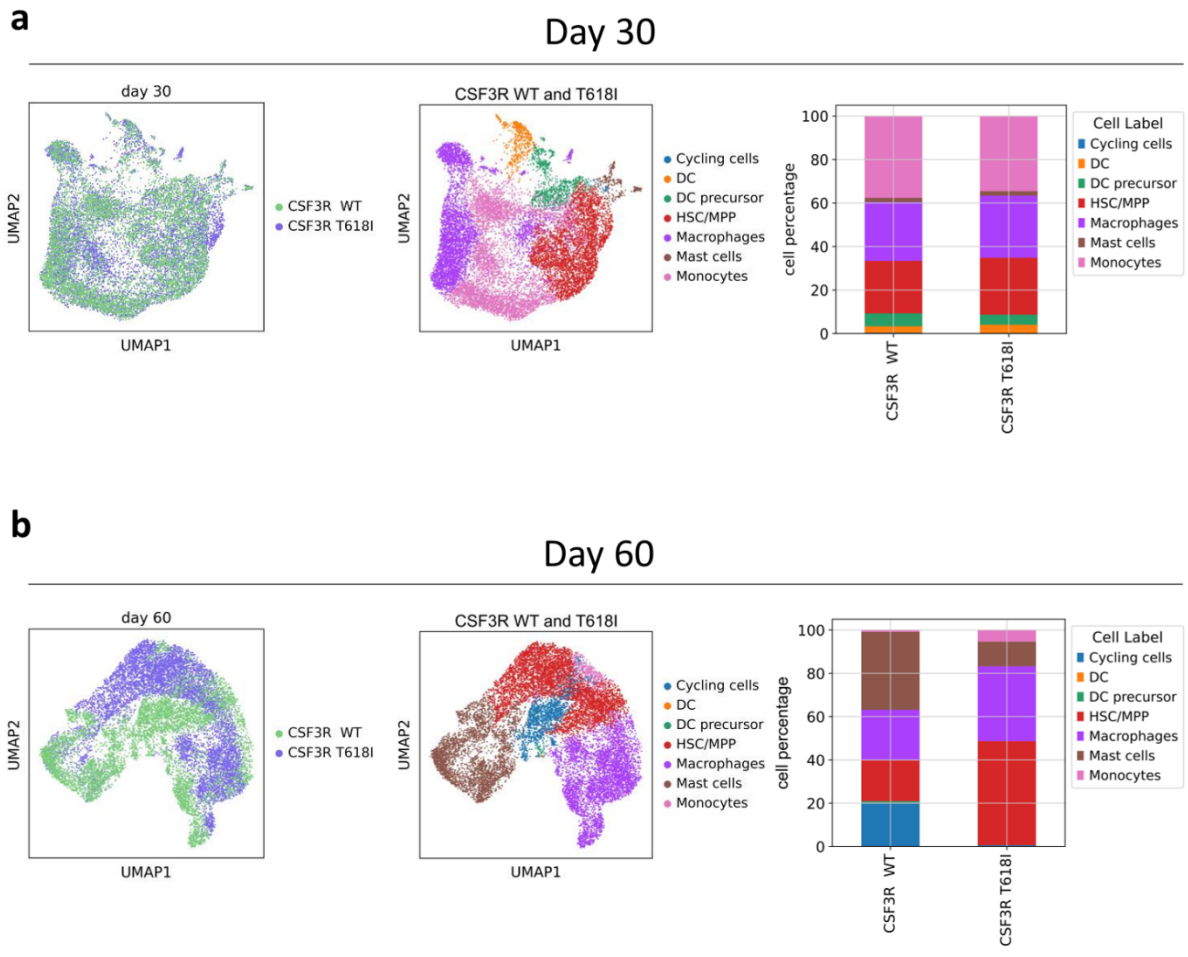

Figure 18: scRNA-seq reveals changes in double transduced populations over time.
a) UMAP showing different subpopulations in the outgrown cells at day 30 resulting from double transduction of RUNX1-RUNX1T1tr and CSF3R WT or CSF3R T618I. **b**) UMAP showing different subpopulations at day 60. Published previously.[195]

2.7 CSF3R T618I confers cytokine independence in the t(8;21) positive cell line SKNO-1

Previous studies in murine t(8;21) models have shown that pre-leukemic clones, expanded by RUNX1-RUNX1T1, are highly cytokine dependent. Therefore, alterations causing proliferation advantages and cytokine mediated survival might be decisive collaborators leading towards leukemic transformation.[15,22,198,201] To this end, the t(8;21)-positive, cytokine dependent cell line SKNO-1 was used for further experiments. In this setting, CSF3R T618I but not CSF3R WT expression caused cytokine independent growth (**Figure 19 a**). On SKNO-1 native cells, vector control or CSF3R WT expressing cells, withdrawal of the cytokine GM-CSF led to cell cycle arrest that could be overcome by expression of CSF3R T618I (**Figure 19 b**).[195]

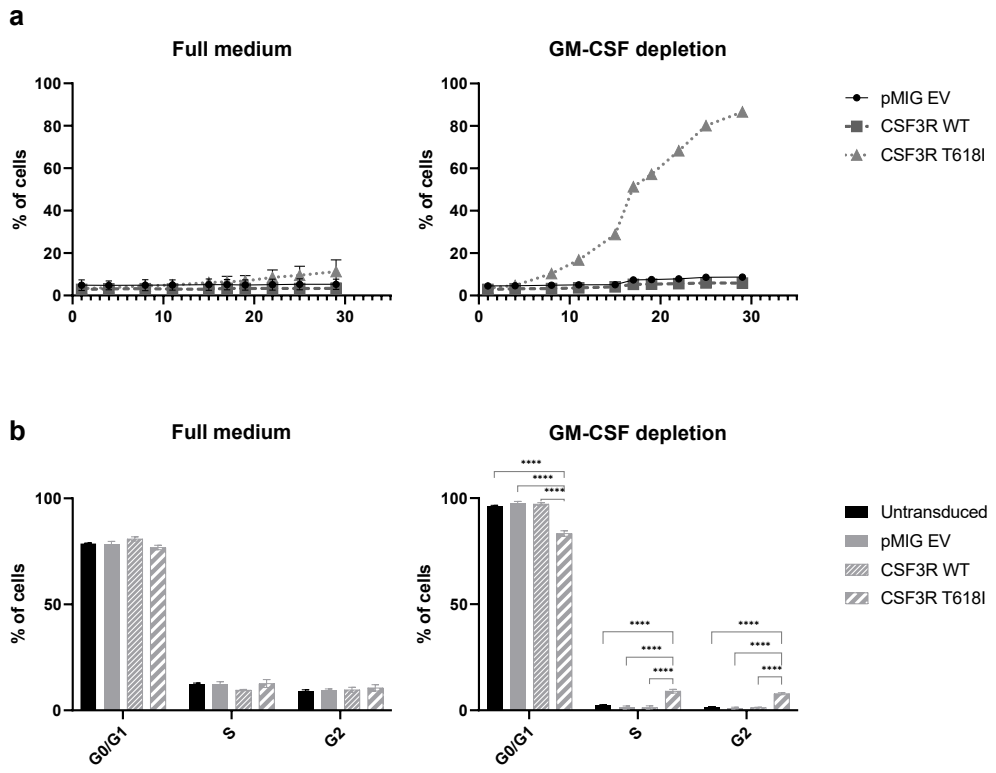

Figure 19: CSF3R T618I confers cytokine independence and increased sensitivity to GLI inhibition.
a) Competitive growth analysis of cell line SKNO-1 virally transduced with vector control (EV), CSF3R WT or T618I, cultivated with or without GM-CSF. Expression of fluorescent marker (GFP) was assessed every 2-3 days using flow cytometry. Error bars represent ± standard error of the mean. **b**) Cell cycle analysis of SKNO-1 untransduced, transduced with vector control (EV), CSF3R WT or T618I and cultured with or without GM-CSF. Cell cycle was assessed after staining with DRAQ5 and detection using flow cytometry. Cell cycle analysis was performed using FlowJo Software. Error bars represent ± standard error of the mean. Comparison was performed using two-tailed unpaired t-test (**** $p < 0.0001$).

2.8 CSF3R T618I sensitizes to GLI inhibition in a RUNX1-RUNX1T1 background.

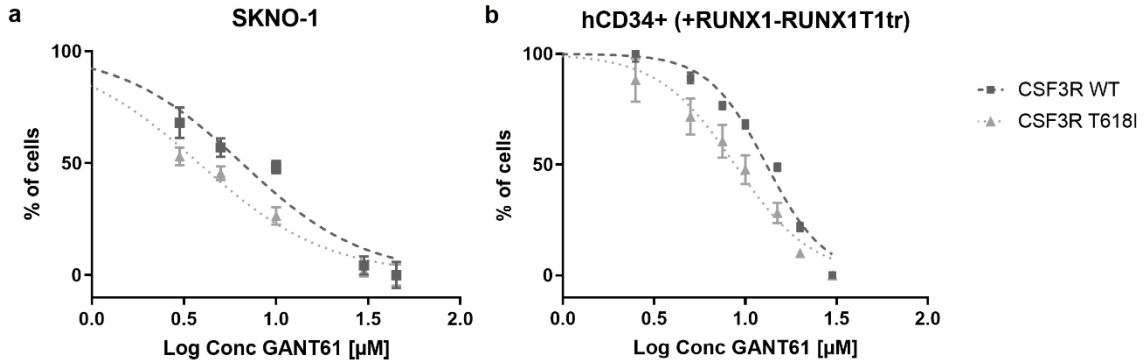

Figure 20: CSF3R T618I sensitizes to GLI inhibition in a RUNX1-RUNX1T1 background
GLI inhibition using escalating doses of GANT61 in a) sorted SKNO 1 and b) expanded hCD34+ cells transduced with CSF3R WT or T618I. Error bars represent ± standard error of the mean. Published previously.[195]

In a next step it was tested if CSF3R T618I signaling can be counteracted by pharmacological inhibition of GLI2 signaling. Outgrown progenitor cells co-transduced with RUNX1-RUNX1T1tr and either CSF3R WT or CSF3R T618I were treated with the GLI inhibitor GANT61. CSF3R T618I expressing cells were significantly sensitive to GLI inhibition (**Figure 19 b**).
Independently, experiments on SKNO-1 cells confirmed that CSF3R T618I expression results in significantly higher sensitivity towards GANT61, compared to vector or CSF3R WT controls (**Figure 19 a**). [195]

Considering previously reported signal transduction of mutated *CSF3R via* JAK2 and STAT3,[112] both pathways were targeted pharmacologicly. However, neither the JAK2 inhibitor Ruxolitinib nor the STAT3 inhibitor C188-9 caused significantly enhanced cell death upon ectopic expression of CSF3R wildtype or mutant (**Figure 21 a**). Interestingly, phosphorylated STAT3 was increased in CSF3R T618I expressing cells compared to CSF3R WT or vector control, while JAK2 total protein expression was majorly decreased with no measurable phosphorylation (**Figure 21 b**).[195]

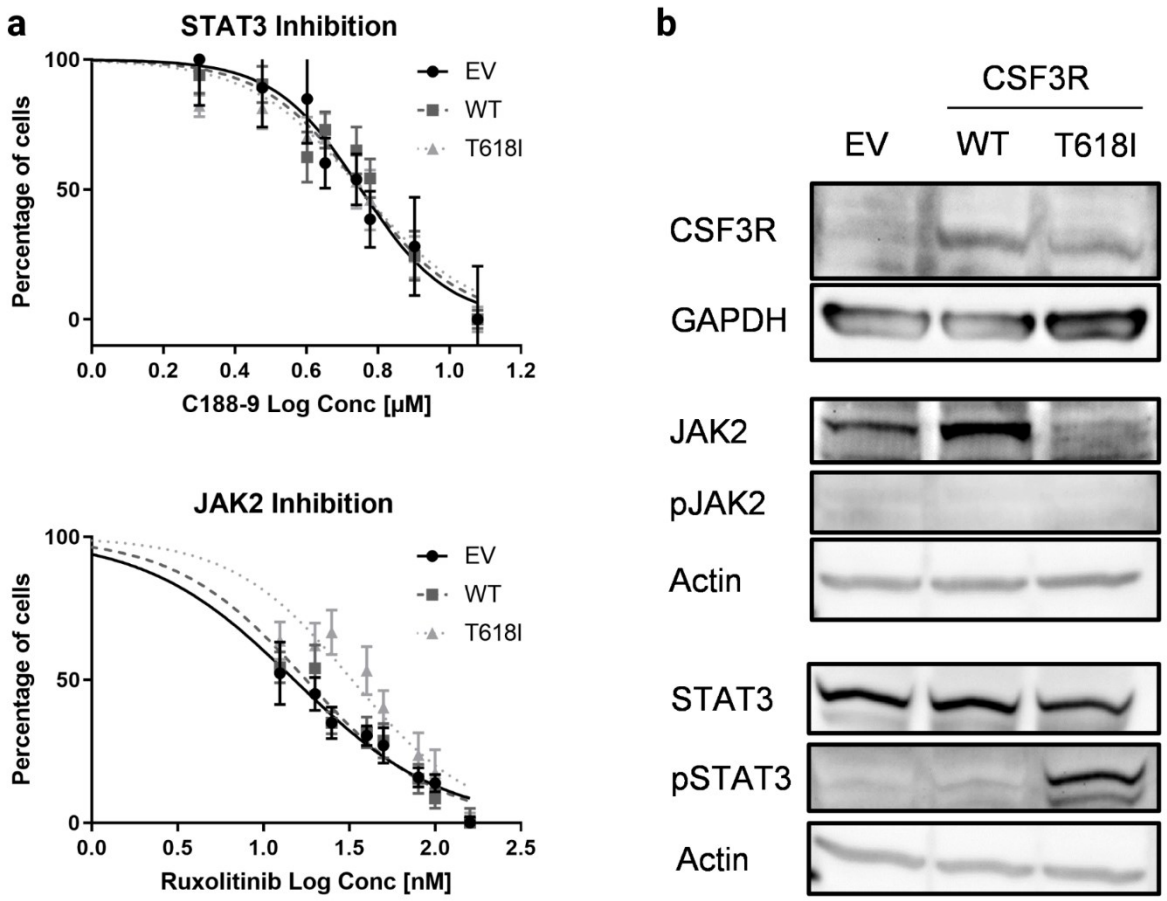

Figure 21: CSF3R T618I alters signaling cascade.
a) Drug sensitivity assay after treatment of cell line SKNO-1 with escalating doses of STAT3 inhibitor C188-9 (upper panel) or JAK inhibitor Ruxolitinib (n=3) (lower panel). SKNO-1 cells have been virally transduced with either empty vector control (EV), CSF3R WT or CSF3R T618I and sorted prior to treatment. Error bars represent ± standard error of the mean. **b**) Western Blot analysis of SKNO-1 cells. Published previously.[195]

Data from RNA-seq showed a slight, however insignificant, trend towards reduction in *JAK2* expression when comparing double oncogene expressing cells with RUNX1-RUNX1T1tr-mediated expansion of cells (**Figure 22 a**). Elevated SOCS3 expression, a direct inhibitor of JAK2 on protein level, advocates for posttranslational regulation and JAK2 degradation in resonance of CSF3R activation via the T618I mutation (**Figure 22 c**). JAK3 is not known to bind activated wildtype CSF3R in the same manner as JAK2, however bulk RNA-seq found it´s expression to be significantly increased upon CSF3R T618I expression in a RUNX1-RUNX1T1tr background (**Figure 22 b**).

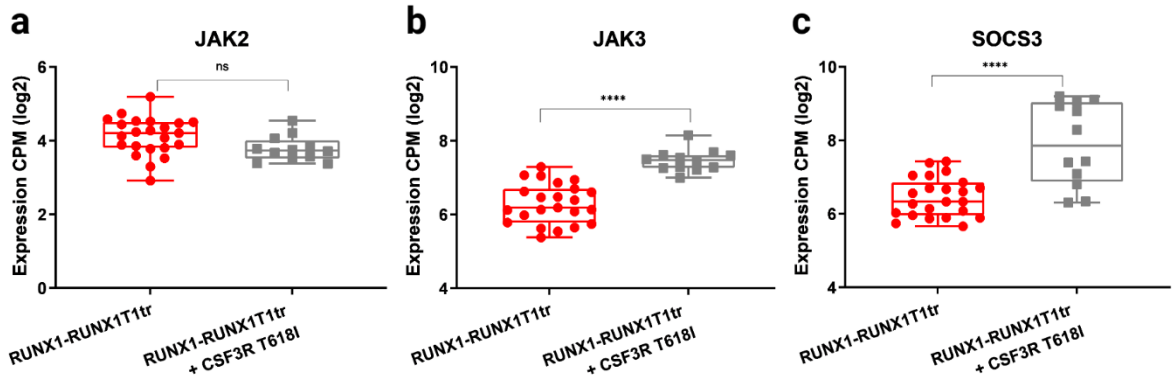

Figure 22: CSF3R T618I alters expression profile of HSPCs.
Expression on *JAK2* **a**), *JAK3* **b**) and *SOCS3* **c**) in HSPCs on day 60 assessed by bulk RNA-seq. Replicates of outgrown RUNX1-RUNX1T1tr populations (in red) resulting from double transduction with *CSF3R* WT (n=12) and pMIG EV (n=11) were pooled together for analysis as they behave similarly in the growth competition assay. Differential expression analysis was performed with edgeR/limma package. **** $p < 0.0001$. Error bars represent ± standard error of the mean. Published previously.[195]

To test, if JAK3 could present an alternative signaling route, it was targeted therapeutically in the cell line SKNO-1, using the selective JAK3 inhibitor Ritlecitinib. Interestingly, analysis of the drug sensitivity assay confirmed only slight sensitivity of CSF3R T618I cells at high dosis (≥ 250µM) (**Figure 23 a**). Testing the multikinase inhibitor Dasatinib revealed that expression of CSF3R T618I conferred increased sensitivity as compared to CSF3R WT or vector control (**Figure 23 b**).

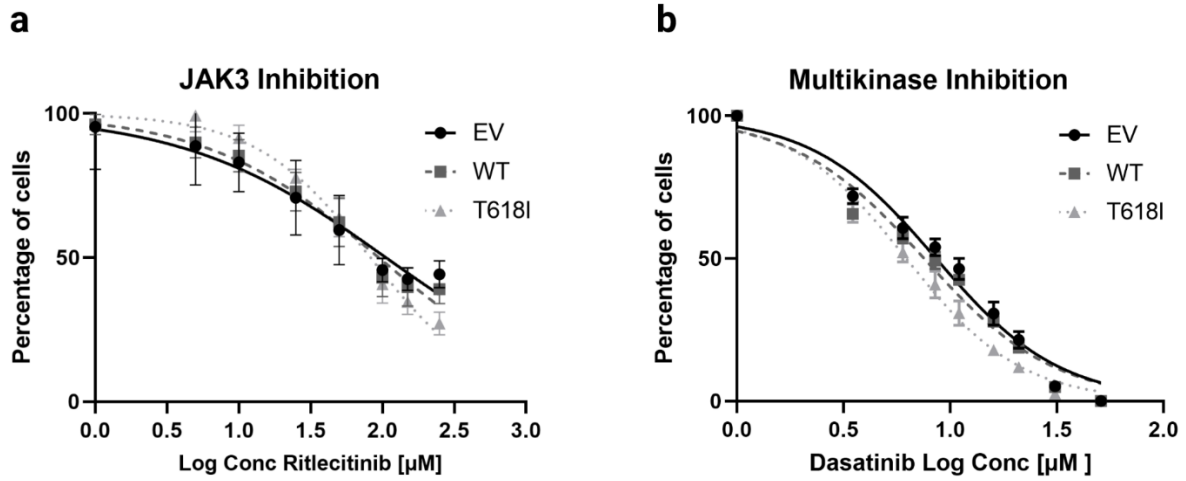

Figure 23: SKNO-1 cells overexpressing CSF3R T618I are more sensitive to Dasatinib than to JAK3 inhibition.
Drug sensitivity assay (n=3). (**a**) Response to the JAK3 inhibitor Ritlecitinib (*CSF3R* T618I cells were sensitive at 250 µM). (**b**) Response to the multikinase inhibitor Dasatinib (*CSF3R* T618I cells were sensitive in the range of 7.5 to 20 µM). Error bars represent ± standard error of the mean.

3 Discussion

In the context of atypical CML and in particular CNL, the CSF3R hotspot mutation T618I has been thoroughly described. In AML, however, it is mainly known in combination with CEBPA mutations[202], where it drastically diminishes survival rates[203].

This study first examined the relevance of the *CSF3R* mutation T618I in clonal competition during leukemogenesis. Various studies showed that early progenitor cells are expanded in consequence of RUNX1-RUNX1T1 fusion expression due to enhanced self-renewal potential and blockade of differentiation pathways.[94,109,204–206] However, in NOD/SCID mice, retroviral expression of the fusion protein does not promote leukemia.[109,205–207] Leukemogenesis requires the presence of a suitable secondary mutation,[108,205,206,208–211] nonetheless, addition of G-CSF significantly increases proliferation of RUNX1-RUNX1T1 expressing cells.[212] In a study published recently, Carratt et al. demonstrated the importance of lesion order on transforming potential.[213] They were able to show that RUNX1-RUNX1T1 expression must be the leading event in mouse bone marrow CFUs. The results of this work confirmed the order of events and, what's more, proved transferability to the human setting. In accordance with the literature[196], for this study, ectopic expression of RUNX1-RUNX1T1tr was sufficient for hematopoietic stem and progenitor cells expansion due to blockage of differentiation. Mouse bone marrow CFUs form no colonies under RUNX1-RUNX1T1 expression alone, as shown by Carratt et al[213]. While this seems to be diverging at first, the results of this work provide an explanation. First, CSF3R T618I enhanced proliferation but further provided cell cycle progression independent of cytokine availability, while cells expressing RUNX1-RUNX1T1 alone cannot be expanded in cytokine free environment. While HSPCs used in this work were supported by a mix of cytokines, including GM-CSF and IL-3, the authors state to have performed mouse bone marrow assays without addition of signaling molecules.

Morphologic analysis revealed that introduction of CSF3R T618I in a RUNX1-RUNX1T1tr background generates an immature cell population with highly increased frequency of cells with self-renewal potential and increased survival potential.[195] While leukemic blasts bear

limited proliferation capacity, a small subset of leukemic stem cells with long-term self-renewal potential drive leukemic progression[5]. Therefore, in this setting the role of CSF3R T618I is not limited to driving proliferation, but further aggravates the block of differentiation.[195] This may not only lead to malignant transformation, but further develop an enlarged subset of leukemic stem cells, known to confer therapy resistance and initiate relapse events[214]. This is in line with a study from Tarlock et al., demonstrating that *CSF3R* mutated pediatric leukemia is associated with increased risk of relapse[4].

In a next step, surface marker expression was used to further characterize HSPCs. Surface expression is an important criterion in routine diagnostics, distinct patterns can even indicate certain cytogenetic properties. While inversion inv(16) is frequently accompanied by expression of T-lineage marker CD2,[198] expression of CD7, CD56[215] or CD19, together with CD34 can hint to translocation t(8;21).[216] This translocation is associated with favorable prognosis, yet, surface expression of CD56 has prognostic impact as it comes along with shorter time to relapse and survival.[215] Human HSPCs expressing both RUNX1-RUNX1T1tr and CSF3R T618I present a surface marker pattern very similar to acute myelomonocytic leukemia (AMML), further advocating for progressed leukemic transformation. While the expression profile of double positive cells clearly identifies them as immature cells of monocytic origin (**Table *1***), it might even indicate the presence of myeloid-derived suppressor cells (MDSCs), commonly described as Lin-CD11b+CD33+HLA-DR-CD14+CD15-CD66b-. RUNX1-RUNX1T1 and CSF3R T618I positive mouse bone marrow presents the homologue surface marker signature CD11b+Ly-6C+Ly-6G-[213]. Originally identified in tumor bearing mice[217], MDSCs have emerged as major immunosuppressive regulator of tumor microenvironment in solid and hematologic cancers. By production and secretion of IL-10 and TGF-β, MDSCs exert a highly suppressive effect on T-Cells and further induce their expansion in a positive feedback loop, promoting tumor growth[218,219]. In support of this hypothesis, GSEA analysis of double oncogene expressing cells revealed enrichment in IL-10 signaling, being one of the most deregulated pathways as compared to RUNX1-RUNX1T1 single positive cells.[195] However, clear identification of this cell type would require further surface marker

analysis and, most important, functional assays determining the suppressive capacity, which is beyond the scope of this study. Yet, it is tempting to speculate that cooperation of both genetic lesions might result in an immunosuppressive phenotype.

To determine leukemic progression and aggressive behavior, engraftment *in vivo* is an important parameter. Wichmann et al. showed in a similar setting, that HSPCs transduced with RUNX1-RUNX1T1 can persist for some time after transplantation into irradiated mice, but do not engraft[196]. In line with that, Carratt et al. found that only cooperation of RUNX1-RUNX1T1 with CSF3R T618I expressed sequentially in mouse bone marrow cells led to disease progression with significantly shortened survival of irradiated mice[213]. For this study, human HSPCs ectopically expressing RUNX1-RUNX1T1 together with CSF3R WT or CSF3R T618I were expanded and transplanted into non-irradiated NSG mice. Diverging from previous studies, no human cells were detected at any measurement during the observation period. The fact that neither single nor double oncogene expression of human HSPCs lead to engraftment or even short time persistence in this setting does not give an indication about leukemic potential or aggressiveness. Rather, technical differences might be key for successful engraftment. On one hand, irradiation of mice before transplantation could help creating an exploitable niche for HSPCs. On the other hand, transplanting transduced cells at an earlier timepoint of expansion might be sufficient for leukemic development in *vivo*.

One major task of this study was the identification of molecular mechanisms leading to malignant transformation and disease progression. Bulk RNA-seq revealed transcription of more than 600 genes was significantly deregulated upon CSF3R T618I expression in a RUNX1-RUNX1T1 background. One of the most upregulated genes, *GLI2*, is a known downstream actor of hedgehog signaling. GSEA analysis showed enrichment of the whole hedgehog pathway upon expression of both oncogenes. This is interesting for two reasons: canonical hedgehog signaling is critical during embryonic development and regulates cell proliferation, differentiation and stem cell maintenance[220]. Non-canonical, ligand-independent hedgehog/GLI signaling on the other hand, is frequently activated in a plethora of cancer

types[221,222]. Single cell RNA-seq of HSPCs revealed that *GLI2* expression was mainly elevated in MPP/HSCs, advocating for a role in maintenance and expansion of immature cells. Patients within the AMLCG-2008 cohort showed that expression of *GLI2* was correlated to shorter survival both indicating that those patients might benefit from targeted therapy, and that this target might be GLI2. Analysis of the Beat AML cohort further confirmed a correlation of *GLI2* expression levels with occurrence of *CSF3R* mutations, or, interestingly, *FLT3*-ITD. *FLT3*-ITD in AML patients is associated with poor prognosis[200,223,224], again highlighting the importance of further investigations into GLI2. Deciphering the types of *CSF3R* variants, this study clearly shows that mainly variants considered malignant or of uncertain significance are capable of rising *GLI2* transcript levels in the background of *FLT3*-ITD or CBF leukemia. In the Beat AML cohort 2 of 3 patients with CBF leukemia in combination with CSF3R mutations had elevated levels of *GLI2* expression. This further suggests that upregulation of *GLI2* is a direct consequence of synergism between translocation t(8;21) and CSF3R T618I. Of note, *GLI2* is not expressed in healthy adult hematologic tissues.

Within the canonical hedgehog pathway, the transcription factor GLI2 is activated downstream of ligand binding (Hedgehog (Hh), Indian Hedgehog (Ihh), Desert Hedgehog (Dhh)) to Patched 1 (PTCH1) and subsequent derepression of Smoothened (SMO). Efforts on targeting activated HH-signaling chemotherapeutically both in solid tumors and hematopoietic malignancies has mainly been directed towards SMO inhibition. For this study, however, upregulation of GLI2 transcription advocated for non-canonical GLI2 signaling. Therefore, antagonizing Hh pathway signaling using a SMO inhibitor was considered unsuitable. Emerging evidence for non-canonical GLI activation beyond SMO[225–227] lead to the discovery of direct GLI1/2 inhibitors. GANT58 and GANT61 directly bind GLI1 and GLI2, inhibiting GLI-DNA binding and target gene transcription[228,229]. Since GANT61 was found to be more efficient[229], further investigations and preclinical trials in a variety of cancer types, including leukemia, followed[230]. Therefore, GANT61 was chosen as GLI2 inhibitor for this study.

Pharmacological intervention of GLI2 signaling using GANT61 showed increased sensitivity of RUNX1-RUNX1T1 and CSF3R T618I co-expressing HSPCs and SKNO-1 cells. This suggests that upregulation of GLI2 is not a byproduct of mutant CSF3R, but rather an active participant and mechanism in driving leukemia progression, mediated by the unique cooperation of RUNX1-RUNX1T1 and CSF3R T618I. Further, it provides an exploitable target, that should be considered for deeper investigations.

Interestingly, inhibition of both JAK2 and STAT3 signaling did not result in increased cell death.[195] In t(8;21) positive AML, activating JAK2 mutations are found recurrently, proposing collaboration during leukemogenesis.[2,231–234] Furthermore, in the context of CNL, signaling through the CSF3 receptor is thought to involve both STAT3 and JAK2 phosphorylation.[112] In this study, JAK2 total protein was significantly decreased, which was not reflected on a transcriptional level. That advocates for a post-translational downregulation mechanism of JAK2 on one hand, as well as an alternative activation of STAT3 within the CSF3R T618I expressing models used in this study. Furthermore, although STAT3 showed increased phosphorylation in CSF3R T618I expressing cells, pharmacological counteraction did not result in measurable differences concerning the IC50. This fact raises the question, whether signal transduction of mutated CSF3R could follow an alternative route in the context of t(8;21) AML. A conceivable solution could be a shift towards different JAK family members. The basis of this hypothesis is given by bulk RNA-seq, were JAK3 was significantly upregulated upon CSF3R T618I expression. Treatment with Ruxolitinib selectively targets JAK1 and JAK2, however shows very low sensitivity towards JAK3.[235] Activation of JAK3 was hypothesized to be an indirect effect, as association with the common γ-chain of cytokine receptors is required, a domain not present in CSF3R. Pharmacologic counteraction of JAK3, using Ritlecitinib only showed increased sensitivity of double oncogene expressing SKNO-1 cells at high concentrations. Ritlecitinib is a highly selective JAK3 inhibitor regarding other JAK kinases, however, is also capable of binding and inhibiting several members of the TEC kinase family. Therefore, sensitivity might be conferred by inhibition of other kinases, at high concentrations

even unspecific, or JAK3 signaling might be redundant. Those results suggest, that JAK3 upregulation may not play a major role in leukemogenesis.

Another hypothesis is that CSF3R T618I in a t(8;21) background is increasingly signaling through the Ras/Raf/MAPK/ERK pathway, associated with proliferation (see **1.4.2.3**). Furthermore, activation of non-canonical GLI2 signaling in cancer is known to be mediated by ERK1/2 signaling downstream of growth factor receptors[222]. Using Dasatinib, a BCR-ABL and Src kinase family inhibitor, this study could reveal higher sensitivity of mutant CSF3R expressing cells compared to CSF3R WT or vector control expressing cells. The Src kinase family includes the adaptor protein Shc, facilitating Ras signaling cascade, LYN, that is thought to be a crucial player in both JAK and PI3K/AKT signaling, HCK and others (**Figure 6**). Sensitivity towards Dasatinib upon CSF3R T618I expression suggests a crucial role of Src family kinases in mutant CSF3R signaling in a t(8;21) background and points towards Ras/Raf/MAPK/ERK signaling as missing link in GLI2 activation. In order to unravel the mechanism, however, further investigations are inevitable.

Taken together, a human in vitro model for clonal competition during the onset and progression of AML was developed. The experiments throughout this thesis provide evidence that CSF3R T618I and RUNX1-RUNX1T1tr collaborate via hedgehog signaling. This proved to be directly targetable by inhibition of its downstream actor GLI. This novel mechanism was confirmed independently in two model systems. In context with its upregulation in *FLT3*-ITD positive AML, the downstream effector *GLI2* becomes an increasingly attractive target for pharmacological intervention in AML.[195]

4 Experimental Procedures and Material

4.1 Experimental Procedures

4.1.1 Plasmids

The expression vector pMSCV-RUNX1-RUNX1T1TR-IRES-tdTomato has been described previously.[196] MSCV-IRES-GFP expression vectors with CSF3R wildtype and T618I mutant as well as vector control were a generous gift from Julia Maxson, Portland, Oregon, USA.[236]

4.1.2 Cell culture and retroviral transduction

SKNO-1 cells (DSMZ, ACC-690) were cultured in RPMI 1640 Glutamax (Invitrogen, Carlsbad, CA, USA) supplemented with 10% fetal bovine serum (FBS) (PAN Biotech, Aidenbach, Germany), 1% penicillin-streptomycin (PAN biotech) and 10ng/ml GM-CSF (Miltenyi Biotech, Bergisch Gladbach, Germany). HEK 293T cells (DSMZ, ACC-635) were cultured in Dulbecco's modified Eagle's medium (DMEM) (PAN Biotech) supplemented with 10% FBS and 1% penicillin-streptomycin. CD34+ bone marrow cells (Lonza, Basel, Switzerland) were cultured in Iscove's modified Dulbecco's medium (IMDM) (Gibco, Carlsbad, CA, USA), supplemented with 20% FBS, 1% penicillin-streptomycin, 4µM L-Glutamine (Gibco), 10 ng/ml interleukin (IL)-3, 20 ng/ml IL-6, 20 ng/ml Flt3-L, 20 ng/ml GM-CSF, 20 ng/ml stem cell factor (SCF), 20 ng/ml thrombopoietin (TPO) (cytokines were obtained from Peprotech, Hamburg, Germany). Retroviral transduction of CD34+ cells was performed as described before.[196,237] Transduction of SKNO-1 was performed accordingly with the culture medium described above. Previously published.[195]

4.1.3 Flow cytometry

Beginning 4 days post transduction, CD34+ progenitor cells were analyzed every 2-3 days for expression of dtTomato and eGFP by FACS. SKNO-1 cells were either sorted 10 days after transduction or left unsorted.

For analysis of cell surface marker expression, allophycocyanin (APC)-, phycoerythrin/cyanine 7 (PE/Cy7)-, or PE-Vio770-conjugated anti-human HLA-DR, CD3, CD10, CD11b, CD11c, CD13, CD14, CD15, CD18, CD19, CD27, CD33, CD34, CD41a, CD49a, CD117 and CD135 antibodies were used (BioLegend, San Diego, CA, USA; BD Life Sciences, Franklin Lakes, NJ, USA; or Miltenyi Biotech, Bergisch Gladbach, Germany). Isotype controls mouse IgG1, mouse IgG2a, mouse IgM and recombinant human IgG1 were used accordingly.

Apoptosis rates were measured by FACS following cell staining with APC-conjugated Annexin V (BD Pharmingen, Franklin Lakes, NJ, USA) according to manufacturer's recommendations in combination with DAPI as vital dye.

Cell cycle was assessed by FACS after DRAQ5 staining (Alexis Biochemicals, San Diego, CA, USA) for 10 minutes at 37°C.

All flow cytometry experiments were performed using FACS Calibur or FACS Canto II (BD Life Sciences). FACS data were analyzed using FlowJo Software (BD Life Sciences). Statistical analysis was performed using GraphPad Prism (GraphPad Software Inc., San Diego, CA, USA). P-values were calculated using the student´s t-test. Previously published.[195]

4.1.4 Cytotoxicity assay

$3*10^4$ SKNO-1 or progenitor cells/well were treated in 96 well plates for 72h with varying concentrations of JAK Inhibitor Ruxolitinib phosphate (ChemScene, Monmoth Junction, NJ, USA), STAT3 Inhibitor XIII, C188-9 (EMD Millipore, Billerica, MA, USA) or GLI Inhibitor GANT61 (TOCRIS, Bristol, UK) or the multikinase (BCR-ABL/SRC) inhibitor Dasatinib (Santa Cruz Biotechnology, Dallas, TX, USA). 68h post treatment, 20µl CellTiterBlue reagent was added to each well of cells as recommended by manufacturer. Plates were incubated for additional 4h at 37°C in the dark. For Analysis, CellTiterBlue® Cell Viability Assay was used. Readout was obtained using the GloMax® Discover plate reader (Both by Promega, Fitchburg, WI, USA). Statistical analysis was performed using GraphPad Prism (GraphPad Software Inc., San Diego, CA, USA). Values were normalized to the DMSO control and drug response was assessed by nonlinear regression (curve fit) using the equation *log(inhibitor) vs. normalized response – Variable slope*. Previously published.[195]

4.1.5 Bulk and single cell RNA sequencing

Human progenitor cells, co-transduced with *RUNX1-RUNX1T1*tr and *CSF3R* WT or T618I were submitted to RNA sequencing (Prime-seq) at day 60 of outgrowth. Library preparation, sequencing, analysis of differential gene expression and pathway analysis was performed as described before.[237–239] For single cell RNA sequencing (scRNA-seq), libraries from cells harvested on day 30 and day 60 were prepared using the Chromium Next GEM Single Cell 3' GEM Kit v3.1 (10x Genomics, Pleasanton, CA, USA) according to the manufacturer's instructions. Paired-end sequencing (Read 1: 28bp; Read 2: 91bp) was performed on an Illumina HiSeq 1500 instrument, with an average of 50.000 reads per cell and 10.000 cells per library. Sample demultiplexing and alignment of the data were done using the Cell Ranger software (v6.1.2) and the human genome GRCh38.p13 from Gencode (release 39). Further data processing (quality control, filtering, normalization, highly variable gene selection, embedding and visualization) was performed using the python package SCANPY v1.9.1.[240] Cell barcodes with less than 3000 counts, more than 100,000 counts or more than 20% of mitochondrial reads were filtered. Additionally, cells with less than 600 genes captured were

removed. This resulted in 29781 cells and 30039 genes across 4 samples (respectively at day 30: 7530 cells for *CSF3R* WT and 7661 cells for *CSF3R* T618I, at day 60: 6432 cells for *CSF3R* WT and 8158 cells for *CSF3R* T618I). Finally, the cell type annotation was done using the package CellTypist v1.3.1.[241] Previously published.[195]

4.1.6 RT-qPCR

RT-qPCR was performed using BioRad PrimePCR® Custom Plate in the 96 Well format. For this purpose, RNA was extracted from SKNO-1 cells using Qiagen RNease Mini Kit according to manufacturer´s recommendations. Genomic DNA was digested using DNase I, RNase-free (ThermoFisher) according to manufacturer´s recommendation. Subsequently cDNA was prepared using iScript cDNA Synthesis Kit (BioRad) as recommended for 2µg RNA. Real-Time PCR reaction was prepared as recommended by manufacturer using iTaq Universal SYBR Green Supermix. RT-qPCR was measured using Real-Time PCR Detection System CFX96 Touch (BioRad).

4.2 Materials

4.2.1 Chemicals

Reagent	Company
2-Propanol	AppliChem (Darmstadt, Germany)
Agarose	Carl Roth (Karlsruhe, Germany)
Albumin Fraction V (pH 7.0) (BSA)	AppliChem (Darmstadt, Germany)
Ampicillin sodium salt	Sigma-Aldrich (St. Louis, MO, USA)
APS (Ammonium persulfate)	Carl Roth (Karlsruhe, Germany)
Bio-Rad Protein Assay Dye	Bio-Rad (Hercules, CA, USA)
BOLT LDS Sample Buffer 4x	Thermo Fisher Scientific (Waltham, MA, USA)
BOLT Sample Reduction Agent 10x	Thermo Fisher Scientific (Waltham, MA, USA)
Bromophenole blue	Sigma-Aldrich (St. Louis, MO, USA)
cOmplete, mini, Protease inhibitor	Roche (Basel, Switzerland)
Coulter Clenz Cleaning Agent	Beckman Coulter (Krefeld, Germany)
Coulter Isoton II Diluent	Beckman Coulter (Krefeld, Germany)
DEPC-treated water, Ambion	Thermo Fisher Scientific (Waltham, MA, USA)
DH5α competent bacteria	New England Biolabs (Frankfurt, Germany)
Dimethyl Sulfoxide (DMSO)	Sigma-Aldrich (St. Louis, MO,USA)
Dithiotreitol (DTT)	Thermo Fisher Scientific (Waltham, MA, USA)
DMEM	PAN Biotech (Aidenbach, Germany)
DNase I, RNase free	Thermo Fisher Scientific (Waltham, MA, USA)
DPBS w/o Mg2+, Ca2+	PAN Biotech (Aidenbach, Germany)
DRAQ5 5mM	Alexis Biochemicals (Lausanne, Switzerland)
eBeads GFP BrightComp Compensation Beads	Thermo Fisher Scientific (Waltham, MA, USA)
eBeads UltraComp, eBio	Thermo Fisher Scientific (Waltham, MA, USA)

EDTA, UltraPure 0,5M, Invitrogen	Thermo Fisher Scientific (Waltham, MA, USA)
Ethanol	Merck Millipore (Darmstadt, Germany)
Fetal Bovine Serum (FBS)	PAN Biotech (Aidenbach, Germany)
Fetal Bovine Serum (FBS) Superior	Biochrom (Berlin, Germany)
Formaledhyde 16% (w/v), methanol-free	Thermo Fisher Scientific (Waltham, MA, USA)
GeneRuler 1kb ladder	Thermo Fisher Scientific (Waltham, MA, USA)
Glycerol	Sigma-Aldrich (St. Louis, MO, USA)
Glycin	Sigma-Aldrich (St. Louis, MO, USA)
HALT Protease inhibtor cocktail	Thermo Fisher Scientific (Waltham, MA, USA)
HEPES	AppliChem (Darmstadt, Germany)
IncuWater Clean	AppliChem (Darmstadt, Germany)
Kaliumchloride (KCL)	Merck Millipore (Darmstadt, Germany)
LB-Agar	Carl Roth (Karlsruhe, Germany)
LB-Medium	Carl Roth (Karlsruhe, Germany)
L-Glutamin 200mM, Gibco	Thermo Fisher Scientific (Waltham, MA, USA)
MagicMark XP Western Protein Standard	Thermo Fisher Scientific (Waltham, MA, USA)
Magnesiumchloride ($MgCl_2$)	Merck Millipore (Darmstadt, Germany)
Methanol	Carl Roth (Karlsruhe, Germany)
MethoCult GFH84444	StemCell Technologies (Vancouver, BC, Canada)
Milk powder (Western Blot)	Carl Roth (Karlsruhe, Germany)
NP-40	AppliChem (Darmstadt, Germany)
Opti-MEM I Reduced Serum Medium, Gibco	Thermo Fisher Scientific (Waltham, MA, USA)
PageRuler Prestained Protein ladder	Thermo Fisher Scientific (Waltham, MA, USA)
Penicillin-Streptomycin, Gibco	Thermo Fisher Scientific (Waltham, MA, USA

PeqGold Protein Marker V Prestained	Peqlab (Wilmington, DE, USA)
Phosphatase inhibitor cocktail 2	Sigma-Aldrich (St. Louis, MO, USA)
Phosphatase inhibitor cocktail 3	Sigma-Aldrich (St. Louis, MO, USA)
Pierce ECL Plus Western Blotting Substrate	Thermo Fisher Scientific (Waltham, MA, USA)
Plasmocin prophylactic	InvivoGen (Toulouse, France)
Polyethylenimine (PEI)	Sigma-Aldrich (St. Louis, MO, USA)
Propidium Iodide	Sigma-Aldrich (St. Louis, MO, USA)
Proteinase K	New England Biolabs (Frankfurt, Germany)
Q5 HF Hot Start Polymerase	New England Biolabs (Frankfurt, Germany)
Quick load purple 2-Log DNA ladder	New England Biolabs (Frankfurt, Germany)
Quick load purple Gel Loading Dye 6x	New England Biolabs (Frankfurt, Germany)
Recombinant Human FLT3-Ligand, Peprotech	Thermo Fisher Scientific (Waltham, MA, USA)
Recombinant Human GM-CSF, Peprotech	Thermo Fisher Scientific (Waltham, MA, USA)
Recombinant Human IL-3, Peprotech	Thermo Fisher Scientific (Waltham, MA, USA)
Recombinant Human IL-6, Peprotech	Thermo Fisher Scientific (Waltham, MA, USA)
Recombinant Human SCF, Peprotech	Thermo Fisher Scientific (Waltham, MA, USA)
Recombinant Human TPO, Peprotech	Thermo Fisher Scientific (Waltham, MA, USA)

Restore Western Blot Sripping Buffer	Thermo Fisher Scientific (Waltham, MA, USA)
RetroNectin	Takara Bio (Kusatsu, Japan)
RNase AWAY	Carl Roth (Karlsruhe, Germany)
Rotiphorese gel 30	Carl Roth (Karlsruhe, Germany)
RPMI 1640 Glutamax	Thermo Fisher Scientific (Waltham, MA, USA)
S.O.C. Medium	Invitrogen (Darmstadt, Germany)
Sodium chloride (NaCl)	Carl Roth (Karlsruhe, Germany)
Sodium dodecyl sulfate (SDS)	Sigma-Aldrich (St. Louis, MO, USA)
ß-Mercaptoethanol	Sigma-Aldrich (St. Louis, MO, USA)
SYBR Safe DNA gel stain	Invitrogen (Darmstadt, Germany)
TAE Buffer 10x	Apotheke LMU Klinikum (Munich, Germany)
TBS Buffer 10x	Apotheke LMU Klinikum (Munich, Germany)
Tetra-methyl-ethylenediamine (TEMED)	Sigma-Aldrich (St. Louis, MO, USA)
Tris-(hydroxymethyl)-aminomethane (TRIS)	Carl Roth (Karlsruhe, Germany)
Triton X-100	Sigma-Aldrich (St. Louis, MO, USA)
Trypan Blue	Sigma-Aldrich (St. Louis, MO, USA)
Trypsin-EDTA (0.05%), phenol red	Thermo Fisher Scientific (Waltham, MA, USA)
TurboFect	Thermo Fisher Scientific (Waltham, MA, USA)
Tween20	Sigma-Aldrich (St. Louis, MO, USA)
Western Blot electrophoresis buffer 10x	Apotheke LMU Klinikum (Munich, Germany)

Table 5: Chemicals

4.2.2 Buffers and solutions

Buffers/Solutions	Composition
Agarose gel (1%-1,5%)	1-1.5% agarose in 1x TAE buffer with SYBR Safe (1:10 000)
Cell Freezing buffer	10% DMSO in FBS, stored at 4°C
FACS buffer	PBS, 1% FCS, 1mg/l propidium iodide; stored at 4°C, light protected
Laemmli buffer 4x	250mM Tris-HCL pH 6.8, 280mM sodiumdodecylsulfate (SDS), 40% glycerol, 8% ß-mercaptoethanol,0,02% bromophenol blue
LB-Agar plates	40g LB-Agar fill up to 1L with H2O dest.
LB-Agar plates Ampicillin	LB-Agar plates with 100µg/ml Ampcillin
LB-Medium	25g LB-Medium fill up to 1L with H2O dest.
Nuclear Extract Buffer A	10mM HEPES-KOH pH 7.9 (stored at 4°C), 1.5mM $MgCl_2$, 10mM KCl, 0.5mM DTT, HALT Protease inhibitor cocktail (added freshly, 1:25)
Nuclear Extract Buffer B	20mM HEPES-KOH pH 7.9, 25% Glycerol, 420mM NaCl, 1.5mM $MgCl_2$, 0.2mM EDTA, 0.5mM DTT, HALT Protease inhibitor cocktail (added freshly, 1:25)
Polyethylenimin (PEI)	1mg/ml in H2O dest.; sterile filtered; stored at -20°C
TAE buffer 10x	400mM Tris base, 200mM acetic acid, 10mM EDTA
TAE buffer 1x	100ml TAE buffer 10x with 900ml H_2O dest.
Tris buffered Saline (TBS) 10x	100mM Tris, 1,65M NaCl, pH 8,0
Tris buffered Saline (TBS) 1x	100ml TBS 10x with 900ml H_2O dest.

TBS-T	1x TBS, 0,1% Tween-20
Tris-HCL-Buffer pH 6,8	1,5M Tris
Tris-HCL-Buffer pH 8,8	1,5M Tris
Western Blot blocking solutions	5% non-fat milk in TBS-T or 5% BSA in TBS-T
Western Blot electrophoresis buffer 10x	250mM Tris base, 1,9M glycine, 1% SDS, pH 8,3
Western Blot electrophoresis buffer 1x	100ml electrophoresis buffer 10x with 900ml H_2O dest.
Whole Cell lysis buffer	50mM Tris-HCL, pH 8.5, 150mM NaCl, 1% Triton X-100

Table 6: Buffers and solutions

4.2.3 Laboratory Equipment

Equipment	Company
Amaxa Nucleofector II device	Lonza (Basel, CH)
Analytical balance ABJ 220-4NM	Kern & Sohn (Balingen-Frommern, Germany)
Bacteria shaker	
Centrifuge 5415D, 5424R	Eppendorf (Hamburg, Germany)
Centrifuge Hareaus Megafuge 40R	Thermo Fisher Scientific (Waltham, MA, USA)
CO2 incubator C 170	BINDER (Tuttlingen, Germany)
E-BOX VX2	Vilber Lourmat (Eberhardzell, Germany)
FACS Calibur	BD Biosciences (Franklin Lakes, NJ, USA)
FACS Canto II	BD Biosciences (Franklin Lakes, NJ, USA)
FACS Vantage SE	BD Biosciences (Franklin Lakes, NJ, USA)
Fluorescent microscope DMi8	Leica Microsystems (Wetzlar, Germany)
Freezer -20°C	Liebherr (Bulle FR, Switzerland)
Freezer -80°C, TLE	Thermo Fisher Scientific (Waltham, MA, USA)
Freezing container "Mr. Frosty"	Thermo Fisher Scientific (Waltham, MA, USA)
Fusion SL4 imaging system	Vilber Lourmat (Eberhardzell, Germany)
Heating block "Thermomixer compact"	Eppendorf (Hamburg, Germany)
Ice machine FM-170AKE	Hoshizaki (Amsterdam, NL)
Incubator 9040-0013	BINDER (Tuttlingen, Germany)
Liquid Nitrogen Tank	Cryoson (Schöllkrippen, Germany)
Magnetic stirrer IKAMAG "Big Squid Hibiskus"	IKA (Staufen, Germany)
Microplate reader GloMax® Discover	Promega (Madison, WI, USA)
Microscope ID03	Carl Zeiss (Oberkochen, Germany)

Nanodrop spectrophotometer 1000	Thermo Fisher Scientific (Waltham, MA, USA)
PCR cycler PeqSTAR 2x Gradient	Peqlab (Wilmington, DE, USA)
PCR cycler PeqSTAR 2x Universal	Peqlab (Wilmington, DE, USA)
pH meter inoLab® pH 7110	WTW (Weilheim, Germany)
Pipettes (0.25-2.00µL, 2.0-20.0µL, 20-200µL, 200-1000µL)	Eppendorf (Hamburg, Germany)
Pipetus accu-jet pro	Brand (Wertheim, Germany)
Precision weighing scale PCB 2500-2	Kern & Sohn (Balingen-Frommern, Germany)
Real-Time PCR Detection System CFX96 Touch	Bio-Rad (Hercules, CA, USA)
Tube roller RS-TR 5	Phoenix instrument (Garbsen, Germany)
Ultrapure water system Milli-Q System	Merck Millipore (Darmstadt, Germany)
VARIOKLAV Type 500	HP Medizintechnik (Oberschleißheim, Germany)
Vertical Autoclave VX-150	Systec (Linden, Germany)
Vi-CELL XR Cell Viability Analyzer	Beckman Coulter (Krefeld, Germany)
Vortex Mixer Vortex-Genie 2	Scientific Industries SI (Bohemia, NY, USA)
Water Bath Hydro	Lauda, GFL-technology (Lauda, Germany)
Xcell SureLock Mini Cell	Invitrogen (Darmstadt, Germany)

Table 7: Laboratory Equipment

4.2.4 Consumables

Consumable	Company
96-well V-bottom	Greiner Bio One (Frickenhausen, Germany)
Amersham Protran Nitrocellulose membrane, 0.45µM	GE Healthcare (Little Chalfont, UK)
Cell scraper	
Combitips advanced 0.5mL	Eppendorf (Hamburg, Germany)
Combitips advanced 1.0mL	Eppendorf (Hamburg, Germany)
Combitips advanced 5.0mL	Eppendorf (Hamburg, Germany)
Cryo Tube Nunc	Thermo Fisher Scientific (Waltham, MA, USA)
Disposable bags	Brand (Wertheim, Germany)
DURAN Erlenmeyer flasks (50mL, 250mL, 500mL, 1000mL)	DURAN Group (Mainz, Germany)
DURAN GL 45 Lab Bottles (100mL, 250mL, 500mL, 1000mL)	DURAN Group (Mainz, Germany)
Gel-loading pipette tips	Sigma-Aldrich (St. Louis, MO, USA)
Micro tube SafeSeal 1.5mL	Sarstedt (Nümbrecht, Germany)
Micro tube SafeSeal 2.0mL	Sarstedt (Nümbrecht, Germany)
Novex Empty Gel Cassette, mini, 1.0mm	Thermo Fisher Scientific (Waltham, MA, USA)
PARAFILM	Sigma-Aldrich (St. Louis, MO, USA)
PCR tubes 0.2mL	Biozym Scientific (Oldendorf, Germany)
Petri dish 10cm	Sarstedt (Nümbrecht, Germany)
Round Base Polystyrene Tube 5ml (FACS)	Thermo Fisher Scientific (Waltham, MA, USA)
Round Base Polystyrene Tube 5ml (FACS)	Sarstedt (Nümbrecht, Germany)

Round Bottom Polypropylene Tube 14ml (Bacteria culture)	Falcon, Corning (Corning, NY, USA)
Serological pipettes 25ml	Greiner Bio One (Frickenhausen, Germany)
Serological pipettes Stripette 10ml	Corning (Corning, NY, USA)
Serological pipettes Stripette 5ml	Corning (Corning, NY, USA)
Sorenson low binding standard tips	Sigma-Aldrich (St. Louis, MO, USA)
TC Flask T25, T75, T175, standard	Sarstedt (Nümbrecht, Germany)
TC Flask T25, T75, T175, suspension	Sarstedt (Nümbrecht, Germany)
TC Plate 6-, 24-, 48-, 96-well, suspension	Sarstedt (Nümbrecht, Germany)
TC Plate 6-, 24-, 48-, 96-well, standard	Sarstedt (Nümbrecht, Germany)
TipOne pipette tips 10µl	Starlab (Hamburg, Germany)
TipOne pipette tips 1000µl	Starlab (Hamburg, Germany)
TipOne pipette tips 200µl	Starlab (Hamburg, Germany)
Tube 15mL	Sarstedt (Nümbrecht, Germany)
Tube 50mL	Sarstedt (Nümbrecht, Germany)
Vasco Nitrile Blue Gloves	B. Braun (Melsungen, Germany)

Table 8: Consumables

4.2.5 Restriction Enzymes

Enzyme/Buffer	Company
Acc65I	Fermentas, Thermo Fisher Scientific (Waltham, MA, USA)
AfeI	Fermentas, Thermo Fisher Scientific (Waltham, MA, USA)
AsiSI	New England Biolabs (Frankfurt, Germany)
BbsI (BpiI)	Fermentas, Thermo Fisher Scientific (Waltham, MA, USA)
BglII	New England Biolabs (Frankfurt, Germany)
DNase I, RNase free	Thermo Fisher Scientific (Waltham, MA, USA)
DpnI	New England Biolabs (Frankfurt, Germany)
EcoRI	New England Biolabs (Frankfurt, Germany)
EcoRI	Fermentas, Thermo Fisher Scientific (Waltham, MA, USA)
NdeI	New England Biolabs (Frankfurt, Germany)
NdeI	Fermentas, Thermo Fisher Scientific (Waltham, MA, USA)
NEBuffer 2.1	New England Biolabs (Frankfurt, Germany)
NEBuffer 3.1	New England Biolabs (Frankfurt, Germany)
NotI	Fermentas, Thermo Fisher Scientific (Waltham, MA, USA)
T4 Ligase	New England Biolabs (Frankfurt, Germany)
T4 Ligation Buffer	New England Biolabs (Frankfurt, Germany)
Tango Buffer	Fermentas, Thermo Fisher Scientific (Waltham, MA, USA)

XbaI	Fermentas, Thermo Fisher Scientific (Waltham, MA, USA)
XhoI	New England Biolabs (Frankfurt, Germany)
XhoI	Fermentas, Thermo Fisher Scientific (Waltham, MA, USA)

Table 9: Restriction Enzymes and buffers

4.2.6 Antibodies

Antibody	Host	Dilution	Company
Actin	Rabbit	1:10000	Santa Cruz Biotechnology (Dallas, TX, USA)
CSF3R	Rabbit	1:2000	Abcam (Cambridge, UK)
ERK 1/2	Rabbit	1:1000	Santa Cruz Biotechnology (Dallas, TX, USA)
GAPDH	Mouse	1:10000	Santa Cruz Biotechnology (Dallas, TX, USA)
GLI2	Rabbit	1:1000	Thermo Fisher Scientific (Waltham, MA, USA)
GLI2	Rabbit	1:1000	Thermo Fisher Scientific (Waltham, MA, USA)
His	Rabbit	1:5000	Santa Cruz Biotechnology (Dallas, TX, USA)
JAK2	Rabbit	1:2000	Cell Signaling Technologies (Danvers, MA, USA)
pERK 1/2	Mouse	1:1000	Santa Cruz Biotechnology (Dallas, TX, USA)

pJAK2 (Tyr1007/1008)	Rabbit	1:2000	Cell Signaling Technologies (Danvers, MA, USA)
pStat3 (Tyr705)	Rabbit	1:2000	Cell Signaling Technologies (Danvers, MA, USA)
Stat3	Rabbit	1:2000	Cell Signaling Technologies (Danvers, MA, USA)

Table 10: Western Blot – Primary Antibodies

Antibody	Host	Dilution	Company
Mouse	Goat	1:10000	Santa Cruz Biotechnology (Dallas, TX, USA)
Rabbit	Goat	1:10000	Santa Cruz Biotechnology (Dallas, TX, USA)

Table 11: Western Blot – Secondary Antibodies

Antibody	Conjugate	Isotype	Dilution	Company
Annexin V	APC	Protein-Dye	1:25	BD Biosciences (Franklin Lakes, NJ, USA)
CD10	PE-Cy7	Mouse IgG1, κ	1:50	Biolegend (San Diego, CA, USA)
CD114	APC	Mouse IgG1, κ	1:11	Miltenyi Biotech (Bergisch Gladbach, Germany)
CD114	PE	Mouse IgG1, κ	1:11	Miltenyi Biotech (Bergisch Gladbach, Germany)
CD117	APC	Mouse IgG1, κ	1:50	BD Biosciences (Franklin Lakes, NJ, USA)

CD11b	PE-Cy7	Mouse IgG1, κ	1:50	BD Biosciences (Franklin Lakes, NJ, USA)
CD11c	APC	Mouse IgG1, κ	1:50	BD Biosciences (Franklin Lakes, NJ, USA)
CD13	APC	Recombinant human IgG1	1:50	Miltenyi Biotech (Bergisch Gladbach, Germany)
CD135	PE-Vio770	Recombinant human IgG1	1:50	Miltenyi Biotech (Bergisch Gladbach, Germany)
CD14	PE-Cy7	Mouse IgG2a, κ	1:50	BD Biosciences (Franklin Lakes, NJ, USA)
CD15	APC	Mouse IgM	1:50	BD Biosciences (Franklin Lakes, NJ, USA)
CD18	PE-Vio770	Mouse IgG1, κ	1:50	Miltenyi Biotech (Bergisch Gladbach, Germany)
CD19	APC	Mouse IgG1, κ	1:50	BD Biosciences (Franklin Lakes, NJ, USA)
CD27	PE-Vio770	Mouse IgG1, κ	1:50	Miltenyi Biotech (Bergisch Gladbach, Germany)
CD3	PE-Vio770	Mouse IgG2a, κ	1:50	Miltenyi Biotech (Bergisch Gladbach, Germany)
CD33	APC	Recombinant human IgG1	1:50	Miltenyi Biotech (Bergisch Gladbach, Germany)
CD34	APC	Mouse IgG1, κ	1:50	BD Biosciences (Franklin Lakes, NJ, USA)
CD41a	PE-Cy7	Mouse IgG1, κ	1:50	Thermo Fisher Scientific (Waltham, MA, USA)

CD45	APC	Mouse IgG1, κ	1:20	Thermo Fisher Scientific (Waltham, MA, USA)
CD49a	APC	Mouse IgG1, κ	1:50	Miltenyi Biotech (Bergisch Gladbach, Germany)
CD80	PE		1:20	
DAPI	Unc.	Dye	1:500	
DRAQ5 5mM	Unc.	Dye	1:500	Alexis Biochemicals (Lausanne, CH)
Fc Block	Unc.	Human IgG1	1:100	BD Biosciences (Franklin Lakes, NJ, USA)
HLA-DR	APC	Recombinant human IgG1	1:50	Miltenyi Biotech (Bergisch Gladbach, Germany)
Isotype Control	APC	Mouse IgG1, κ	1:50	BD Biosciences (Franklin Lakes, NJ, USA)
Isotype Control	PE-Vio770	Mouse IgG2a, κ	1:50	Miltenyi Biotech (Bergisch Gladbach, Germany)
Isotype Control	PE-Cy7	Mouse IgG2a, κ	1:50	BD Biosciences (Franklin Lakes, NJ, USA)
Isotype Control	APC	Mouse IgG1, κ	1:50	BD Biosciences (Franklin Lakes, NJ, USA)
Isotype Control	PE-Cy7	Mouse IgG1, κ	1:50	BD Biosciences (Franklin Lakes, NJ, USA)
Isotype Control	PE-Vio770	Mouse IgG1, κ	1:50	Miltenyi Biotech (Bergisch Gladbach, Germany)
Isotype Control	APC	Mouse IgM	1:50	BD Biosciences (Franklin Lakes, NJ, USA)

Isotype Control	APC	Recombinant human IgG1	1:50	Miltenyi Biotech (Bergisch Gladbach, Germany)
Isotype Control	PE-Vio770	Recombinant human IgG1	1:50	Miltenyi Biotech (Bergisch Gladbach, Germany)
Isotype Control	PE	Mouse IgG2a, κ	1:50	BD Biosciences (Franklin Lakes, NJ, USA)
Isotype Control	PE	Mouse IgG1, κ	1:50	BD Biosciences (Franklin Lakes, NJ, USA)
pStat3 (pY705)	PE	Mouse IgG2a, κ	1:20	BD Biosciences (Franklin Lakes, NJ, USA)

Table 12: FACS Antibodies

4.2.7 Commercial Kits

Kit	Company
Cell line nucleofector kit	Lonza (Basel, CH)
Cell line optimization nucleofector kit	Lonza (Basel, CH)
Endofree Plasmid Maxi Kit	Qiagen (Hilden, Germany)
MycoAlert Mycoplasma Deetection Kit	Lonza (Basel, CH)
QIAamp DNA Blood Mini Kit	Qiagen (Hilden, Germany)
QIAprep Spin Miniprep Kit	Qiagen (Hilden, Germany)
QIAquick Gel Extraction Kit	Qiagen (Hilden, Germany)
QIAquick PCR Purification Kit	Qiagen (Hilden, Germany)
RNeasy Mini Kit	Qiagen (Hilden, Germany)
NEBuilder HiFi DNA Assembly Kit	New England Biolabs (Frankfurt, Germany)
Chromium Next GEM Single Cell 3' Kit v3.1	10x Genomics (Pleasanton, CA, USA)

Cell titer Blue Viability Assay	Promega (Madison, WI, USA)
iScript cDNA Synthesis Kit	Bio-Rad (Hercules, CA, USA)
iTaq Universal SYBR Green Supermix	Bio-Rad (Hercules, CA, USA)
PrimePCR Custom Assay	Bio-Rad (Hercules, CA, USA)

Table 13: Commercial Kits

4.2.8 Inhibitors and Cytostatics

Inhibitor	Provider	Solvent	Temp (°C)
Ruxolitinib Phosphate	ChemScene (Monmoth Junction, NJ, USA)	DMSO	-80
C188-9	EMD Merck Millipore (Darmstadt, Germany)	DMSO	-80
GANT 61	Tocris Bioscience (Bristol, UK)	DMSO	-20

Table 14: Inhibitors and Cytostatics

4.2.9 Software

Software	Application	Provider
Biorender	Illustrations and figure design	Biorender AG (Münchwilen TG, CH)
CFX-Manager	RT-qPCR data analysis	Bio-Rad (Hercules, CA, USA)
E-Capt 15.06	Agarose gel recording	Vilber Lourmat (Eberhardzell, Germany)
FACSDiva Software	Flow cytometry data acquisation	BD Biosciences (Franklin Lakes, NJ, USA)
FlowJo Software v.10	Flow cytometry data analysis	BD Biosciences (Franklin Lakes, NJ, USA)
FusionCapt Advance 16.11	Western blot recording	Vilber Lourmat (Eberhardzell, Germany)
GraphPad Prism 9	Data visualization, statistical analysis	GraphPad Software (La Jolla, CA, USA)
IBS	Design and presentation of biological sequences	CUCKOO Workgroup, webbased
Microsoft Office 2010, 365	Text editing, Data analysis, Presentations	Microsoft (Redmond, WA, USA)
SnapGene 3.3.4	Primer design, creation and inspection of vector maps	GSL Biotech LLC (Chicago, IL, USA)

Table 15: Software

References

1. Zhang, Y. *et al.* CSF3R Mutations are frequently associated with abnormalities of RUNX1, CBFB, CEBPA, and NPM1 genes in acute myeloid leukemia. *Cancer* (2018) doi:10.1002/cncr.31586.

2. Opatz, S. *et al.* The clinical mutatome of core binding factor leukemia. *Leukemia* **34**, 1553–1562 (2020).

3. Christen, F. *et al.* Genomic landscape and clonal evolution of acute myeloid leukemia with t(8;21): an international study on 331 patients. (2019).

4. Tarlock, K. *et al.* Prognostic impact of CSF3R mutations in favorable risk childhood acute myeloid leukemia. *Blood* **135**, 1603–1606 (2020).

5. Bonnet, D. & Dick, J. E. Human acute myeloid leukemia is organized as a hierarchy that originates from a primitive hematopoietic cell. *Nat Med* (1997) doi:10.1038/nm0797-730.

6. Fialkow, P. J. *et al.* Clonal development, stem-cell differentiation, and clinical remissions in acute nonlymphocytic leukemia. *N Engl J Med* **317**, 468–473 (1987).

7. Onciu, M. Acute Lymphoblastic Leukemia. *Hematol Oncol Clin North Am* **23**, 655–674 (2009).

8. De Kouchkovsky, I. & Abdul-Hay, M. 'Acute myeloid leukemia: a comprehensive review and 2016 update'. *Blood Cancer J* **6**, e441–e441 (2016).

9. Döhner, H., Weisdorf, D. J. & Bloomfield, C. D. Acute Myeloid Leukemia. *New England Journal of Medicine* **373**, 1136–1152 (2015).

10. WHO. World fact sheets cancers. *Globocan 2020* **419**, 1–2 (2020).

11. Tumorregister München. *Akute Myeloische Leukämie - Inzidenz Und Mortalität*. https://www.tumorregister-muenchen.de (2021).

12. MLL Münchner Leukämielabor GmbH. AML (akute myeloische Leukämie) - Diagnostische Empfehlung. 1–9 https://www.mll.com/erkrankungendiagnostik/akute-myeloische-leukaemie-aml/akute-myeloische-leukaemie-aml.html (2020).

13. Döhner, H. *et al.* Diagnosis and management of acute myeloid leukemia in adults: Recommendations from an international expert panel, on behalf of the European LeukemiaNet. *Blood* **115**, 453–474 (2010).

14. Thol, F. & Ganser, A. Treatment of Relapsed Acute Myeloid Leukemia. *Curr Treat Options Oncol* **21**, 66 (2020).

15. Sekeres, M. A. & Gerds, A. T. Mitigating Fear and Loathing in Managing Acute Myeloid Leukemia. *Semin Hematol* **52**, 249–255 (2015).

16. Swerdlow, S. H. *et al.* WHO Classification of Tumours of Haematopoietic and Lymphoid Tissues. Preprint at http://apps.who.int/bookorders/anglais/detart1.jsp?codlan=1&codcol=70&codcch=4002 (2008).

17. Khoury, J. D. *et al.* The 5th edition of the World Health Organization Classification of Haematolymphoid Tumours: Myeloid and Histiocytic/Dendritic Neoplasms. *Leukemia 2022 36:7* **36**, 1703–1719 (2022).

18. Grimwade, D. & Mrózek, K. Diagnostic and Prognostic Value of Cytogenetics in Acute Myeloid Leukemia. *Hematol Oncol Clin North Am* **25**, 1135–1161 (2011).

19. Arber, D. A. *et al.* The 2016 revision to the World Health Organization classification of myeloid neoplasms and acute leukemia. *Blood* **127**, 2391–2405 (2016).

20. Craig, F. E. & Foon, K. A. Flow cytometric immunophenotyping for hematologic neoplasms. *Blood* **111**, 3941–3967 (2008).

21. Bene, M. C. *et al.* Proposals for the immunological classification of acute leukemias. European Group for the Immunological Characterization of Leukemias (EGIL). *Leukemia* vol. 9 1783–1786 Preprint at (1995).

22. Khalidi, H. S. *et al.* The immunophenotype of adult acute myeloid leukemia: high frequency of lymphoid antigen expression and comparison of immunophenotype, French-American-British classification, and karyotypic abnormalities. *Am J Clin Pathol* **109**, 211–220 (1998).

23. Mrózek, K. *et al.* Comparison of cytogenetic and molecular genetic detection of t(8;21) and inv(16) in a prospective series of adults with de novo acute myeloid leukemia: a Cancer and Leukemia Group B Study. *J Clin Oncol* **19**, 2482–2492 (2001).

24. Grimwade, D. Screening for core binding factor gene rearrangements in acute myeloid leukemia. *Leukemia* **16**, 964–969 (2002).

25. Döhner, H. *et al.* Diagnosis and management of AML in adults: 2017 ELN recommendations from an international expert panel. *Blood* **129**, 424–447 (2017).

26. Haferlach, T. Advancing leukemia diagnostics: Role of Next Generation Sequencing (NGS) in acute myeloid leukemia. *Hematol Rep* **12**, 8957 (2020).

27. Bennett, J. M. *et al.* Proposals for the Classification of the Acute Leukaemias French-American-British (FAB) Co-operative Group. *Br J Haematol* **33**, 451–458 (1976).

28. Vardiman, J. W. *et al.* The 2008 revision of the World Health Organization (WHO) classification of myeloid neoplasms and acute leukemia: rationale and important changes. *Blood* **114**, 937–951 (2009).

29. Jaffe, E. S. *Pathology and Genetics of Tumours of Haematopoietic and Lymphoid Tissues*. vol. 3 (Iarc, 2001).

30. Tallman, M. S. *et al.* Acute myeloid leukemia, version 3.2019. *JNCCN Journal of the National Comprehensive Cancer Network* **17**, 721–749 (2019).

31. Dombret, H. & Gardin, C. An update of current treatments for adult acute myeloid leukemia. *Blood* **127**, 53–61 (2016).

32. Petersdorf, S. H. *et al.* A phase 3 study of gemtuzumab ozogamicin during induction and postconsolidation therapy in younger patients with acute myeloid leukemia. *Blood* **121**, 4854–4860 (2013).

33. Burnett, A. K. *et al.* Identification of Patients With Acute Myeloblastic Leukemia Who Benefit From the Addition of Gemtuzumab Ozogamicin: Results of the MRC AML15 Trial. *Journal of Clinical Oncology* **29**, 369–377 (2010).

34. Hills, R. K. *et al.* Addition of gemtuzumab ozogamicin to induction chemotherapy in adult patients with acute myeloid leukaemia: a meta-analysis of individual patient data from randomised controlled trials. *Lancet Oncol* **15**, 986–996 (2014).

35. Castaigne, S. *et al.* Effect of gemtuzumab ozogamicin on survival of adult patients with de-novo acute myeloid leukaemia (ALFA-0701): a randomised, open-label, phase 3 study. *Lancet* **379**, 1508–1516 (2012).

36. Burnett, A. K. *et al.* Addition of gemtuzumab ozogamicin to induction chemotherapy improves survival in older patients with acute myeloid leukemia. *J Clin Oncol* **30**, 3924–3931 (2012).

37. Amadori, S. *et al.* Sequential combination of gemtuzumab ozogamicin and standard chemotherapy in older patients with newly diagnosed acute myeloid leukemia: results of a randomized phase III trial by the EORTC and GIMEMA consortium (AML-17). *J Clin Oncol* **31**, 4424–4430 (2013).

38. Stone, R. M. *et al.* Midostaurin plus Chemotherapy for Acute Myeloid Leukemia with a FLT3 Mutation. *N Engl J Med* **377**, 454–464 (2017).

39. Stone, R. M. *et al.* Phase IB study of the FLT3 kinase inhibitor midostaurin with chemotherapy in younger newly diagnosed adult patients with acute myeloid leukemia. *Leukemia* **26**, 2061–2068 (2012).

40. Fischer, T. *et al.* Phase IIB trial of oral Midostaurin (PKC412), the FMS-like tyrosine kinase 3 receptor (FLT3) and multi-targeted kinase inhibitor, in patients with acute myeloid leukemia and high-risk myelodysplastic syndrome with either wild-type or mutated FLT3. *J Clin Oncol* **28**, 4339–4345 (2010).

41. European Medicines Agency. Summary of opinion (initial authorisation): Daurismo (glasdegib). vol. 1 222209 https://www.ema.europa.eu/en/documents/smop-initial/chmp-summary-positive-opinion-daurismo_en.pdf (2020).

42. US Food and Drug Administration. Highlights of prescribing information: DAURISMO™ 2018. https://www.accessdata.fda.gov/drugsatfda_docs/label/2018/210656s000lbl.pdf (2018).

43. Speck, N. A. & Gilliland, D. G. Core-binding factors in haematopoiesis and leukaemia. *Nat Rev Cancer* **2**, 502–513 (2002).

44. Cozzio, A. *et al.* Similar MLL-associated leukemias arising from self-renewing stem cells and short-lived myeloid progenitors. *Genes Dev* **17**, 3029 (2003).

45. Tan, B. T., Park, C. Y., Ailles, L. E. & Weissman, I. L. The cancer stem cell hypothesis: a work in progress. *Laboratory Investigation 2006 86:12* **86**, 1203–1207 (2006).

46. Chopra, M. & Bohlander, S. K. The cell of origin and the leukemia stem cell in acute myeloid leukemia. *Genes Chromosomes Cancer* **58**, 850–858 (2019).

47. Rowley, J. D. Identificaton of a translocation with quinacrine fluorescence in a patient with acute leukemia. *Ann Genet* **16**, 109–112 (1973).

48. Rowley, J. D., Golomb, H. M. & Dougherty, C. 15/17 translocation, a consistent chromosomal change in acute promyelocytic leukaemia. *Lancet (London, England)* vol. 1 549–550 Preprint at https://doi.org/10.1016/s0140-6736(77)91415-5 (1977).

49. Beghini, A. Core binding factor Leukemia: Chromatin remodeling moves towards oncogenic transcription. *Cancers* vol. 11 1973 Preprint at https://doi.org/10.3390/cancers11121973 (2019).

50. Okuda, T., Van Deursen, J., Hiebert, S. W., Grosveld, G. & Downing, J. R. AML1, the target of multiple chromosomal translocations in human leukemia, is essential for normal fetal liver hematopoiesis. *Cell* **84**, 321–330 (1996).

51. Wang, Q. *et al.* Disruption of the Cbfa2 gene causes necrosis and hemorrhaging in the central nervous system and blocks definitive hematopoiesis. *Proc Natl Acad Sci U S A* **93**, 3444–3449 (1996).

52. Ducy, P. & Zhang, R. *Osf2/Cbfa1: A Transcriptional Activator of Osteoblast Differentiation*. *Cell* vol. 89 (1997).

53. Banerjee, C. *et al.* Runt homology domain proteins in osteoblast differentiation: AML3/CBFA1 is a major component of a bone-specific complex. *J Cell Biochem* **66**, (1997).

54. Levanon, D. *et al.* Transcription Factor Runx3 Regulates Interleukin-15-Dependent Natural Killer Cell Activation. *Mol Cell Biol* **34**, 1158 (2014).

55. Fainaru, O. *et al.* Runx3 regulates mouse TGF-β-mediated dendritic cell function and its absence results in airway inflammation. *EMBO Journal* **23**, 969–979 (2004).

56. Fainaru, O., Shseyov, D., Hantisteanu, S. & Groner, Y. Accelerated chemokine receptor 7-mediated dendritic cell migration in RunxB knockout mice and the spontaneous development of asthma-like disease. *Proc Natl Acad Sci U S A* **102**, 10598–10603 (2005).

57. Wang, C. Q. *et al.* Runx3 deficiency results in myeloproliferative disorder in aged mice. *Blood* **122**, 562–566 (2013).

58. Levanon, D. *et al.* The Runx3 transcription factor regulates development and survival of TrkC dorsal root ganglia neurons. *EMBO J* **21**, 3454 (2002).

59. Lallemend, F. *et al.* Positional differences of axon growth rates between sensory neurons encoded by runx3. *EMBO Journal* **31**, 3718–3729 (2012).

60. Inoue, K. ichi *et al.* Runx3 controls the axonal projection of proprioceptive dorsal root ganglion neurons. *Nature Neuroscience 2002 5:10* **5**, 946–954 (2002).

61. Li, Q. L. *et al.* Causal relationship between the loss of RUNX3 expression and gastric cancer. *Cell* **109**, 113–124 (2002).

62. Fukamachi, H. Runx3 controls growth and differentiation of gastric epithelial cells in mammals. *Dev Growth Differ* **48**, 1–13 (2006).

63. Fukamachi, H. & Ito, K. Growth regulation of gastric epithelial cells by Runx3. *Oncogene* **23**, 4330–4335 (2004).

64. Chi, X.-Z. *et al.* RUNX3 Suppresses Gastric Epithelial Cell Growth by Inducing p21 WAF1 / Cip1 Expression in Cooperation with Transforming Growth Factor β-Activated SMAD . *Mol Cell Biol* **25**, 8097–8107 (2005).

65. Ogawa, E. *et al.* Molecular cloning and characterization of pebp2β, the heterodimeric partner of a novel drosophila runt-related dna binding protein pebp2α. *Virology* **194**, 314–331 (1993).

66. Wang, S. *et al. Cloning and Characterization of Subunits of the T-Cell Receptor and Murine Leukemia Virus Enhancer Core-Binding Factor*. *MOLECULAR AND CELLULAR BIOLOGY* vol. 13 (1993).

67. Huang, G. *et al.* Dimerization with PEBP2β protects RUNX1/AML1 from ubiquitin-proteasome-mediated degradation. *EMBO Journal* **20**, 723–733 (2001).

68. Li, L. H. & Gergen, J. P. Differential interactions between Brother proteins and Runt domain proteins in the Drosophila embryo and eye. *Development* **126**, 3313–3322 (1999).

69. Wang, Q. *et al.* The CBFβ Subunit Is Essential for CBFα2 (AML1) Function In Vivo. *Cell* **87**, 697–708 (1996).

70. Lukasik, S. M. *et al.* Altered affinity of a cbfβ-smmhc for runx1 explains its role in leukemogenesis. *Nat Struct Biol* **9**, 674–679 (2002).

71. Huang, G. *et al.* Molecular basis for a dominant inactivation of RUNX1/AML1 by the leukemogenic inversion 16 chimera. *Blood* **103**, 3200–3207 (2004).

72. Yi, G. *et al.* CBFβ-MYH11 interferes with megakaryocyte differentiation via modulating a gene program that includes GATA2 and KLF1. *Blood Cancer J* **9**, 1–13 (2019).

73. Zhen, T. *et al.* RUNX1 and CBFb-SMMHC transactivate target genes together in abnormal myeloid progenitors for leukemia development. *Blood* **136**, 2373–2385 (2020).

74. Hyde, R. K., Zhao, L., Alemu, L. & Liu, P. P. Runx1 is required for hematopoietic defects and leukemogenesis in Cbfb-MYH11 knock-in mice. *Leukemia* **29**, 1771–1778 (2015).

75. Richter, L. E. *et al.* HDAC1 is a required cofactor of CBFb-SMMHC and a potential therapeutic target in inversion 16 acute myeloid leukemia. *Molecular Cancer Research* **17**, 1241–1252 (2019).

76. Kamikubo, Y. *et al.* Accelerated Leukemogenesis by Truncated CBFβ-SMMHC Defective in High-Affinity Binding with RUNX1. *Cancer Cell* **17**, 455–468 (2010).

77. Meyers, S., Lenny, N. & Hiebert, S. W. The t(8;21) fusion protein interferes with AML-1B-dependent transcriptional activation. *Mol Cell Biol* **15**, 1974–1982 (1995).

78. Vangala, R. K. *et al.* The myeloid master regulator transcription factor PU.1 is inactivated by AML1-ETO in t(8;21) myeloid leukemia. *Blood* **101**, 270–277 (2003).

79. Pabst, T. *et al.* AML1-ETO downregulates the granulocytic differentiation factor C/EBPα in t(8;21) myeloid leukemia. *Nat Med* **7**, 444–451 (2001).

80. Linggi, B. *et al.* The t(8;21) fusion protein, AML1-ETO, specifically represses the transcription of the p14ARF tumor suppressor in acute myeloid leukemia. *Nat Med* **8**, 743–750 (2002).

81. Liu, S. *et al.* Interplay of RUNX1/MTG8 and DNA methyltransferase 1 in acute myeloid leukemia. *Cancer Res* **65**, 1277–1284 (2005).

82. Wang, J., Hoshino, T., Redner, R. L., Kajigaya, S. & Liu, J. M. ETO, fusion partner in t(8;21) acute myeloid leukemia, represses transcription by interaction with the human N-CoR/mSin3/HDAC1 complex. *Proc Natl Acad Sci U S A* **95**, 10860–10865 (1998).

83. Friedman, A. D. C/EBPα in normal and malignant myelopoiesis. *International Journal of Hematology* vol. 101 330–341 Preprint at https://doi.org/10.1007/s12185-015-1764-6 (2015).

84. Gao, X. N. *et al.* AML1/ETO cooperates with HIF1α to promote leukemogenesis through DNMT3a transactivation. *Leukemia* **29**, 1730–1740 (2015).

85. Lutterbach, B. *et al.* ETO, a Target of t(8;21) in Acute Leukemia, Interacts with the N-CoR and mSin3 Corepressors. *Mol Cell Biol* **18**, 7176–7184 (1998).

86. Gelmetti, V. *et al.* Aberrant Recruitment of the Nuclear Receptor Corepressor-Histone Deacetylase Complex by the Acute Myeloid Leukemia Fusion Partner ETO. *Mol Cell Biol* **18**, 7185–7191 (1998).

87. Rhoades, K. L. *et al.* Synergistic up-regulation of the myeloid-specific promoter for the macrophage colony-stimulating factor receptor by AML1 and the t(8;21) fusion protein may contribute to leukemogenesis. *Proc Natl Acad Sci U S A* **93**, 11895–11900 (1996).

88. Shimizu, K. *et al.* AML1-MTG8 leukemic protein induces the expression of granulocyte colony-stimulating factor (G-CSF) receptor through the up-regulation of CCAAT/enhancer binding protein epsilon. *Blood* **96**, 288–296 (2000).

89. Kundu, M. & Liu, P. P. Function of the inv(16) fusion gene CBFB-MYH11. *Current Opinion in Hematology* vol. 8 201–205 Preprint at https://doi.org/10.1097/00062752-200107000-00004 (2001).

90. Castilla, L. H. *et al.* The fusion gene Cbfb-MYH11 blocks myeloid differentiation and predisposes mice to acute myelomonocytic leukaemia [4]. *Nature Genetics* vol. 23 144–146 Preprint at https://doi.org/10.1038/13776 (1999).

91. Kuo, Y. H. *et al.* Cbfβ-SMMHC induces distinct abnormal myeloid progenitors able to develop acute myeloid leukemia. *Cancer Cell* **9**, 57–68 (2006).

92. Higuchi, M. *et al.* Expression of a conditional AML1-ETO oncogene bypasses embryonic lethality and establishes a murine model of human t(8;21) acute myeloid leukemia. *Cancer Cell* **1**, 63–74 (2002).

93. Downing, J. R. AML1/CBFβ transcription complex: Its role in normal hematopoiesis and leukemia. *Leukemia* vol. 15 664–665 Preprint at https://doi.org/10.1038/sj.leu.2402035 (2001).

94. Mulloy, J. C. *et al.* The AML1-ETO fusion protein promotes the expansion of human hematopoietic stem cells. *Blood* **99**, 15–23 (2002).

95. Faber, Z. J. *et al.* The genomic landscape of core-binding factor acute myeloid leukemias. *Nat Genet* **48**, 1551–1556 (2016).

96. Boissel, N. *et al.* Incidence and prognostic impact of c-Kit, FLT3, and Ras gene mutations in core binding factor acute myeloid leukemia (CBF-AML). *Leukemia* **20**, 965–970 (2006).

97. Bowen, D. T. *et al.* RAS mutation in acute myeloid leukemia is associated with distinct cytogenetic subgroups but does not influence outcome in patients younger than 60 years. *Blood* **106**, 2113–2119 (2005).

98. Goemans, B. F. *et al.* Mutations in KIT and RAS are frequent events in pediatric core-binding factor acute myeloid leukemia. *Leukemia* **19**, 1536–1542 (2005).

99. Valk, P. *et al.* Second hit mutations in the RTK/RAS signaling pathway in acute myeloid leukemia with inv(16). *Haematologica* **89**, 106–106 (2004).

100. Beghini, A. *et al.* C-kit mutations in core binding factor leukemias [3]. *Blood* vol. 95 726–727 Preprint at https://doi.org/10.1182/blood.v95.2.726 (2000).

101. Kühn, M. W. M. *et al.* High-resolution genomic profiling of adult and pediatric core-binding factor acute myeloid leukemia reveals new recurrent genomic alterations. *Blood* **119**, e67 (2012).

102. Shima, T. *et al.* The ordered acquisition of Class II and Class I mutations directs formation of human t(8;21) acute myelogenous leukemia stem cell. *Exp Hematol* **42**, 955-965.e5 (2014).

103. Castilla, L. H. *et al.* Failure of embryonic hematopoiesis and lethal hemorrhages in mouse embryos heterozygous for a knocked-in leukemia gene CBFB-MYH11. *Cell* **87**, 687–696 (1996).

104. Castilla, L. H. *et al.* Identification of genes that synergize with Cbfb-MYH11 in the pathogenesis of acute myeloid leukemia. *Proc Natl Acad Sci U S A* **101**, 4924–4929 (2004).

105. Schoch, C. *et al.* Acute myeloid leukemias with reciprocal rearrangements can be distinguished by specific gene expression profiles. *Proc Natl Acad Sci U S A* **99**, 10008–10013 (2002).

106. Tyner, J. W. *et al.* Functional genomic landscape of acute myeloid leukaemia. *Nature* **562**, 526–531 (2018).

107. Müller-Tidow, C. *et al.* Translocation Products in Acute Myeloid Leukemia Activate the Wnt Signaling Pathway in Hematopoietic Cells. *Mol Cell Biol* **24**, 2890–2904 (2004).

108. Yuan, Y. *et al.* AML1-ETO expression is directly involved in the development of acute myeloid leukemia in the presence of additional mutations. *Proc Natl Acad Sci U S A* **98**, 10398–10403 (2001).

109. Mulloy, J. C. *et al.* Maintaining the self-renewal and differentiation potential of human CD34+ hematopoietic cells using a single genetic element. *Blood* **102**, 4369–4376 (2003).

110. Mulloy, J. C. *et al.* AML1-ETO fusion protein up-regulates TRKA mRNA expression in human CD34+ cells, allowing nerve growth factor-induced expansion. *Proc Natl Acad Sci U S A* **102**, 4016–4021 (2005).

111. Beekman, R. *et al.* Sequential gain of mutations in severe congenital neutropenia progressing to acute myeloid leukemia. *Blood* **119**, 5071–5077 (2012).

112. Maxson, J. E. *et al.* Oncogenic *CSF3R* Mutations in Chronic Neutrophilic Leukemia and Atypical CML. *New England Journal of Medicine* **368**, 1781–1790 (2013).

113. Touw, I. P. & Beekman, R. Severe congenital neutropenia and chronic neutrophilic leukemia: An intriguing molecular connection unveiled by oncogenic mutations in CSF3R. *Haematologica* vol. 98 1490–1492 Preprint at https://doi.org/10.3324/haematol.2013.090571 (2013).

114. Anderlini, P. & Champlin, R. E. Biologic and molecular effects of granulocyte colony-stimulating factor in healthy individuals: Recent findings and current challenges. *Blood* vol. 111 Preprint at https://doi.org/10.1182/blood-2007-07-097543 (2008).

115. Dwivedi, P. & Greis, K. D. Granulocyte colony-stimulating factor receptor signaling in severe congenital neutropenia, chronic neutrophilic leukemia, and related malignancies. *Experimental Hematology* vol. 46 9–20 Preprint at https://doi.org/10.1016/j.exphem.2016.10.008 (2017).

116. Fukunaga, R., Ishizaka-Ikeda, E., Pan, C. X., Seto, Y. & Nagata, S. Functional domains of the granulocyte colony-stimulating factor receptor. *EMBO Journal* **10**, 2855–2866 (1991).

117. Demetri, G. D. & Griffin, J. D. Granulocyte Colony-Stimulating Factor and Its Receptor. *Blood* **78**, 2791–2808 (1991).

118. Cosman, D. *et al.* A new cytokine receptor superfamily. *Trends Biochem Sci* **15**, 265–270 (1990).

119. Bazan, J. F. A novel family of growth factor receptors: A common binding domain in the growth hormone, prolactin, erythropoietin and IL-6 receptors, and the p75 IL-2 receptor β-chain. *Biochem Biophys Res Commun* **164**, 788–795 (1989).

120. Touw, I. P. & Van De Geijn, G.-J. M. Granulocyte colony-stimulating factor and its receptor in normal myeloid cell development, leukemia and related blood cell disorders. *Frontiers in Bioscience* **12**, 800–815 (2007).

121. Beekman, R. & Touw, I. P. G-CSF and its receptor in myeloid malignancy. *Blood* vol. 115 Preprint at https://doi.org/10.1182/blood-2010-01-234120 (2010).

122. Layton, J. E. & Hall, N. E. The interaction of G-CSF with its receptor. *Frontiers in Bioscience* vol. 11 3181–3189 Preprint at https://doi.org/10.2741/2041 (2006).

123. Santini, V. *et al.* The carboxy-terminal region of the granulocyte colony-stimulating factor receptor transduces a phagocytic signal. *Blood* **101**, 4615–4622 (2003).

124. Fukunaga, R., Ishizaka-Ikeda, E. & Nagata, S. Growth and differentiation signals mediated by different regions in the cytoplasmic domain of granulocyte colony-stimulating factor receptor. *Cell* **74**, 1079–1087 (1993).

125. Hermans, M. H. A. *et al.* Signaling mechanisms coupled to tyrosines in the granulocyte colony-stimulating factor receptor orchestrate G-CSF-induced expansion of myeloid progenitor cells. *Blood* **101**, 2584–2590 (2003).

126. Koay, D. C. & Sartorelli, A. C. Functional differentiation signals mediated by distinct regions of the cytoplasmic domain of the granulocyte colony-stimulating factor receptor. *Blood* **93**, 3774–3784 (1999).

127. Dong, F. *et al.* The C-terminal cytoplasmic region of the granulocyte colony-stimulating factor receptor mediates apoptosis in maturation-incompetent murine myeloid cells. in *Experimental Hematology* vol. 24 214–220 (1996).

128. Palande, K., Meenhuis, A., Jevdjovic, T. & Touw, I. P. *Scratching the Surface: Signaling and Routing Dynamics of the CSF3 Receptor*. *Frontiers in Bioscience* vol. 18 https://repository.ubn.ru.nl/bitstream/handle/2066/117625/1/117625.pdf (2013).

129. Ward, A. C. The role of the granulocyte colony-stimulating factor receptor (G-CSF-R) in disease. *Frontiers in Bioscience* **12**, 608 (2007).

130. Liongue, C. & Ward, A. C. Granulocyte Colony-Stimulating Factor Receptor Mutations in Myeloid Malignancy. *Front Oncol* **4**, 93 (2014).

131. Nicholson, S. E., Novak, U., Ziegler, S. F. & Layton, J. E. Distinct regions of the granulocyte colony-stimulating factor receptor are required for tyrosine phosphorylation of the signaling molecules JAK2, Stat3, and p42, p44(MAPK). *Blood* **86**, 3698–3704 (1995).

132. Nicholson, S. E. *et al.* Tyrosine kinase JAK1 is associated with the granulocyte-colony-stimulating factor receptor and both become tyrosine-phosphorylated after receptor activation. *Proc Natl Acad Sci U S A* **91**, 2985–2988 (1994).

133. Zhu, Q. S. *et al.* G-CSF induced reactive oxygen species involves Lyn-PI3-kinase-Akt and contributes to myeloid cell growth. *Blood* **107**, 1847–1856 (2006).

134. Corey, S. J. *et al.* Granulocyte colony-stimulating factor receptor signaling involves the formation of a three-component complex with Lyn and Syk protein-tyrosine kinases. *Proc Natl Acad Sci U S A* **91**, 4683–4687 (1994).

135. Hermans, M. *et al.* Sustained receptor activation and hyperproliferation in response to granulocyte colony-stimulating factor (G-CSF) in mice with a severe congenital neutropenia/acute. *Journal of Experimental Medicine* **189**, 683–691 (1999).

136. Ward, A. C., Monkhouse, J. L., Csar, X. F., Touw, I. P. & Bello, P. A. The Src-like tyrosine kinase Hck is activated by granulocyte colony-stimulating factor (G-CSF) and docks to the activated G-CSF receptor. *Biochem Biophys Res Commun* **251**, 117–123 (1998).

137. Barge, R. M. Y. *et al.* Tryptophan 650 of human granulocyte colony-stimulating factor (G-CSF) receptor, implicated in the activation of JAK2, is also required for G-CSF-mediated activation of signaling complexes of the p21ras route. *Blood* **87**, 2148–2153 (1996).

138. Tian, S. S. *et al.* Multiple signaling pathways induced by granulocyte colony-stimulating factor involving activation of JAKs, STAT5, and/or STAT3 are required for regulation of three distinct classes of immediate early genes. *Blood* **88**, 4435–4444 (1996).

139. Ward, A. C., Smith, L., De Koning, J. P., Van Aesch, Y. & Touw, I. P. Multiple signals mediate proliferation, differentiation, and survival from the granulocyte colony-stimulating factor receptor in myeloid 32D cells. *Journal of Biological Chemistry* **274**, 14956–14962 (1999).

140. Ward, A. C. *et al.* Tyrosine-Dependent and -Independent Mechanisms of STAT3 Activation by the Human Granulocyte Colony-Stimulating Factor (G-CSF) Receptor Are Differentially Utilized Depending on G-CSF Concentration. *Blood* **93**, 113–124 (1999).

141. Boyle, K. *et al.* The SOCS box of suppressor of cytokine signaling-3 contributes to the control of G-CSF responsiveness in vivo. *Blood* **110**, 1466–1474 (2007).

142. Babon, J. J. *et al.* Suppression of Cytokine Signaling by SOCS3: Characterization of the Mode of Inhibition and the Basis of Its Specificity. *Immunity* **36**, 239–250 (2012).

143. Bartalucci, N. *et al.* Co-targeting the PI3K/mTOR and JAK2 signalling pathways produces synergistic activity against myeloproliferative neoplasms. *J Cell Mol Med* **17**, 1385–1396 (2013).

144. Corey, S. J. *et al.* Requirement of src kinase lyn for induction of DNA synthesis by granulocyte colony-stimulating factor. *Journal of Biological Chemistry* **273**, 3230–3235 (1998).

145. Dombrosky-Ferlan, P. M. & Corey, S. J. Yeast two-hybrid in vivo association of the Src kinase Lyn with the protooncogene product Cbl but not with the p85 subunit of PI 3-kinase. *Oncogene* **14**, 2019–2024 (1997).

146. Grishin, A. *et al.* Involvement of she and Cbl-PI 3-kinase in Lyn-dependent proliferative signaling pathways for G-CSF. *Oncogene* **19**, 97–105 (2000).

147. Sinha, S. *et al.* Suppression of apoptosis and granulocyte colony-stimulating factor-induced differentiation by an oncogenic form of Cbl. *Exp Hematol* **29**, 746–755 (2001).

148. Zhan, Y., Lieschke, G. J., Grail, D., Dunn, A. R. & Cheers, C. Essential Roles for Granulocyte-Macrophage Colony-Stimulating Factor (GM-CSF) and G-CSF in the Sustained Hematopoietic Response ofListeria monocytogenes–Infected Mice. *Blood* **91**, 863–869 (1998).

149. Lieschke, G. J. *et al.* Mice lacking granulocyte colony-stimulating factor have chronic neutropenia, granulocyte and macrophage progenitor cell deficiency, and impaired neutrophil mobilization. *Blood* **84**, 1737–1746 (1994).

150. Omori, F. *et al.* Levels of human serum granulocyte colony-stimulating factor and granulocyte-macrophage colony-stimulating factor under pathological conditions. *Biotherapy* **4**, 147–153 (1992).

151. Pauksen, K., Elfman, L., Ulfgren, A. K. & Venge, P. Serum levels of granulocyte-colony stimulating factor (G-CSF) in bacterial and viral infections, and in atypical pneumonia. *Br J Haematol* **88**, 256–260 (1994).

152. Cheers, C. *et al.* Production of colony-stimulating factors (CFSs) during infection: Separate determinations of macrophage-, granulocyte-, granulocyte-macrophage-, and multi-CSFs. *Infect Immun* **56**, 247–251 (1988).

153. Kawakami, M. *et al.* Levels of serum granulocyte colony-stimulating factor in patients with infections. *Blood* **76**, 1962–1964 (1990).

154. Zhan, Y. & Cheers, C. Haemopoiesis in mice genetically lacking granulocyte-macrophage colony stimulating factor during chronic infection with Mycobacterium avium. *Immunol Cell Biol* **78**, 118–123 (2000).

155. Basu, S. *et al.* 'Emergency' granulopoiesis in G-CSF-deficient mice in response to Candida albicans infection. *Blood* **95**, 3725–3733 (2000).

156. Martins, A., Han, J. & Kim, S. O. The multifaceted effects of granulocyte colony-stimulating factor in immunomodulation and potential roles in intestinal immune homeostasis. *IUBMB Life* **62**, 611–617 (2010).

157. Carulli, G. Effects of recombinant human granulocyte colony-stimulating factor administration on neutrophil phenotype and functions. *Haematologica* vol. 82 606–616 Preprint at (1997).

158. De Haas, M. *et al.* Granulocyte colony-stimulating factor administration to healthy volunteers: Analysis of the immediate activating effects on circulating neutrophils. *Blood* **84**, 3885–3894 (1994).

159. Barth, E. *et al.* Peaks of endogenous G-CSF serum concentrations are followed by an increase in respiratory burst activity of granulocytes in patients with septic shock. *Cytokine* **17**, 275–284 (2002).

160. Boneberg, E.-M., Hareng, L., Gantner, F., Wendel, A. & Hartung, T. Human monocytes express functional receptors for granulocyte colony– stimulating factor that mediate suppression of monokines and interferon-γ. *Blood* **95**, 270–276 (2000).

161. Saito, M. *et al.* Granulocyte colony-stimulating factor directly affects human monocytes and modulates cytokine secretion. *Exp Hematol* **30**, 1115–1123 (2002).

162. Nishiki, S. *et al.* Selective activation of STAT3 in human monocytes stimulated by G-CSF: Implication in inhibition of LPS-induced TNF-α production. *Am J Physiol Cell Physiol* **286**, (2004).

163. Rutella, S. *et al.* Granulocyte colony-stimulating factor promotes the generation of regulatory DC through induction of IL-10 and IFN-α. *Eur J Immunol* **34**, 1291–1302 (2004).

164. Kim, S. O., Sheikh, H. I., Ha, S. D., Martins, A. & Reid, G. G-CSF-mediated inhibition of JNK is a key mechanism for Lactobacillus rhamnosus-induced suppression of TNF production in macrophages. *Cell Microbiol* **8**, 1958–1971 (2006).

165. Dale, D. C. *et al.* A randomized controlled phase III trial of recombinant human granulocyte colony-stimulating factor (filgrastim) for treatment of severe chronic neutropenia. *Blood* **81**, 2496–2502 (1993).

166. Horowitz, M. M. & Confer, D. L. Evaluation of hematopoietic stem cell donors. *Hematology / the Education Program of the American Society of Hematology. American Society of Hematology. Education Program* (2005) doi:10.1182/asheducation-2005.1.469.

167. Russell, N. H., Gratwohl, A. & Schmitz, N. The place of blood stem cells in allogeneic transplantation. *British Journal of Haematology* vol. 93 Preprint at https://doi.org/10.1046/j.1365-2141.1996.d01-1712.x (1996).

168. Liongue, C., Wright, C., Russell, A. P. & Ward, A. C. Granulocyte colony-stimulating factor receptor: stimulating granulopoiesis and much more. *Int J Biochem Cell Biol* **41**, 2372–2375 (2009).

169. Ward, A. C. *et al.* Novel point mutation in the extracellular domain of the granulocyte colony-stimulating factor (G-CSF) receptor in a case of severe congenital neutropenia hyporesponsive to G-CSF treatment. *J Exp Med* **190**, 497–507 (1999).

170. Druhan, L. J. *et al.* Novel mechanism of G-CSF refractoriness in patients with severe congenital neutropenia. *Blood* **105**, 584–591 (2005).

171. Sinha, S., Zhu, Q. S., Romero, G. & Corey, S. J. Deletional mutation of the external domain of the human granulocyte colony-stimulating factor receptor in a patient with severe chronic neutropenia refractory to granulocyte colony-stimulating factor. *J Pediatr Hematol Oncol* **25**, 791–796 (2003).

172. Papadaki, H. A. *et al.* Acute myeloid/NK precursor cell leukemia with trisomy 4 and a novel point mutation in the extracellular domain of the G-CSF receptor in a patient with chronic idiopathic neutropenia. *Ann Hematol* **83**, 345–348 (2004).

173. Pardanani, A. *et al.* CSF3R T618I is a highly prevalent and specific mutation in chronic neutrophilic leukemia. *Leukemia* **27**, 1870–1873 (2013).

174. Mehta, H. M. *et al.* Granulocyte colony-stimulating factor receptor T595I (T618I) mutation confers ligand independence and enhanced signaling. *Leukemia* **27**, 2407–2410 (2013).

175. Maniaci, B., Chung, J., Sanz-Altamira, P., DeAngelo, D. J. & Maxson, J. E. A Novel CSF3R Activating Mutation Identified in a Patient with Chronic Neutrophilic Leukemia. *Blood* **138**, 3582 (2021).

176. Beekman, R., Valkhof, M., van Strien, P., Valk, P. J. M. & Touw, I. P. Prevalence of a new auto-activating colony stimulating factor 3 receptor mutation (CSF3R-T595I) in acute myeloid leukemia and severe congenital neutropenia. *Haematologica* **98**, e62 (2013).

177. Bernard, T., Gale, R. E. & Linch, D. C. Analysis of granulocyte colony stimulating factor receptor isoforms, polymorphisms and mutations in normal haemopoietic cells and acute myeloid leukaemia blasts. *Br J Haematol* **93**, 527–533 (1996).

178. Forbes, L. V. *et al.* An activating mutation in the transmembrane domain of the granulocyte colony-stimulating factor receptor in patients with acute myeloid leukemia. *Oncogene* **21**, 5981–5989 (2002).

179. Plo, I. *et al.* An activating mutation in the CSF3R gene induces a hereditary chronic neutrophilia. *J Exp Med* **206**, 1701–1707 (2009).

180. Dong, F. *et al.* Mutations in the gene for the granulocyte colony-stimulating-factor receptor in patients with acute myeloid leukemia preceded by severe congenital neutropenia. *N Engl J Med* **333**, 487–493 (1995).

181. Dong, F. *et al.* Mutations in the granulocyte colony-stimulating factor receptor gene in patients with severe congenital neutropenia. *Leukemia 1997 11:1* **11**, 120–125 (1997).

182. Germeshausen, M., Ballmaier, M. & Welte, K. Incidence of CSF3R mutations in severe congenital neutropenia and relevance for leukemogenesis: Results of a long-term survey. *Blood* **109**, 93–99 (2007).

183. Zhang, H. *et al.* Characterization of the leukemogenic potential of distal cytoplasmic CSF3R truncation and missense mutations. *Leukemia* **31**, 2752–2760 (2017).

184. Ward, A. C., Van Aesch, Y. M., Schelen, A. M. & Touw, I. P. Defective Internalization and Sustained Activation of Truncated Granulocyte Colony-Stimulating Factor Receptor Found in Severe Congenital Neutropenia/Acute Myeloid Leukemia. *Blood* **93**, 447–458 (1999).

185. Hunter, M. G. & Avalos, B. R. Deletion of a Critical Internalization Domain in the G-CSFR in Acute Myelogenous Leukemia Preceded by Severe Congenital Neutropenia. *Blood* **93**, 440–446 (1999).

186. Dong, F. *et al.* Stimulation of Stat5 by Granulocyte Colony-Stimulating Factor (G-CSF) Is Modulated by Two Distinct Cytoplasmic Regions of the G-CSF Receptor. *The Journal of Immunology* **161**, 6503 (1998).

187. Dong, F., Qiu, Y., Yi, T., Touw, I. P. & Larner, A. C. The carboxyl terminus of the granulocyte colony-stimulating factor receptor, truncated in patients with severe congenital neutropenia/acute myeloid leukemia, is required for SH2-containing phosphatase-1 suppression of Stat activation. *J Immunol* **167**, 6447–6452 (2001).

188. Hunter, M. G. *et al.* Loss of SHIP and CIS recruitment to the granulocyte colony-stimulating factor receptor contribute to hyperproliferative responses in severe congenital neutropenia/acute myelogenous leukemia. *J Immunol* **173**, 5036–45 (2004).

189. Van De Geijn, G. J. M., Gits, J., Aarts, L. H. J., Heijmans-Antonissen, C. & Touw, I. P. G-CSF receptor truncations found in SCN/AML relieve SOCS3-controlled inhibition of STAT5 but leave suppression of STAT3 intact. *Blood* **104**, 667–674 (2004).

190. Liu, F. *et al.* Csf3r mutations in mice confer a strong clonal HSC advantage via activation of Stat5. *J Clin Invest* **118**, 946–955 (2008).

191. Hermans, M. H. A. *et al.* Perturbed Granulopoiesis in Mice With a Targeted Mutation in the Granulocyte Colony-Stimulating Factor Receptor Gene Associated With Severe Chronic Neutropenia. *Blood* **92**, 32–39 (1998).

192. Gotlib, J., Maxson, J. E., George, T. I. & Tyner, J. W. The new genetics of chronic neutrophilic leukemia and atypical CML: implications for diagnosis and treatment. *Blood* **122**, 1707–1711 (2013).

193. Maxson, J. E. *et al.* CSF3R mutations have a high degree of overlap with CEBPA mutations in pediatric AML. *Blood* (2016) doi:10.1182/blood-2016-04-709899.

194. Swoboda, A. *et al.* CSF3R T618I Collaborates with RUNX1-RUNX1T1 to Expand Human Haematopoietic Stem and Progenitor Cells. *Blood* **138**, 2233–2233 (2021).

195. Swoboda, A. S. *et al.* CSF3R T618I Collaborates With RUNX1-RUNX1T1 to Expand Hematopoietic Progenitors and Sensitizes to GLI Inhibition. *Hemasphere* **7**, E958 (2023).

196. Wichmann, C. *et al.* Activating c-KIT mutations confer oncogenic cooperativity and rescue RUNX1/ETO-induced DNA damage and apoptosis in human primary CD34+ hematopoietic progenitors. *Leukemia* **29**, 279–289 (2015).

197. Xu, Y. *et al.* Immunophenotypic identification of acute myeloid leukemia with monocytic differentiation. *Leukemia* **20**, 1321–1324 (2006).

198. Adriaansen, H. J. *et al.* Acute myeloid leukemia M4 with bone marrow eosinophilia (M4Eo) and inv(16)(p13q22) exhibits a specific immunophenotype with CD2 expression. *Blood* **81**, 3043–51 (1993).

199. Baer, M. R. *et al.* Acute myeloid leukemia with 11q23 translocations: myelomonocytic immunophenotype by multiparameter flow cytometry. *Leukemia* **12**, 317–325 (1998).

200. Wellbrock, J. *et al.* Expression of hedgehog pathway mediator GLI represents a negative prognostic marker in human acute myeloid leukemia and its inhibition exerts Antileukemic effects. *Clinical Cancer Research* **21**, 2388–2398 (2015).

201. Grimwade, D. The clinical significance of cytogenetic abnormalities in acute myeloid leukaemia. *Best Pract Res Clin Haematol* **14**, 497–529 (2001).

202. Lavallée, V.-P. *et al.* Chemo-genomic interrogation of CEBPA mutated AML reveals recurrent CSF3R mutations and subgroup sensitivity to JAK inhibitors. *Blood* **127**, 3054 (2016).

203. Su, L. *et al.* CSF3R mutations were associated with an unfavorable prognosis in patients with acute myeloid leukemia with CEBPA double mutations. *Ann Hematol* **98**, 1641–1646 (2019).

204. Tonks, A. *et al.* The AML1-ETO fusion gene promotes extensive self-renewal of human primary erythroid cells. *Blood* **101**, 624–632 (2003).

205. Okuda, T. *et al.* Expression of a knocked-in AML1-ETO leukemia gene inhibits the establishment of normal definitive hematopoiesis and directly generates dysplastic hematopoietic progenitors. *Blood* **91**, 3134–3143 (1998).

206. Peterson, L. F. & Zhang, D.-E. The 8;21 translocation in leukemogenesis. *Oncogene* **23**, 4255–4262 (2004).

207. Rhoades, K. L. *et al.* Analysis of the role of AML1-ETO in leukemogenesis, using an inducible transgenic mouse model. *Blood* **96**, 2108–15 (2000).

208. de Guzman, C. G. *et al.* Hematopoietic stem cell expansion and distinct myeloid developmental abnormalities in a murine model of the AML1-ETO translocation. *Mol Cell Biol* **22**, 5506–5517 (2002).

209. Yergeau, D. A. *et al.* Embryonic lethality and impairment of haematopoiesis in mice heterozygous for an AML1-ETO fusion gene. *Nat Genet* **15**, 303–306 (1997).

210. Schwieger, M. *et al.* AML1-ETO inhibits maturation of multiple lymphohematopoietic lineages and induces myeloblast transformation in synergy with ICSBP deficiency. *J Exp Med* **196**, 1227–1240 (2002).

211. Grisolano, J. L., O'Neal, J., Cain, J. & Tomasson, M. H. An activated receptor tyrosine kinase, TEL/PDGFbetaR, cooperates with AML1/ETO to induce acute myeloid leukemia in mice. *Proc Natl Acad Sci U S A* **100**, 9506–9511 (2003).

212. Shimada, H. *et al.* Analysis of genes under the downstream control of the t(8;21) fusion protein AML1-MTG8: overexpression of the TIS11b (ERF-1, cMG1) gene induces myeloid cell proliferation in response to G-CSF. *Blood* **96**, 655–63 (2000).

213. Carratt, S. A. *et al.* RUNX1::ETO translocations must precede CSF3R mutations to promote acute myeloid leukemia development. *Leukemia* **37**, 1141–1146 (2023).

214. Stelmach, P. & Trumpp, A. Leukemic stem cells and therapy resistance in acute myeloid leukemia. *Haematologica* **108**, 353–366 (2023).

215. Baer, M. R. *et al.* Expression of the Neural Cell Adhesion Molecule CD56 Is Associated With Short Remission Duration and Survival in Acute Myeloid Leukemia With t(8; 21)(q22; q22). *Blood* **90**, 1643–1648 (1997).

216. Kita, K. *et al.* Phenotypical characteristics of acute myelocytic leukemia associated with the t(8;21)(q22;q22) chromosomal abnormality: frequent expression of immature B-cell antigen CD19 together with stem cell antigen CD34. *Blood* **80**, 470–477 (1992).

217. Bronte, V. *et al.* Apoptotic Death of CD8+ T Lymphocytes After Immunization: Induction of a Suppressive Population of Mac-1+/Gr-1+ Cells. *J Immunol* **161**, 5313 (1998).

218. Gabrilovich, D. I., Ostrand-Rosenberg, S. & Bronte, V. Coordinated regulation of myeloid cells by tumours. *Nat Rev Immunol* **12**, 253–268 (2012).

219. Yu, S., Ren, X. & Li, L. Myeloid-derived suppressor cells in hematologic malignancies: two sides of the same coin. *Experimental Hematology & Oncology 2022 11:1* **11**, 1–15 (2022).

220. Ingham, P. W. & McMahon, A. P. Hedgehog signaling in animal development: paradigms and principles. *Genes Dev* **15**, 3059–3087 (2001).

221. Sigafoos, A. N., Paradise, B. D. & Fernandez-Zapico, M. E. Hedgehog/GLI Signaling Pathway: Transduction, Regulation, and Implications for Disease. *Cancers (Basel)* **13**, (2021).

222. Pietrobono, S., Gagliardi, S. & Stecca, B. Non-canonical hedgehog signaling pathway in cancer: Activation of GLI transcription factors beyond smoothened. *Front Genet* **10**, 465464 (2019).

223. Tao, S. *et al.* Prognosis and outcome of patients with acute myeloid leukemia based on FLT3-ITD mutation with or without additional abnormal cytogenetics. *Oncol Lett* **18**, 6766 (2019).

224. Lim, Y. *et al.* Integration of Hedgehog and mutant FLT3 signaling in myeloid leukemia. *Sci Transl Med* **7**, (2015).

225. Aberger, F. & Ruiz i Altaba, A. Context-dependent signal integration by the GLI code: the oncogenic load, pathways, modifiers and implications for cancer therapy. *Semin Cell Dev Biol* **33**, 93–104 (2014).

226. Onishi, H. & Katano, M. Hedgehog signaling pathway as a therapeutic target in various types of cancer. *Cancer Sci* **102**, 1756–1760 (2011).

227. Stecca, B. & Ruiz I Altaba, A. Context-dependent regulation of the GLI code in cancer by HEDGEHOG and non-HEDGEHOG signals. *J Mol Cell Biol* **2**, 84–95 (2010).

228. Agyeman, A., Jha, B. K., Mazumdar, T. & Houghton, J. A. Mode and specificity of binding of the small molecule GANT61 to GLI determines inhibition of GLI-DNA binding. *Oncotarget* **5**, 4492–4503 (2014).

229. Lauth, M., Bergström, Å., Shimokawa, T. & Toftgård, R. Inhibition of GLI-mediated transcription and tumor cell growth by small-molecule antagonists. *Proc Natl Acad Sci U S A* **104**, 8455 (2007).

230. Pan, D. *et al.* Gli inhibitor GANT61 causes apoptosis in myeloid leukemia cells and acts in synergy with rapamycin. *Leuk Res* **36**, 742–748 (2012).

231. Schneider, F. *et al.* AML1–ETO meets JAK2: clinical evidence for the two hit model of leukemogenesis from a myeloproliferative syndrome progressing to acute myeloid leukemia. *Leukemia* **21**, 2199–2201 (2007).

232. Schnittger, S., Bacher, U., Kern, W., Haferlach, C. & Haferlach, T. JAK2 seems to be a typical cooperating mutation in therapy-related t(8;21)/ AML1-ETO-positive AML. *Leukemia* **21**, 183–184 (2007).

233. Lee, J. W. *et al.* The JAK2 V617F mutation in de novo acute myelogenous leukemias. *Oncogene* **25**, 1434–1436 (2006).

234. K Dohner *et al.* JAK2V617F mutations as cooperative genetic lesions in t(8;21)-positive acute myeloid leukemia. *Haematologica* **91**, 1569–1570 (2006).

235. Quintás-Cardama, A. *et al.* Preclinical characterization of the selective JAK1/2 inhibitor INCB018424: therapeutic implications for the treatment of myeloproliferative neoplasms. *Blood* **115**, 3109–3117 (2010).

236. Maxson, J. E. *et al.* Ligand independence of the T618I mutation in the colony-stimulating factor 3 receptor (CSF3R) protein results from loss of O-linked glycosylation and increased receptor dimerization. *Journal of Biological Chemistry* (2014) doi:10.1074/jbc.M113.508440.

237. Redondo Monte, E. *et al.* ZBTB7A prevents RUNX1-RUNX1T1-dependent clonal expansion of human hematopoietic stem and progenitor cells. *Oncogene* **39**, 3195–3205 (2020).

238. Bagnoli, J. W. *et al.* Sensitive and powerful single-cell RNA sequencing using mcSCRB-seq. *Nat Commun* **9**, 2937 (2018).

239. Janjic, A. *et al.* Prime-seq, efficient and powerful bulk RNA sequencing. *Genome Biol* **23**, 1–27 (2022).

240. Wolf, F. A., Angerer, P. & Theis, F. J. SCANPY: Large-scale single-cell gene expression data analysis. *Genome Biol* **19**, 1–5 (2018).

241. Domínguez Conde, C. *et al.* Cross-tissue immune cell analysis reveals tissue-specific features in humans. *Science (1979)* **376**, (2022).

Appendix 1

HGNC Symbol	Average Expression CSF3R T618I	logFC CSF3R T618I vs WT	adj.P.Val T618I vs WT	logFC CSF3R T618I vs EV	adj.P.Val T618I vs EV
CD177	1,666982546	5,827634415	4,64518E-13	4,687744191	4,80249E-11
HGF	1,479858714	4,199388603	7,07912E-08	4,508932471	4,99623E-08
ADCYAP1	5,649992336	3,362010028	4,62313E-08	3,626651168	7,15839E-09
ADGRG1	2,809819285	2,941304663	7,28341E-06	1,827137557	0,000390543
GLI2	2,818716232	2,827631199	5,37525E-06	3,007745783	1,15677E-06
LOXL1	3,53900136	2,799381841	5,57948E-09	1,95934201	4,7876E-07
RETN	4,776043636	2,743697876	1,80598E-10	5,506104462	1,90999E-14
CACNA2D4	2,749904189	2,617035123	3,33693E-06	1,435887996	0,000520271
AC011498.4	5,633704325	2,539248635	4,56369E-10	3,024279648	4,56893E-12
DYSF	3,134165418	2,508413942	3,07753E-07	3,706091452	6,47178E-10
PTGER3	3,07032389	2,504266554	3,02828E-06	2,209172091	3,99307E-06
DGAT2	3,135331339	2,344192861	0,000741664	2,730370459	0,000180548
ANXA3	5,515687106	2,320162484	1,42665E-11	2,759397393	7,11225E-14
AL807752.6	3,209760381	2,271157064	4,86117E-07	2,379491495	5,55355E-08
Z94721.2	3,673700254	2,253709013	4,05632E-06	2,025041289	3,47244E-06
SOCS3	6,949029902	2,199094611	2,08062E-13	2,753355134	3,44642E-16
TMEM176B	8,758513426	2,184802184	4,77685E-15	2,931431073	1,25856E-18
CST7	7,225040687	2,131569778	2,98052E-09	2,143067568	2,10459E-09
FCGR1CP	4,827299207	2,11417732	1,58372E-09	2,539093944	2,90091E-11
TMEM176A	7,625322169	1,978773358	2,08062E-13	2,495044606	3,44642E-16
HSBP1L1	2,945550622	1,918829923	0,000271674	2,48425297	2,03368E-05
ALDH1L2	2,458255068	1,913407565	0,001849081	2,955066701	1,21466E-05
SNORD3B-2	2,011443263	1,901802651	0,02174405	3,092872922	0,000731215
HPR	4,672484705	1,852028217	5,83888E-06	2,146055486	1,36567E-07
HP	6,707470778	1,851965813	4,30019E-09	2,134372297	9,8659E-11
PIEZO2	4,447638605	1,835427923	4,78921E-06	1,403451678	6,31502E-05
PADI4	5,563962169	1,820658357	1,80598E-10	1,3615127	5,01428E-08
PPARG	3,195027571	1,809868054	0,001693096	2,987445684	6,97529E-06
FCGR1B	4,980177511	1,77874934	1,80598E-10	2,271426197	1,73815E-13
CYSTM1	4,644421887	1,751412653	2,71273E-06	2,884866165	3,86102E-10
IFITM3	6,905988831	1,746019096	3,00761E-14	2,005999353	3,44642E-16
ITGA1	4,801151026	1,723979037	2,25337E-09	1,612179402	4,95281E-09
SNHG22	3,148809606	1,684763565	0,001024125	1,937997286	5,49686E-05
GOLM1	5,164036246	1,674440289	2,16538E-08	1,937264627	3,86102E-10
FCGR1A	5,91006344	1,666699983	3,07687E-10	2,35439196	4,1027E-14
SLPI	3,680606864	1,663534408	0,000580835	2,320210492	3,53286E-06
TMEM45B	3,609413101	1,663497151	0,001566397	2,80704489	2,75692E-06
STON1	4,82400896	1,65303571	3,73525E-09	1,561276523	4,90814E-09
NCOA7	5,91045748	1,64082345	5,86351E-11	1,845165336	1,17149E-12
CCDC26	3,065191412	1,634356362	0,000463603	1,392734735	0,000889602
IFITM2	8,280681302	1,625885999	2,99194E-17	1,407483817	2,22066E-15

ACSL1	6,794376738	1,613575126	4,0275E-12	1,987880713	9,34907E-15
BATF3	3,037874669	1,602361729	0,000985561	2,431723448	6,46803E-06
RNF144B	3,130101809	1,591430786	0,010007624	1,382525817	0,010489534
ORM1	3,524806677	1,589703743	3,45813E-05	2,855959013	1,00484E-09
AC006970.1	3,329409301	1,584228725	0,000174483	2,263796767	5,75664E-07
STEAP4	4,367596773	1,571903527	0,00019702	2,172138603	1,15004E-06
FPR2	4,667398126	1,541509294	0,000145517	2,185695552	4,37122E-07
S100P	7,207604386	1,528786548	5,57948E-09	1,870264976	4,31847E-11
FAM89A	4,138463595	1,522569927	6,49663E-05	1,937801267	8,42609E-07
ADRB3	3,068446532	1,520443676	0,017525285	2,415926611	0,000259772
TUBB6	5,754544954	1,518656593	2,59169E-07	1,603210092	2,48961E-08
ADGRG3	5,830891963	1,512377564	4,30019E-09	2,037886465	2,7597E-12
CSF1	3,481247601	1,490784393	0,040451865	2,740684945	0,000280041
KBTBD11	3,820254106	1,485454226	0,000526497	1,486989318	0,00025472
SIPA1L2	3,622989689	1,485260025	0,004651308	2,53009904	1,52902E-05
SEL1L3	5,096191583	1,470300016	6,11939E-07	1,374362278	6,3076E-07
GGTLC2	3,362169668	1,470035116	0,001482741	1,424314693	0,001307499
NACC2	3,935379972	1,462742005	0,002779836	1,433708779	0,001365605
RGL4	3,779634635	1,454997317	0,017725797	1,672686691	0,002668409
DUSP2	4,47675994	1,432439298	0,000302554	1,948087094	1,97293E-06
GGT1	4,658567374	1,413826701	0,000260833	1,166582601	0,001619519
CEACAM4	5,339093849	1,411568695	3,37009E-06	1,349556314	3,28393E-06
HOOK2	4,470001925	1,390763324	2,01115E-05	1,470189812	2,78939E-06
IL15RA	3,664727288	1,389157595	0,000446149	1,681421576	1,43139E-05
COCH	3,686847074	1,355818486	0,00465378	1,354879371	0,001648666
CD55	6,949024145	1,355586872	1,46313E-10	1,268569647	4,82584E-10
TSPAN2	4,74556814	1,35345329	7,04656E-05	1,357114411	3,27043E-05
MMP25	5,945764587	1,340257004	3,73137E-06	1,667688453	3,06492E-08
CYTL1	8,930720067	1,323460479	8,36763E-10	1,593274043	7,18255E-12
SEMA4C	3,175921926	1,321715587	0,019085595	2,025949028	0,00028271
RAB1B	3,048301756	1,315100391	0,028397169	1,509250407	0,006557242
ENTPD1	4,221645143	1,291897736	0,000362351	1,645540913	8,05236E-06
CLU	7,190614857	1,276728291	2,89127E-09	1,257668941	3,39552E-09
JUNB	8,131424852	1,274671519	1,34664E-08	1,854415626	1,20007E-12
PFKFB3	5,789685009	1,272820375	2,54033E-08	1,914654278	1,0655E-12
CSF3R	7,92542365	1,272760923	8,76703E-11	1,531931063	5,40808E-13
LIN7A	4,100374251	1,263044824	0,002096681	1,082789681	0,003956277
NIBAN1	6,556040839	1,254513473	1,41228E-08	1,368855344	1,43083E-09
AQP9	3,669211329	1,25438115	0,001588722	2,339558213	2,83134E-07
MIR155HG	4,262914682	1,253710853	0,002945989	0,791027589	0,046543976
OTUD1	5,052895467	1,247376949	5,17764E-05	1,685377876	1,46116E-07
SNTB1	6,361821612	1,244833271	4,32409E-10	1,16048784	1,58726E-09
BCL2A1	6,026394988	1,2421632	2,68137E-07	1,530137596	1,55492E-09
FAM160A2	4,829131381	1,238543944	6,89022E-06	0,933050523	0,000201634
TMEM107	4,795692932	1,220752954	0,000404005	1,643235588	3,26725E-06
NFKBIZ	6,03048094	1,210942393	4,06672E-07	1,5521008	1,18377E-09
LDLR	5,847795377	1,209234383	2,30281E-05	1,155587678	1,98629E-05

IL1R1	3,759328138	1,197654469	0,017440835	1,120009983	0,010012605
PADI2	5,653766464	1,189919187	0,00087786	1,923900371	4,48447E-07
MCEMP1	5,36155492	1,188842278	2,05259E-05	2,514674579	3,52222E-12
SLC26A2	4,615822203	1,188777124	3,21839E-05	1,189791155	9,76773E-06
JAK3	6,699556802	1,166926142	1,86717E-06	1,52898637	4,66107E-09
RDH10	4,180287185	1,165313099	0,009687486	1,783581857	7,0847E-05
GPR160	4,832431303	1,159134823	0,000653676	1,013864425	0,001263563
TRIB3	6,180425609	1,152442014	4,65906E-06	0,845652325	0,00030313
IFITM9P	3,66691335	1,145099875	0,011395137	1,486447014	0,000697728
IL1RN	5,856544396	1,139876886	0,00010389	1,32402768	5,93619E-06
BEX1	6,657391039	1,133496579	0,000936322	2,315208288	3,31825E-09
TNFSF10	5,647145351	1,110227027	7,04656E-05	1,288596392	3,47244E-06
MGST1	7,492373666	1,101317895	6,36572E-08	1,329289632	6,77298E-10
TPT1P1	4,79342886	1,098353767	0,000527021	0,711279734	0,016906335
RHBDD2	4,532859435	1,081574525	0,001618363	1,059644134	0,000968238
AP5B1	4,173120999	1,073121945	0,005662672	1,249624683	0,000494397
DNASE2	6,302899185	1,06195687	7,28341E-06	1,34444411	5,93224E-08
FAM47E-STBD1	3,198098583	1,060489892	0,036697104	0,9881439	0,030418656
ALPK1	5,177155749	1,058117626	2,49887E-06	1,217634297	8,09583E-08
AC116049.2	3,607752889	1,054429933	0,048020846	0,979702637	0,039751925
SNHG29	4,264144393	1,045902972	0,00465378	1,06437215	0,002008959
NMB	3,572677892	1,044535492	0,026531277	0,97871099	0,016890432
VAMP5	5,373580791	1,023452451	4,63208E-06	0,730803195	0,000405878
LIMK2	5,525583118	1,021397653	4,63208E-06	1,117994379	4,53049E-07
TRIQK	4,975652426	1,018636947	0,000467183	0,78121341	0,004145362
RHOB	4,449751595	1,013349279	0,001587146	2,063253901	1,37099E-08
BASP1	5,54969002	1,007581226	0,004345445	1,76438008	1,23551E-06
FAM124A	4,184542035	1,002980215	0,002945989	0,898155218	0,003859532
LAIR1	5,931408164	0,999789181	6,89022E-06	1,184559803	1,60947E-07
PLSCR1	6,404255448	0,998288261	4,44628E-07	1,123273081	2,48961E-08
SYNGR1	5,505335815	0,994047994	0,000815617	0,882865714	0,001619519
CBSL	4,48660724	0,993996836	0,019934646	0,865035903	0,02896404
AL591806.4	5,87502457	0,990845025	6,10598E-05	0,576683373	0,015231677
SMARCD3	4,287493608	0,984687035	0,017525285	1,803316277	8,38803E-06
KLHL2	4,47253874	0,981967941	0,007744365	1,275288931	0,000255595
ALOX5	6,794933112	0,981922395	2,03378E-06	1,263104269	7,15839E-09
CCPG1	7,087939029	0,981593526	3,60888E-06	1,067515729	5,65287E-07
NAMPT	7,07565334	0,98149557	1,20903E-06	1,001967476	5,98555E-07
KIAA0040	4,522644025	0,979348876	0,001828737	0,940467211	0,001459778
STAT3	5,67888266	0,972789808	0,000110592	1,03098882	2,27211E-05
SORT1	5,100441541	0,966418776	0,001097426	1,382306107	4,08124E-06
USP13	3,222729265	0,966388054	0,046923117	1,582873058	0,000368421
ADGRE2	3,660354391	0,965454729	0,034458443	0,840120196	0,035085209
SERPINA1	7,086336839	0,96067525	4,46129E-05	1,820209462	6,81786E-11
FSTL3	3,719004687	0,960273932	0,027820764	1,576521807	0,000124076
FOLR3	4,749298976	0,956499845	0,049364621	1,737684995	0,000183463
RAB34	5,998887083	0,955900695	1,2701E-05	0,48919062	0,019035997

MTHFS	6,036547326	0,942387136	0,00019702	1,102284603	1,35177E-05
TRAF3	4,215007628	0,93998763	0,016734362	0,906494185	0,012203248
MNDA	7,655844151	0,933700413	6,50157E-07	1,543769987	3,75657E-12
TXNP1	4,448178567	0,919157238	0,004707439	0,607672762	0,049592941
RMND1	4,263491554	0,918958164	0,024524291	0,859604741	0,023567305
TCF4	4,492930349	0,91848372	0,006320111	0,924144677	0,00260032
BCL3	5,420242036	0,913328776	0,000543435	1,188882083	6,97529E-06
WARS	6,776406717	0,912967198	5,40638E-06	0,779314537	4,961E-05
CEP120	4,012592302	0,909038719	0,022391877	0,784472238	0,032351518
CARS	5,685146753	0,90425285	9,23708E-05	1,057601069	5,09473E-06
NKG7	5,503121211	0,901160073	0,000771135	0,748742602	0,00322051
CSTA	6,806776133	0,898334801	0,001425031	1,134749699	4,47951E-05
CPEB4	4,418607446	0,894651507	0,033200139	1,320249009	0,000683359
IGF1R	4,185039403	0,893492232	0,01008545	1,355069778	3,55189E-05
C19orf38	6,057261848	0,882033268	4,46129E-05	0,829083179	6,97291E-05
SERPINB1	9,339311126	0,879488901	1,58798E-08	0,606954855	2,21384E-05
FAM241A	6,008321919	0,879338628	0,000123145	0,47134804	0,035350105
KLF10	6,788935794	0,877446913	2,18899E-05	0,607040669	0,002038922
PGD	8,41248048	0,876916914	1,11875E-08	1,058568192	1,14477E-10
UPP1	6,662166044	0,876728771	4,29707E-05	1,673026037	5,21185E-11
RCN1	6,307511616	0,869619514	9,67651E-06	0,504228268	0,006709651
MSRB1	6,437538792	0,868195617	0,000260833	1,297515387	2,08888E-07
CPD	6,712047447	0,865513684	3,20595E-07	1,121486964	6,47178E-10
PDSS1	4,995228641	0,864423669	0,000816154	1,218419592	2,75692E-06
STAC	4,558454724	0,862927815	0,038913537	1,476498374	0,000132696
LITAF	7,596819381	0,861151665	6,08304E-06	1,045197273	1,23853E-07
TRGC2	6,311670834	0,855250679	0,000167503	1,115295954	1,42637E-06
KSR1	4,539135953	0,853690552	0,020759312	1,11600896	0,001365183
VLDLR	4,764617239	0,852291549	0,014353034	0,993584576	0,002038922
APMAP	8,236311034	0,846916023	6,20361E-07	1,045588319	5,77419E-09
IL1RAP	6,286778657	0,844374159	8,46702E-05	1,049472061	1,42637E-06
IER2	7,504859454	0,842932308	0,000640684	1,260821149	8,74907E-07
KCNE3	5,293474361	0,839182448	0,000816154	0,720709525	0,002465084
JUN	7,60106662	0,838697855	0,000718991	1,472777435	4,73943E-08
CLEC5A	6,252494897	0,834970829	0,0007534	1,001286277	3,53922E-05
PIM3	6,597080718	0,830046437	3,35498E-05	1,230723287	1,12769E-08
CLDND1	6,728014189	0,827554236	4,07553E-05	0,750110682	0,000121036
JDP2	5,834391097	0,826788664	0,00110886	0,918935833	0,000190505
SMCO4	4,822998299	0,823777749	0,005432667	1,436728133	1,39018E-06
TXNP4	4,456517593	0,822262902	0,008573032	0,832914163	0,003859532
PPM1M	4,979296082	0,809997256	0,006160199	0,804997476	0,003940331
YRDC	5,116028406	0,806309155	0,008565459	1,027949737	0,000371018
IRF2	4,42041651	0,804046736	0,017471386	0,835578788	0,007991006
FAM210B	4,869262809	0,803166626	0,002651677	0,912804739	0,000305357
MLST8	5,401953192	0,798956713	0,001318615	0,94533591	8,86262E-05
ELANE	10,32030073	0,797582704	0,007940212	1,171686559	6,76178E-05
CGREF1	4,199223413	0,795501429	0,028014223	1,222437515	0,000235854

ARSD	4,622355271	0,787770589	0,002892716	0,690153879	0,00510428
DENND10	6,935061008	0,785600833	3,72868E-05	0,616401386	0,000752381
PGDP1	5,014088001	0,783673478	0,001687165	1,263368672	7,29219E-07
ABHD5	4,511685126	0,781526631	0,016611121	0,983833838	0,001146063
SETD7	4,69451793	0,770351451	0,019828377	1,052327685	0,000431822
GLIPR2	6,817353729	0,767165375	0,000383956	1,250670788	6,07898E-08
TPT1-AS1	6,359532435	0,76522943	3,45813E-05	0,518809194	0,003157139
BAZ1A	6,51604968	0,760077256	0,000164258	0,980842679	1,7147E-06
NCF1	5,376655785	0,757140973	0,002228133	0,909330216	0,000126336
PSAT1	7,097730893	0,756704727	0,001425031	0,753631865	0,001118623
CASP1	5,934134486	0,756456944	0,000745598	0,951998068	1,70181E-05
ERO1A	6,103183415	0,75533499	0,001502125	0,814027557	0,000348817
ASNS	5,62597205	0,755244286	0,008698834	0,723698801	0,007943646
NCF1B	5,435887124	0,750322756	0,006423524	0,919252506	0,000390543
CCNL1	7,437190263	0,745946398	4,47311E-05	0,834407656	5,3466E-06
PRELID1P1	4,344832868	0,744810061	0,023128055	0,85862486	0,005440386
SERPINB2	6,81954003	0,744227039	0,031667945	0,95414342	0,003073326
FNDC3B	6,82164169	0,740686994	0,004393657	0,93682153	0,000189159
SESN2	5,780919524	0,740196947	0,020446686	0,692441317	0,021723707
CLEC12A	6,51921516	0,738881339	3,67926E-05	0,753731546	1,52524E-05
TUBA4A	5,250681282	0,737216086	0,011719868	1,103466783	8,22461E-05
BST1	6,286607031	0,733182731	0,002149637	1,056368672	8,12853E-06
MARS	6,667821967	0,732607084	0,00044653	0,811472842	7,19022E-05
METTL9	8,540832198	0,732562846	4,48718E-07	0,730992071	4,48447E-07
GAPDHP44	4,911977918	0,731088179	0,006933307	0,57462619	0,024864393
MICOS10-NBL1	4,608354357	0,729005501	0,028302688	0,760617518	0,011657537
DENND10P1	4,544612036	0,725055119	0,049166391	0,826847974	0,011646451
STK17A	4,47730011	0,724385779	0,042438652	0,95261679	0,003261202
CFH	5,63760146	0,721982005	0,00415427	0,789567699	0,000916381
GYG1	6,299547253	0,72167283	0,000467625	1,054740122	5,82597E-07
APOL6	6,644260788	0,718858097	5,85929E-05	0,999964473	1,07184E-07
S100A11	9,033942877	0,714014773	2,36046E-05	1,080378684	4,95281E-09
NAMPTP1	6,593417947	0,714010879	0,001516022	0,54933459	0,012163884
F11R	6,467250833	0,710429931	0,000116862	0,552849896	0,001928997
TYMP	4,866621404	0,710357731	0,034248377	1,458483992	6,18546E-06
SEMA6B	5,813591619	0,707094758	0,008170325	1,613519201	2,63909E-08
PHGDH	7,972652626	0,706947493	0,000580835	0,517039691	0,010770984
NDRG1	7,039654802	0,699745154	5,68969E-05	0,590579242	0,000463431
MYC	6,805026929	0,694933903	0,001230132	0,46487164	0,029426133
HCK	7,751096201	0,694354645	2,18899E-05	1,200474146	1,61676E-10
SLC25A37	6,634025263	0,693186451	0,025592363	0,966587371	0,000844001
TPI1P3	5,792466649	0,690804246	0,005737641	0,515842672	0,031022646
MAPK14	6,945865916	0,690389792	6,65992E-05	0,591723167	0,000424742
L2HGDH	4,455396947	0,688271197	0,034398569	0,702293738	0,017582933
MTHFD2	7,932588493	0,68799563	4,45857E-05	0,473881453	0,003890086
CR1	6,664463148	0,68678858	0,000609882	1,055142089	3,63125E-07
MAP3K20	6,383510109	0,684090545	0,001793318	1,101358141	1,00213E-06

CNIH4	7,026380785	0,683818867	0,000594415	0,872790649	1,11329E-05
S100A9	10,28095784	0,682991076	0,005702617	1,8008355	2,95595E-10
EGR1	7,829931778	0,681660749	0,010423655	1,074721914	3,42228E-05
BCAP29	5,157200555	0,677835918	0,013818956	0,575294125	0,026276315
SQOR	6,280862891	0,677647369	0,003028214	1,244363409	2,11143E-07
GADD45A	6,164671724	0,675235595	0,004376318	0,595085287	0,008834889
CD44	9,076964418	0,675104184	1,04953E-07	0,39975855	0,000654162
MAP3K1	5,713880655	0,673159395	0,003328001	0,796809117	0,000273795
CARD16	6,294068797	0,67271746	0,001364344	0,955166079	5,70906E-06
TMEM87A	6,200194539	0,670555691	0,000741664	0,853780578	1,28033E-05
TSPO	9,743458477	0,668580601	1,67907E-06	0,920306543	1,28263E-09
ADD3	7,368883169	0,66636443	4,63208E-06	0,860436259	2,08747E-08
SDCCAG8	5,506901242	0,665828894	0,022484619	0,886207931	0,001010673
CEBPD	7,648292929	0,665025314	0,000169061	0,877941779	1,40747E-06
CEBPZOS	5,592083234	0,661660089	0,020446686	0,722833994	0,006004205
HSPA13	5,066861492	0,656290411	0,028609541	0,614738207	0,028383073
AL159163.1	8,128551846	0,654784698	2,79255E-07	0,55436138	5,85767E-06
KLF2	6,097342247	0,65225381	0,016255986	1,010432912	8,83036E-05
IL1B	5,068500249	0,6521804	0,036274681	0,58858658	0,042196925
AC092368.3	5,103947005	0,639524022	0,025516017	0,750399104	0,004138124
PIK3CB	5,978008442	0,63909938	0,013361617	0,590383534	0,015592669
NCF1C	5,558887602	0,639080424	0,011487527	0,746884491	0,00159964
GINM1	5,376263052	0,638900117	0,016734362	0,530832806	0,034822859
IDI1	6,191375474	0,638791513	0,000697784	0,612491468	0,000731215
RABAC1	6,452681446	0,637504955	0,004376318	0,799898614	0,00021729
ST20-MTHFS	5,424884167	0,636205829	0,007744365	0,946967715	3,55189E-05
HIP1	6,564907625	0,633220513	0,004576569	0,976592333	9,26365E-06
GPI	8,27918139	0,633047347	0,000580835	0,449963416	0,013485014
SBNO2	5,738474524	0,631715893	0,00538256	1,201882055	3,01335E-07
MTO1	4,880406692	0,627856641	0,023128055	0,703501595	0,006070651
MPC1	5,57351145	0,627398952	0,017365716	0,891063451	0,00030313
STAT1	6,696863868	0,626452237	0,005432667	0,55675906	0,010718844
VEGFA	5,75575952	0,625293903	0,027820764	0,544327145	0,045410582
LRPAP1	10,06582642	0,625067832	3,12742E-07	0,665058085	7,94821E-08
TBL1X	5,536892915	0,623658411	0,028921168	0,765940291	0,003545097
AGTRAP	6,578371466	0,622885167	0,004133	1,044456761	1,9029E-06
DNAJC1	5,899069526	0,622343222	0,00118801	0,476082423	0,009894034
AC002985.1	5,522841365	0,621603611	0,011473667	1,064618621	8,4995E-06
RAB13	7,387234721	0,617955335	0,000442928	0,660939588	0,000132497
EIF4EBP1	7,774656328	0,611177261	0,000356802	0,745345189	1,35177E-05
ZNF516	5,02999123	0,611127852	0,009924209	0,866049928	0,000108385
S100A8	9,531106945	0,610733887	0,028302688	1,487420934	1,70686E-07
AC009163.5	5,598117978	0,60889736	0,020014519	0,575455299	0,019144056
FYB1	7,460480633	0,604633023	0,001613458	0,638886227	0,000638935
RNF157	7,948371317	0,604027744	7,90312E-05	0,676765538	1,02813E-05
GAPDH	9,535469901	0,60131991	0,00027017	0,393851045	0,016673334
CD300LF	7,706554316	0,600503395	0,000219325	0,804714112	1,41392E-06

GALNT2	6,182985816	0,598663913	0,005116041	0,413482022	0,049173588
FLOT1	5,525045907	0,597769642	0,016734362	1,171549261	2,49813E-06
IRF1	5,621320324	0,597076165	0,012838799	1,025720444	1,05838E-05
C1RL	5,45125716	0,591053718	0,005036076	0,867187861	2,07958E-05
ERLIN1	6,185435163	0,590515781	0,011910441	0,522619257	0,019560161
GCA	6,602319775	0,588314503	0,01103131	0,819547804	0,000206872
NDUFC2-KCTD14	7,607394543	0,587575279	4,46129E-05	0,61986034	1,40239E-05
IL3RA	5,171687507	0,587308189	0,02022368	0,559126967	0,017978094
MSRB3	5,620618361	0,584381638	0,006461518	0,601533154	0,002804744
AAK1	6,229793057	0,582716613	0,004221531	0,615235068	0,001570524
CHSY1	6,321105378	0,58253512	0,001786241	0,377042733	0,042704895
H2AFJ	6,112744758	0,579118628	0,038684768	0,786467956	0,002237845
TIMP2	6,701253791	0,57911207	0,016282083	1,133743615	2,19532E-06
SAMSN1	7,853967065	0,578693451	0,000599215	0,351614817	0,038910751
FAM126B	5,512124289	0,576161415	0,016451433	0,521102799	0,02096343
SEC62	8,052270802	0,571575129	0,00136083	0,959335738	2,84551E-07
COL23A1	5,862414569	0,570407224	0,036274681	0,984011065	0,000102678
APP	6,815370094	0,566464932	0,004556783	0,604127585	0,001619519
FADS1	6,654379871	0,564564914	0,005691288	0,419333972	0,036927874
BSG	5,197255893	0,563437161	0,012838799	0,553540924	0,008636185
SRA1	5,570384182	0,563133134	0,028622816	1,238395911	1,04906E-06
PGS1	5,644726314	0,562035875	0,030504798	0,7154994	0,002648307
MIDN	8,118302656	0,557284142	3,51742E-05	0,754895649	9,62825E-08
PPP1R15B	6,10486196	0,557009683	0,005993125	0,761387644	0,000102678
TUBA1C	5,388879247	0,555135806	0,04893387	0,699331009	0,005653617
PSTPIP2	7,013702366	0,553853453	0,013818956	0,781215501	0,00027096
TPI1	9,334203091	0,552846351	0,000230563	0,315603231	0,03814508
NUCB1	6,0105243	0,547851668	0,032923415	0,58471394	0,014680176
CXCL8	9,690766642	0,544442909	0,0068795	1,366627418	1,26778E-09
MYDGF	7,662375902	0,543275763	0,000412209	0,657789895	1,77441E-05
AARS	6,955770297	0,543158206	0,010211952	0,708208983	0,000440314
UBASH3B	6,038429484	0,542800429	0,019897325	0,570351522	0,008636185
CEBPG	5,903667597	0,542292098	0,034458443	0,519491953	0,030594741
ATF4	9,079320286	0,541556964	9,57976E-05	0,578220115	2,90388E-05
ORAI2	6,4125497	0,539112534	0,012737003	0,572583548	0,005060143
ATF4P4	7,857135005	0,536826575	0,000117521	0,605901639	1,40514E-05
DENND3	6,194421292	0,529318386	0,012592988	0,673993488	0,000751676
AGFG1	5,310495932	0,527007234	0,046272216	0,556879339	0,020705176
XBP1	8,294715513	0,525851402	4,49489E-05	0,527412352	3,44086E-05
YBX3	6,557190617	0,52565193	0,019911002	0,775373026	0,000276124
RNF181	6,962394965	0,522670773	0,007083276	0,474798875	0,011514507
SLC44A1	8,916295403	0,521789072	0,000135602	1,062970641	4,80249E-11
FBXL5	6,457951638	0,516013682	0,005155848	1,0118647	1,37739E-07
PLD3	7,194909268	0,514852395	0,01301307	0,654039685	0,000916381
THEMIS2	6,749180575	0,513093217	0,019695101	1,053423228	1,51204E-06
FAM107B	7,836216346	0,5092303	0,001706678	0,497180373	0,001703174
SLC20A1	5,686715028	0,505120149	0,014284757	0,562396756	0,003359812

EIF1	9,965628183	0,500242255	2,73277E-06	0,385424724	0,000167327
ITGB2	9,613767003	0,49727436	7,97877E-05	0,863118851	1,16587E-09
GNAQ	6,988007339	0,495012844	0,009894417	0,5600624	0,00218267
SARS	6,083700225	0,493902054	0,012867894	0,688972321	0,000238364
ADGRE5	7,213016362	0,491356364	0,0050736	0,69632342	4,57515E-05
SHMT2	7,679833941	0,486817532	0,002457599	0,500699311	0,001377181
P4HB	8,859791501	0,486259109	0,001774703	0,321396165	0,041438992
ECI1	6,493080526	0,485225313	0,006541817	0,563891883	0,000931782
ANXA11	7,799375517	0,48336745	0,002284578	0,73849599	3,99307E-06
PSMD11	6,25379383	0,479935302	0,002916921	0,556013651	0,000318484
NOP10	7,66565056	0,479359335	0,019911002	0,863014821	1,45891E-05
CSRP1	6,595528466	0,47923061	0,034458443	0,528986876	0,011959618
SFT2D1	6,606680266	0,476693532	0,011089916	0,667547361	0,000189038
C16orf72	6,448881995	0,475648849	0,027820764	0,66747139	0,000870464
ARPC5L	6,322991978	0,473886791	0,024032545	0,475361014	0,016440544
RNF187	6,215567358	0,47057627	0,037648436	0,487186434	0,021198044
UBE2D1	6,253079394	0,469196403	0,038046273	0,989793951	4,83812E-06
CFLAR	7,104850096	0,468175202	0,00465378	0,555552185	0,000488834
SEC16A	5,868217621	0,467229491	0,037542535	0,653565191	0,001487434
VAT1	8,677868674	0,467142821	0,004004915	0,574030987	0,000276124
PHC2	6,127302537	0,464576801	0,021395131	0,530143344	0,004799913
GRINA	6,064566121	0,464496275	0,049242304	0,978536245	9,36073E-06
YARS	7,180212498	0,463216337	0,015058166	0,482165597	0,007984275
IL4R	6,293105918	0,463170363	0,02474685	0,440430464	0,02369877
LONP1	6,750863522	0,462766776	0,03582341	0,416355033	0,048258348
TAX1BP1	7,148202013	0,461047713	0,009924209	0,615001727	0,00030313
LINC01619	7,206683587	0,458568292	0,001460796	0,462549081	0,000979838
GNB4	6,081693803	0,449193213	0,049166391	0,51502985	0,013407728
HLA-A	6,751405102	0,447315254	0,031411663	0,499781874	0,01029538
IRAK3	6,462861556	0,445053983	0,008615451	0,528027462	0,001062653
COMT	7,270147528	0,441241209	0,012479555	0,647143617	0,000131051
LBR	7,174823655	0,439848239	0,004484	0,541119232	0,00028929
RAB27A	8,20249991	0,437435554	0,014897197	0,573536201	0,000797735
PIM1	9,495454809	0,436416495	0,003328001	0,390295495	0,007382079
NUDT4	7,044328201	0,434109183	0,018961841	0,462824315	0,008314826
CASP4	6,685300962	0,433806657	0,039485667	0,620508741	0,001321339
AC079228.1	6,404924279	0,431237064	0,025533735	0,394115677	0,031164171
AGPAT2	7,046648493	0,431144181	0,014940977	0,530535866	0,00154499
GPCPD1	6,279578121	0,430471606	0,032784025	0,541582579	0,003456869
GLRX	6,614826181	0,427620293	0,015948832	0,849543321	1,28485E-06
UBALD2	7,667247394	0,427150136	0,014597956	0,48645585	0,003456457
RALGAPA2	6,24550708	0,423617084	0,043899886	0,661728222	0,000576489
ARID3A	7,048556655	0,423070015	0,04342343	0,806281888	3,44086E-05
RPN2	7,588842177	0,423035011	0,001693096	0,335435725	0,011566113
ALDOA	10,05512121	0,419670008	0,001159593	0,296777443	0,021384994
ZKSCAN1	6,645321866	0,408816219	0,0413273	0,409080023	0,029045002
H3F3C	7,766834053	0,408347134	0,018607019	0,641344266	0,000109366

EEF1A1P5	11,25187401	0,395223144	0,000973379	0,277364986	0,020681366
EIF2S2	7,836517824	0,393090895	0,014532384	0,476653123	0,001832044
GADD45GIP1	7,633851138	0,39111242	0,009169968	0,519561277	0,000298345
SSR4	7,999759566	0,390910731	0,003594158	0,397985424	0,002237845
CD164	7,451453028	0,390356138	0,018056373	0,363327521	0,022286138
EMILIN2	7,229169423	0,389773009	0,042002019	1,010890002	1,24084E-07
LYN	6,825369771	0,388820908	0,049166391	0,444114252	0,014458018
PYGL	8,271539142	0,388165397	0,003546284	0,596165807	7,0512E-06
PECAM1	6,744499522	0,385202066	0,035569382	0,739950478	1,70181E-05
UBE2J1	6,931013003	0,383876314	0,029449721	0,403948292	0,015214814
CAT	8,254402967	0,383700396	0,027820764	0,366937616	0,028088168
C5orf34	9,375313825	0,382329462	0,006052756	0,293798792	0,034136864
DPP7	6,966775625	0,374911447	0,032681399	0,412254859	0,012037868
WDPCP	6,588151273	0,370116047	0,02945327	0,322040538	0,049166003
EEF1A1	12,15253967	0,370053688	0,000904864	0,247152788	0,02801166
KIF5B	7,207384933	0,365394288	0,042866148	0,402295732	0,016588307
NDUFB9	7,768693232	0,362377206	0,007322292	0,421627324	0,001175632
H3F3B	10,04399365	0,361262237	0,000904764	0,488087649	8,05283E-06
SURF4	7,757446197	0,349188279	0,033035319	0,590948615	0,000117686
RTN3	7,775332567	0,349002663	0,027820764	0,323834699	0,033755377
APLP2	8,855210772	0,33644564	0,018274941	0,696733507	9,6129E-07
TXN	8,487119506	0,32062569	0,027710573	0,417657193	0,00219788
ARF1	7,785379639	0,316005527	0,017390988	0,472969331	0,000180548
SENP3-EIF4A1	9,642615029	0,304757402	0,003398085	0,362888472	0,000324508
ACTB	11,81044089	0,282054685	0,003093513	0,485641205	6,0455E-07
TMBIM6	8,907037944	0,2326503	0,041575512	0,3762819	0,000341657
MT-CO2	12,54167096	-0,270696907	0,032627242	-0,335824578	0,004709204
MTATP8P1	10,68570175	-0,307394319	0,011955168	-0,400103631	0,000556844
SRRM2	8,756467406	-0,338069767	0,002916921	-0,539573705	1,9029E-06
MTCO2P12	9,372006213	-0,344700487	0,006160199	-0,268361686	0,032351518
STMN1	8,823701947	-0,345114431	0,016736183	-0,705933343	5,75664E-07
SARAF	8,014998316	-0,355022091	0,016070757	-0,583498322	2,84437E-05
MTRNR2L10	10,466411	-0,358204667	0,003307425	-0,306453038	0,010623392
SNRNP200	6,972473235	-0,359102728	0,031171368	-0,484123564	0,001570524
MT-ATP8	11,35541451	-0,361937723	0,001641992	-0,466604077	3,50088E-05
TOP1	7,1448218	-0,364421516	0,047593832	-0,353777025	0,041684468
PTMA	11,06207291	-0,371345951	0,007009387	-0,518944278	8,82871E-05
FUS	9,005766875	-0,381290918	0,001014671	-0,517178112	7,56578E-06
DYNLL2	7,25157317	-0,40082547	0,016734362	-0,569108457	0,000280748
PTMAP5	9,455136305	-0,405344088	0,006605248	-0,535611287	0,000183463
SPN	8,29315138	-0,408083465	0,009316358	-0,566114637	0,000149654
TOP2B	7,201955111	-0,408744764	0,00339353	-0,604844268	9,02419E-06
APEX1	7,421276617	-0,410112822	0,019769186	-0,577090359	0,000432227
ATP5MC3	8,061585067	-0,410864553	0,010960041	-0,397967059	0,010611962
ITM2C	7,827354882	-0,416356944	0,035639476	-1,003406084	1,46116E-07
HSPE1	6,890354625	-0,422367528	0,035771446	-0,482666014	0,009553032
IQGAP2	7,17792413	-0,428172642	0,035650668	-1,051824364	8,95226E-08

HMGA1	7,383754032	-0,434906947	0,028877069	-0,796279645	1,65395E-05
ELF1	6,833489883	-0,438167188	0,042002019	-0,590462808	0,002536933
NFKBIA	7,360468291	-0,438633338	0,006489704	-0,332766708	0,038182997
H2AFY	8,331864788	-0,460972662	0,000963775	-0,511665736	0,000183463
SEPTIN9	7,501742724	-0,461276007	0,008096727	-0,419243604	0,013279641
SAMHD1	7,523324316	-0,463725026	0,008170325	0,609238903	0,000444266
NDUFB6	6,48631772	-0,471962754	0,017365716	-0,523758407	0,004845528
POLR2C	5,661570285	-0,474221952	0,041841713	-0,480922337	0,024955162
PPM1G	7,789478068	-0,474779296	0,024196664	-0,430158777	0,034833303
PEX26	6,218321192	-0,478005795	0,020877109	-0,486668928	0,012636055
PPA1	6,592823173	-0,489941725	0,045383522	-0,646511535	0,003412345
TAB2	5,979388673	-0,492718546	0,020014519	-0,608298978	0,001918638
CD47	6,971778163	-0,492912786	0,016255986	-0,738246169	0,000117686
PARP1	6,552546671	-0,497021276	0,027710573	-0,818454059	7,66759E-05
METTL7A	6,421930557	-0,506222916	0,024032545	-0,669718787	0,001193341
CXXC5	6,359676402	-0,509372107	0,011719868	-0,578400571	0,002310584
NUDT1	6,07894119	-0,514785473	0,007902539	-0,661102649	0,000282109
AKR1A1	5,962179738	-0,516557169	0,033035319	-0,495490563	0,02931546
ID2	6,465927841	-0,517541681	0,035161791	-0,48192526	0,038819377
PEBP1	7,977933145	-0,520030649	0,000941831	-0,354529379	0,025449338
FEN1	6,33581441	-0,524219954	0,035639476	-0,533060108	0,022106427
CITED2	8,317266211	-0,528874746	0,000662431	-0,538291823	0,000389477
TIMP1	7,48793117	-0,529314718	0,012302057	-0,455924064	0,02730231
SSB	6,732439571	-0,557659714	0,011487415	-0,599757167	0,004054114
ITM2A	6,441384858	-0,56914149	0,035248023	-1,704699556	4,82584E-10
IDH2	7,936466598	-0,596812748	0,000145517	-0,428211963	0,006190802
LGALS9	6,612168709	-0,59780215	0,006953788	-0,600494312	0,00458842
OCIAD2	5,094754286	-0,60972935	0,031206649	-0,717899385	0,005434874
SLFN11	5,159962041	-0,618031277	0,027710573	-0,631930189	0,015355229
AP001972.5	5,793527149	-0,618818078	0,026102065	-0,971464123	0,000123914
GNG2	5,55098339	-0,633131786	0,012441594	-0,547892809	0,02400915
HMGN3	6,599621609	-0,633706647	0,001907485	-0,92276889	4,39355E-06
WIPI2	5,448010022	-0,636726568	0,046205427	-0,595703301	0,046280752
ULK3	4,823163365	-0,647087761	0,046923117	-0,751435824	0,010228182
FLNA	6,784664	-0,650713901	0,004935425	-0,503413511	0,028141067
AC004687.1	5,084130087	-0,6564732	0,027820764	-1,161587704	1,88457E-05
MSH2	5,617119913	-0,658473285	0,006052493	-0,821597553	0,000269989
RGS10	6,902433962	-0,659070044	0,000167503	-0,662868193	0,000116318
PAK1	4,866884593	-0,664292828	0,049430457	-0,910669263	0,002276904
AP1B1	6,864120452	-0,665041022	0,001981756	-0,542104859	0,010593229
BEX4	6,483887561	-0,66551414	0,007029653	-1,04015315	1,11329E-05
TCEAL8	5,193975612	-0,682216	0,018471853	-0,68718415	0,011188463
RASA3	4,757428419	-0,684143621	0,035771446	-0,858399366	0,003503868
LY6E	6,206337459	-0,687339613	0,008096727	-1,012878291	3,53922E-05
ING2	5,743969973	-0,687903649	0,011089916	-0,644419783	0,012044522
ELL	5,340900905	-0,688466968	0,004324604	-0,591047981	0,010911452
ETS2	6,522928858	-0,692291707	0,000650765	-1,025147229	5,62506E-07

TNIK	5,026410703	-0,692782513	0,025689494	-1,084798669	0,0001185
ANXA4	6,030161438	-0,69762411	0,013072559	-0,665133951	0,012819847
AF241726.2	6,575218497	-0,700287492	0,000894595	0,592568543	0,006280607
CDKN1B	5,571034201	-0,709073506	0,007492864	-0,800777756	0,001291691
TCEAL4	5,250296654	-0,710641727	0,035761093	-0,926488959	0,00236381
SLC29A1	6,698465358	-0,712957906	0,000147762	-0,6051669	0,001011347
LPIN1	4,630368833	-0,738169567	0,039485667	-1,046793669	0,001025468
NTRK1	5,853819031	-0,738634767	0,011955168	-1,442106468	4,11561E-07
LINC00926	5,54277825	-0,754369863	0,012815317	-1,038369069	0,000211732
HSH2D	5,492235575	-0,754656711	0,004004915	-0,761964043	0,00219788
MTSS1	5,224879164	-0,776195651	0,007448866	-0,74202586	0,007018359
TNFRSF14	6,136022978	-0,777176998	0,002076201	-0,644092962	0,008931074
MYCBP2	6,791379598	-0,800764159	0,000146416	-0,793632486	0,000119397
MOB1B	4,709914292	-0,80396414	0,035761093	-0,980313886	0,004458802
RPS6KA4	5,143908302	-0,807101839	0,009262283	-0,99743911	0,000556844
EPAS1	6,348223752	-0,808811817	0,004004915	-0,675229765	0,013768356
S100A4	8,237131027	-0,808984313	4,74253E-05	-0,930595303	3,17392E-06
PDLIM5	5,357505202	-0,814928184	0,005737641	-0,64196374	0,025745239
CD2AP	5,086017654	-0,816200183	0,033186507	-0,837242917	0,018547863
CCR2	5,504883936	-0,821469132	0,004176767	-0,672392412	0,016064154
MAP4K4	5,266602966	-0,830288518	0,004667506	-1,04114883	0,000167327
SOX4	8,214359752	-0,838282767	0,032546367	-1,210732592	0,000721187
NLN	4,664444897	-0,839396072	0,010585724	-0,847440322	0,00597129
LMNA	7,116677454	-0,845468995	2,03458E-05	-0,6221626	0,001234008
TMEM273	5,700176251	-0,878269163	0,002687208	-0,85795289	0,002204413
GRAP2	5,93653443	-0,880222307	7,75283E-05	-0,931921084	1,90979E-05
ELK1	5,287949584	-0,884455314	0,003199666	-1,078306311	0,000144665
NIPAL3	4,342178876	-0,889347667	0,022581296	-1,0411189	0,003482187
KLHDC3	5,718356116	-0,894776098	4,47311E-05	-0,851572795	6,20439E-05
RAPGEF2	5,402658807	-0,907424522	0,005095027	-1,221758372	6,45566E-05
RAMP1	4,50064747	-0,914394744	0,024150605	-2,131309789	4,99623E-08
MORN2	3,691781839	-0,916588365	0,017700153	-1,147050807	0,00113589
MEF2D	6,087488879	-0,927865044	0,00023604	-0,716161435	0,00364961
SERPINE2	5,358871606	-0,942479208	0,00365101	-1,652456658	2,69396E-07
TAL1	4,639747741	-0,95309258	0,041258204	-1,41263248	0,000668342
MPO	11,42045309	-0,963127433	0,000124812	-0,936502941	0,000149683
EMID1	4,361437082	-0,963847209	0,049242304	-1,591974396	0,000206872
OTULINL	6,237036849	-0,96890571	3,65407E-05	-0,876646432	0,000114689
LDLRAD4	3,803937776	-0,968916213	0,049871098	-1,375474134	0,001597989
INSIG1	6,624890345	-0,9740124	6,44804E-05	-0,514284648	0,039551274
CD74	9,216599919	-0,97611731	3,9126E-05	-0,697651013	0,002852937
ANGPT1	4,65245511	-0,979721378	0,042571609	-1,865656443	1,43139E-05
GCNT1	5,952813855	-0,987433352	8,46301E-06	-0,954588573	1,0046E-05
GSN	5,869668566	-0,987803917	0,00010389	-0,821446683	0,000904452
CAMK1D	5,304259594	-0,99625475	0,001230401	-0,757525288	0,012188115
PCMTD2	4,038940786	-0,996746696	0,021259847	-0,94260275	0,020305845
C12orf76	4,451124255	-1,03332972	0,031797648	-1,585773879	0,000240216

NMT2	4,37719333	-1,035447524	0,008323566	-1,424814369	9,33244E-05
AHNAK	7,416127179	-1,039479216	1,5374E-06	-1,374640242	1,65279E-09
JUP	6,828187988	-1,040405254	2,70184E-07	-1,451721694	4,31847E-11
IL17RB	6,58383687	-1,046948188	0,004906668	-1,637940353	4,9271E-06
STON2	5,438384954	-1,076922624	0,011312329	-1,156060176	0,003582262
FGL2	5,765264063	-1,080739664	5,17764E-05	-0,832343706	0,001310246
MTURN	4,929658098	-1,101773219	0,006769892	-1,809043913	3,30099E-06
ENSG00000274735	3,731711361	-1,105140846	0,029709239	-1,277551141	0,005731647
TTYH3	6,035493079	-1,111908827	4,0923E-05	-0,895515297	0,000634252
FABP5P2	4,971730805	-1,123749975	0,000332571	-0,715547642	0,021198044
WT1-AS	3,777375391	-1,127729069	0,026974629	-1,769149941	0,000116187
SLC40A1	5,221463715	-1,129970921	0,001460796	-1,973936522	4,82212E-08
MAGED1	5,742272238	-1,139862745	3,60888E-06	-1,352000112	5,88378E-08
MEX3D	3,446577519	-1,156535843	0,03582341	-1,289499949	0,009729194
TSPAN33	4,36329801	-1,16027514	0,004194557	-0,911323135	0,020853771
EPB41L2	4,881823946	-1,181380321	0,001839076	-1,177284343	0,001181339
MEF2C	4,795427616	-1,186325984	0,001596226	-1,163068415	0,001196119
SEMA7A	6,859315994	-1,188830616	0,000344223	-1,524116442	3,95933E-06
LMO4	7,887761069	-1,191230547	9,02372E-05	-1,922607718	3,39552E-09
RAB27B	4,837163159	-1,191637276	0,026209573	-1,735547774	0,000315961
CST3	8,030487681	-1,210225132	7,2555E-07	-0,580027264	0,015980537
ATRN	4,05774942	-1,226821585	0,00659939	-0,918133288	0,039097208
EMILIN1	4,879664006	-1,254304689	0,000300552	-1,379312805	3,92284E-05
TOX	3,740870144	-1,292821241	0,006541817	-1,947220707	1,41246E-05
LSP1	4,226809792	-1,303088988	0,020446686	-1,586215738	0,002009053
TSC22D1	4,688909526	-1,31109983	0,006093514	-2,04737638	7,59505E-06
MEX3B	3,65524625	-1,324839633	0,028925993	-2,585603047	3,99307E-06
ATP1B1	4,164537891	-1,334302884	0,003192485	-1,478914814	0,000520271
AL157895.1	4,011887883	-1,344799095	0,046272216	-2,022156793	0,000735441
HLA-DRA	7,393293587	-1,361311582	1,12884E-05	-1,022049123	0,000702099
USP6NL	3,374211737	-1,366328845	0,011089916	-1,068504668	0,041291596
NRXN2	5,026976054	-1,378420271	4,74253E-05	-1,837232758	1,01364E-07
SMYD3	5,641841438	-1,38912627	5,83355E-06	-1,369341183	4,9271E-06
MIR4458HG	3,092385943	-1,410652827	0,012945815	-1,445495392	0,006430091
IGFBP4	3,987455487	-1,419276757	0,010566611	-1,317678365	0,01230584
RAB7B	4,296380847	-1,425615398	0,003303463	-1,592281857	0,000511151
ARL15	3,303140262	-1,42568722	0,023181052	-1,278158452	0,030314723
CSF1R	6,567807785	-1,427340017	4,4869E-07	-0,725601485	0,007644363
MAP7	3,564058845	-1,427897863	0,034122889	-2,314286138	0,00012887
EPHB6	3,16731313	-1,470930297	0,014649487	-1,455274026	0,009653876
SPARC	4,879004353	-1,481364915	0,001293205	-1,148511423	0,010611962
CD84	5,851704607	-1,496190962	7,28341E-06	-1,365961128	2,23312E-05
CTSH	6,479307342	-1,499037267	4,21659E-07	-0,614929572	0,035872112
UNC5B	2,959850673	-1,511753122	0,048020846	-1,553878727	0,024640854
AL031733.2	3,159879234	-1,535980989	0,031722618	-1,454909594	0,029653942
FAM30A	2,943072972	-1,536373682	0,006489704	-2,320870204	1,25417E-05
ZNF704	4,494887591	-1,539081535	0,0002861	-1,039042834	0,01307384

SCRN1	4,409427859	-1,556822157	0,000470708	-1,80170505	2,90388E-05
HLA-DPB1	5,595334065	-1,573590446	0,002260624	-1,104469779	0,031643201
IRF8	4,785897831	-1,599579007	5,68969E-05	-1,074579709	0,005746525
SFXN3	4,113281502	-1,611797923	0,00068757	-1,033404196	0,028383073
RAB6B	4,241877892	-1,614441306	0,000697784	-1,391917345	0,002414401
CPQ	3,587487911	-1,629958712	0,005036076	-1,287414373	0,022138806
LY86	4,768669085	-1,63171723	0,000406496	-1,2312485	0,006253973
PRSS21	3,902457602	-1,635873475	0,049537988	-4,658662873	6,04703E-09
SEPTIN8	3,182179235	-1,658003591	0,002955778	-1,594752958	0,002665037
AC109460.3	4,702942779	-1,673156289	0,000716006	-2,042797544	1,98629E-05
CD109	4,754175984	-1,680248207	7,32706E-05	-1,987712322	2,19532E-06
MS4A6A	6,430761787	-1,685809583	1,86872E-09	-0,593733808	0,022286138
SLC16A10	3,79979764	-1,688616969	0,004870192	-1,846800619	0,001097835
CFP	4,648273404	-1,697766869	6,06374E-05	-1,19881871	0,003628416
FCER1A	6,420139283	-1,700715638	9,18256E-05	-1,890247165	1,0046E-05
PLXNC1	3,647725301	-1,704554488	0,004317586	-1,665492683	0,003325925
CROT	3,923462745	-1,742272061	0,000298137	-1,679314737	0,000290898
DHRS3	4,445514551	-1,7426821	0,000165115	-1,001840572	0,030836258
POU2F2	4,708652294	-1,750714949	4,99752E-06	-1,145380091	0,001825905
TIMP3	4,962170414	-1,761211568	0,004079465	-2,565643139	1,27988E-05
SLC22A17	3,6174829	-1,797093352	0,00194633	-1,79615659	0,001156766
LIF	4,36474638	-1,798728205	0,001556392	-1,839454893	0,000708492
MYO5A	3,604240506	-1,814977889	0,011955168	-1,655252574	0,01607379
CARD11	2,656921857	-1,897524536	0,018056373	-2,836703654	9,06835E-05
MYCN	2,211678089	-1,935691043	0,026321037	-4,097036113	2,09277E-07
HOXA9	5,107421513	-1,986056953	6,37649E-07	-2,273583383	1,96046E-08
ADRB1	2,692641809	-1,995531185	0,000763932	-1,54799518	0,007698414
GNA12	4,327785403	-1,998438559	0,000215077	-2,639272624	1,07077E-06
ASGR2	5,856119568	-2,005048091	2,79255E-07	-1,623594864	1,11599E-05
SLC24A3	3,012658157	-2,009028973	0,013361617	-3,013888285	4,72479E-05
COL24A1	3,039427813	-2,047122597	0,004297536	-2,536647555	0,00017319
PTGER2	4,434157755	-2,133322175	5,68969E-05	-2,198834511	1,94851E-05
SCPEP1	5,993990228	-2,141882865	1,72319E-07	-1,404396075	0,000224359
TPSAB1	3,403838862	-2,185509628	0,03817007	-2,510751299	0,008989986
CNRIP1	4,010425348	-2,249561918	0,001379716	-2,609931609	0,000116318
GNAI1	2,960860762	-2,257345869	0,001893306	-3,126725678	7,93027E-06
PRG2	10,20750631	-2,296326398	4,4869E-07	-2,509645522	4,73943E-08
TFR2	3,796643709	-2,315806716	0,000105951	-2,632458116	7,58964E-06
DPP4	5,194671389	-2,33862116	0,000137197	-1,274334458	0,042170696
CLEC10A	4,12267992	-2,346466579	1,14605E-05	-1,967951547	0,000126973
SPP1	8,387341382	-2,380800955	1,94902E-07	-1,950979314	8,05283E-06
ADAM28	4,778262843	-2,422253139	6,80155E-09	-2,116389548	1,09537E-07
TPSB2	4,265402811	-2,477308477	0,020014519	-2,512051807	0,012040071
TGFBI	7,181366481	-2,526811767	3,2426E-10	-1,763173819	1,29581E-06
RNASE6	5,030475647	-2,536035866	8,91996E-09	-1,983671017	1,40747E-06
MS4A6E	3,535963948	-2,554707389	4,46129E-05	-1,681269758	0,005882622
HLA-DQA1	5,51610527	-2,590416431	0,000117521	-2,049369383	0,001688967

MAF	6,030086744	-2,640558166	5,57948E-09	-2,32161038	8,84075E-08
PBX1	2,915818412	-2,643162064	9,37187E-05	-2,122950081	0,001216752
NDFIP2	3,935853732	-2,700409296	7,30987E-06	-2,828122115	1,88728E-06
BACE2	4,040864186	-2,723178495	0,002169656	-2,73028992	0,001335717
ADAMDEC1	3,028443693	-2,727626526	8,26653E-05	-1,781784672	0,009192299
RGL1	4,559768325	-2,800667088	5,76416E-07	-1,600940915	0,002361647
CD200R1	3,353020428	-2,873763468	5,87714E-05	-1,952691615	0,005163933
C11orf21	3,121073641	-2,874115628	2,78924E-05	-3,011458873	6,66166E-06
LGMN	6,802759652	-2,977131264	4,61773E-05	-1,493678451	0,046280752
KCNH2	4,765306304	-3,01297737	2,80385E-06	-3,287153061	2,83134E-07
MPEG1	4,237995123	-3,129851357	9,60348E-06	-2,330601789	0,000549934
KIT	4,292303842	-3,165780968	1,86717E-06	-3,121050311	1,42637E-06
EPX	8,371815594	-3,196662996	1,92095E-09	-3,557843345	7,02492E-11
ARL4C	4,527468083	-3,290492519	9,18256E-05	-1,932790663	0,020116723
ST8SIA6	3,110884788	-3,311840069	1,0757E-05	-4,274220901	3,29595E-08
B3GNT7	4,270876701	-3,706129559	8,78352E-07	-2,541271032	0,000305342
RNASE1	7,229498466	-3,723485997	6,14659E-11	-2,569231032	3,20519E-07
CLC	8,489967558	-4,08718993	7,35037E-11	-4,10919428	3,9722E-11
HBB	2,829016623	-4,490637109	6,8667E-07	-4,458597023	5,09889E-07
PRG3	3,726966258	-4,561611369	0,046799317	-4,22578724	0,049905646
CCL18	6,840881747	-5,01062797	0,000501231	-3,720717523	0,007800748

Supplementary Table 1: significantly (p<0.05) deregulated genes in hCD34+ cells after 60 days of competitive outgrowth with RUNX1-RUNX1T1tr and CSF3R T618I compared to co-transduction of vector control (EV) or CSF3R WT.

Data was obtained after performance of bulk RNAseq analysis. (n=2 independent transductions per construct; n=6 replicates per transduction). Results and table were published previously.[194,195]

Appendix 2

Position (hg38)	Aachange (NM_000760.4)	MAF (gnomAD)	VAF	Patient sample	GLI2 expression (TPM (log2))	ClinVar
Chr1: 36472668-A-G	p.Met231Thr	0.02412	0,45	14-00240	0	
			0,43	15-00595	0,057829736	
Chr1: 36472277-C-T	p.Asp320Asn	0.02046	0,45	13-00118	0	
			0,50	13-00163	0	
			0,50	13-00262	2,375118828	
			0,53	13-00500	0	
			0,50	13-00515	0,212393625	
			0,25	13-00537	3,29806423	
			0,49	13-00593	0,286437359	
			0,56	14-00193	0	
			0,48	14-00376	0	
			0,31	14-00473	0,727985953	
			0,49	14-00476	0	
			0,42	14-00567	0	
			1,00	14-00618	0,034524206	
			0,50	14-00672	0,062664034	
			0,52	14-00714	0	
			0,49	15-00018	0	
			0,51	15-00029	0	
			0,49	15-00075	0,018350036	
			0,54	15-00479	0	Benign
			0,47	15-00633	0,030665758	
			0,48	15-00650	0	
			0,45	15-00756	0	
			0,36	15-00763	0,110840583	
			0,49	16-00001	0	
			0,48	16-00303	1,057263835	
			0,47	20-00095	0	
			0,53	20-00325	0,01613982	
			0,50	20-00449	0	
			0,46	20-00450	0	
			0,30	20-00494	3,001662916	
			0,41	20-00508	0,010250282	
Chr1: 36472100-T-C	p.Gln346Arg	0.02401	0,49	14-00240	0	
			0,47	15-00595	0,057829736	
Chr1: 36471505-C-T	p.Glu405Lys	0.00492	0,43	15-00534	0,038022834	
			0,50	20-00500	0	
Chr1: 36469807-C-T	p.Arg440Gln	0.00363	0,48	13-00204	4,99708147	
			0,46	15-00406	0,091013659	
			0,47	15-00534	0,038022834	
			0,45	15-00670	0,021375615	

			0,51	15-00680	0,049628814
			0,47	20-00347	0
Chr1: 36469204-C-G	p.Asp510His	0.05254	0,50	13-00166	0
			0,47	13-00260	0
			0,40	13-00396	0,073222915
			0,47	13-00660	0,051774262
			0,44	14-00126	2,571988498
			0,42	15-00043	0
			0,43	15-00269	0
			0,42	15-00302	0,057081885
			0,48	15-00383	0,28055805
			0,39	15-00417	0,013944937
			0,48	15-00563	0,034438628
			0,47	15-00653	0
			0,44	15-00702	0
			0,48	16-00088	4,327696991
			0,49	16-00115	0
			0,48	20-00052	0,012215892
			0,45	20-00453	3,94692218
			0,40	20-00456	4,235903819
			0,49	20-00460	0
			0,51	20-00492	4,73999919
Chr1: 36468114-A-G	p.Tyr562His	0.00676	0,49	12-00150	0,075021649
			0,45	13-00551	0,046645587
			0,17	13-00552	0
			0,47	14-00228	0
			0,49	15-00482	0
Chr1: 36466902-C-T	p.Gly683Arg	0.04832	0,27	13-00660	0,051774262
			0,10	16-00115	0
			0,17	20-00460	0
Chr1: 36466862-A-G	p.Met696Thr	N/A	0,81	13-00166	0
			0,61	15-00269	0
			0,67	15-00302	0,057081885
			0,71	15-00417	0,013944937
			0,74	15-00563	0,034438628
			0,62	20-00453	3,94692218
			0,40	20-00456	4,235903819
			0,74	20-00492	4,73999919
Chr1: 36466671-G-T	p.Pro760Thr	0.0005718	0,47	20-00491	0,108982288
Chr1: 36466446-C-T	p.Glu835Lys	0.00532	0,53	14-00231	0
			0,51	14-00464	0
			0,73	15-00717	0,013540033
			0,62	15-00763	0,110840583
			0,50	20-00080	0
			0,55	20-00088	0,010937129
			0,53	20-00507	0

Chr1: 36475383-C-T	p.Ala119Thr	0.0008280	0,55	13-00145	0	Uncertain significance
			0,49	15-00872	0,636438678	
Chr1: 36473802-C-G	p.Glu149Asp	0.002943	0,42	13-00273	1,42933714	
			0,41	14-00021	0	
			0,44	14-00714	0	
			0,42	15-00309	0,544203879	
			0,35	20-00502	0	
Chr1: 36471564-A-C	p.Leu385Arg	N/A	0,51	20-00080	0	
Chr1: 36469717-G-A	p.Ala470Val	No Frequency (NF)	0,45	20-00335	0,022670902	
Chr1: 36468168-G-C	p.Gln544Glu	N/A	0,49	20-00057	0	
Chr1: 36466857-G-A	p.Arg698Cys	0.00269	0,29	13-00552	0	
			0,06	13-00557	1,247921597	
			0,48	15-00701	0,017848198	
Chr1: 36472114-C-A	p.Trp341Cys	N/A	0,40	14-00608	0,045726637	Likely Pathogenic
Chr1: 36468158-C-T	p.Trp547*	0.00026	0,30	15-00717	0,013540033	
Chr1: 36467951-T-A	p.Asn579Tyr	N/A	0,39	13-00245	1,639861344	
Chr1: 36466612-A-T	p.Tyr779*	N/A	0,22	15-00572	1,034624051	
			0,99	20-00091	3,205326691	
Chr1: 36467833-G-A	p.Thr618Ile	NF	0,08	13-00342	0,011580059	Pathogenic
			0,55	13-00468	0,950294861	
			0,48	13-00557	1,247921597	
			0,26	13-00558	1,567485062	
			0,11	14-00273	0	
Chr1: 36467597-G-T	p.Thr640Asn	NF	0,13	20-00498	0	
Chr1: 36466623-G-A	p.Gln776*	NF	0,20	13-00625	0,072980056	
Chr1: 36466496-C-T	p.Trp818*	N/A	0,51	13-00245	1,639861344	
			0,51	14-00608	0,045726637	

Supplementary Table 2: ClinVar prediction of CSF3R Variants
Table and results were previously published.[195]

Acknowledgements

Working on a big research project never comes without challenges, the more I am deeply thankful for everyone who guided me and walked this way by my side.

First and foremost, I deeply thank my first supervisor Prof. Dr. med. Philipp Greif for his guidance and his support throughout my time as part of his team. His valuable insights, great expertise, and ever open door were exceptional.

My deepest thank also goes to Prof. Dr. med. Oliver Weigert. I am very grateful for his critical thinking, challenging questions, and great support as second supervisor.

Another huge thank you goes to Dr. Binje Vick for her ideas and support and all the words of encouragement and wisdom.

Next, I want to thank the Greif lab group and everyone in the ELLF. It was a pleasure! Thank you for hours of brainstorming, making long days light, and all the laughter.

A very special thank you goes to my family. My parents and my sisters, who always believe in me and support me in every way. My husband, who always has my back. My kids, for being more than patient. And finally, my parents in law. Without all your support, this would not have been possible.

Affidavid

LMU LUDWIG-MAXIMILIANS-UNIVERSITÄT MÜNCHEN | Promotionsbüro Medizinische Fakultät | MMRS

Affidavit

Swoboda, Anja

Surname, first name

Max-Lebsche-Platz 30

Street

81377, München, Germany

Zip code, town, country

I hereby declare, that the submitted thesis entitled:

Characterization of CSF3R mutations in Core Binding Factor Leukemia

……

is my own work. I have only used the sources indicated and have not made unauthorised use of services of a third party. Where the work of others has been quoted or reproduced, the source is always given.

I further declare that the dissertation presented here has not been submitted in the same or similar form to any other institution for the purpose of obtaining an academic degree.

München, 06.08.2024 — Anja S. Swoboda

place, date — Signature doctoral candidate

Confirmation of congruency

LMU LUDWIG-MAXIMILIANS-UNIVERSITÄT MÜNCHEN

Promotionsbüro
Medizinische Fakultät

MMRS

Confirmation of congruency between printed and electronic version of the doctoral thesis

Swoboda, Anja
Surname, first name

Max-Lebsche-Platz 30
Street

81377, München, Germany
Zip code, town, country

I hereby declare, that the submitted thesis entitled:

Characterization of CSF3R mutations in Core Binding Factor Leukemia

……

is congruent with the printed version both in content and format.

München, 06.08.2024
place, date

Anja S. Swoboda
Signature doctoral candidate

List of publications

Swoboda, A.S., Arfelli, V.C., Danese, A., Windisch, R., Kerbs, P., Redondo Monte, E., Bagnoli, J.W., Chen-Wichmann, L., Caroleo, A., Cusan, M., Krebs, S., Blum, H., Sterr, M., Enard, W., Herold, T., Colomé-Tatché, M., Wichmann, C., Greif, P.A. CSF3R T618I Collaborates With RUNX1-RUNX1T1 to Expand Hematopoietic Progenitors and Sensitizes to GLI Inhibition. *Hemasphere* **7**, E958 (2023)

Caroleo, A., Kerbs, P., **Swoboda, A.S.,** Wange, L., Heinzlmeir, S., Chang, Y., Küster, B., Enard, W., von Bergwelt, M., Greif, P.A., Cusan, M. Synergistic Antileukemic Effect of Mek and Lsd1 Inhibitors Correlates with Decreased Phospho-Serine 315 of TP53. *Blood* **140**, 5870–5871 (2022)

Kerbs, P., Vosberg, S., Krebs, S., Graf, A., Blum, H., **Swoboda, A.S.,** Batcha A.M.N., Mansmann, U., Metzler, D., Heckman, C.A., Herold, T., Greif, P.A. Fusion gene detection by RNA-sequencing complements diagnostics of acute myeloid leukemia and identifies recurring NRIP1-MIR99AHG rearrangements. *Haematologica* **107**, 100–111 (2022).

Swoboda, A.S., Arfelli, V.C., Danese, A., Windisch, R., Kerbs, P., Redondo Monte, E., Bagnoli, J.W., Chen-Wichmann, L., Caroleo, A., Cusan, M., Krebs, S., Blum, H., Sterr, M., Enard, W., Herold, T., Colomé-Tatché, M., Wichmann, C., Greif, P.A. CSF3R T618I Collaborates with RUNX1-RUNX1T1 to Expand Human Haematopoietic Stem and Progenitor Cells. *Blood* **138**, 2233–2233 (2021).

Redondo Monte, E., **Wilding, A.S.,** Leubolt, G., Kerbs, P., Bagnoli, J.W., Hartmann, L., Hiddemann, W., Chen-Wichmann, L., Krebs, S., Blum, H., Cusan, M., Vick, B., Jeremias, I., Enard W., Theurich, S. Wichmann, C., Greif, P. ZBTB7A prevents RUNX1-RUNX1T1-dependent clonal expansion of human hematopoietic stem and progenitor cells. *Oncogene* **39**, 3195–3205 (2020).

Leubolt, G., Redondo Monte, E., **Wilding, A.S.,** Kerbs, P., Cusan, M., Bagnoli, J.W., Enard, W., Hiddemann, W., Wichmann, C., Schotta, G., Greif, P.A. GATA2 Zinc Finger Mutations Influence Erythroid Differentiation and Chemotherapy Response. *Blood* **134**, 1459–1459 (2019).

Redondo Monte, E., **Wilding, A.S.,** Leubolt, G., Kerbs, P., Bagnoli, J.W., Hiddemann, W., Enard, W., Theurich, S., Greif, P.A., Loss of ZBTB7A Enhances Glycolysis and Beta Oxidation in Myeloid Leukemia. *Blood* **134**, 1453–1453 (2019).

Redondo Monte, E., **Wilding, A.S.,** Leubolt, G., Hartmann, L., Dutta, S., Hiddemann, W., Chen-Wichmann, L., Wichmann, C., Greif, P.A. Loss of ZBTB7A Facilitates RUNX1/RUNX1T1-Dependent Clonal Expansion and Sensitizes for Metabolic Inhibition. *Blood* **132**, 1499–1499 (2018).

Contributions

I planned all experiments described in this thesis and performed all functional assays and cell handling. I analyzed all data and performed statistical analysis. Sequencing for bulk and single cell RNAseq was performed externally. Raw data handling and statistics for RNAseq and patient cohort data were performed by biostatisticians with my assistance. Subsequently, I interpreted all RNA data and performed pathway analysis. Mouse handling was performed externally. I performed preparation and flow cytometry of mouse blood samples. Finally, I wrote the manuscripts for all publications containing data used in this thesis.